STUDIES ON MAC PROTOCOLS AND TRANSMISSION IMPAIRMENTS IN WDM-BASED OPTICAL ACCESS NETWORKS

Thesis Submitted to
Indian Institute of Technology, Kharagpur
for the Award of the degree of

Doctor of Philosophy

by

Jayashree Ratnam (02EC9601)

Under the supervision of

Prof. Debasish Datta
Department of Electronics and Electrical Communication Engineering
and
Prof. Saswat Chakrabarti
G. S. Sanyal School of Telecommunications

Department of Electronics and Electrical Communication Engineering
Indian Institute of Technology, Kharagpur
June 2009

INSTITUTE OF
TECHNOLOGY
KHARAGPUR-721302

EPARTMENT OF ELECTRONICS AND ELECTRICAL
OMMUNICATION ENGINEERING

CERTIFICATE OF APPROVAL

Date: … June, 2009

Certified that the thesis entitled "**Studies on MAC Protocols and Transmission Impairments in WDM-Based Optical Access Networks**" submitted by **Jayashree Ratnam** to **Indian Institute of Technology, Kharagpur**, for the award of the degree of Doctor of Philosophy has been accepted by the external examiners and that the student has successfully defended the thesis in the viva-voce examination held today.

Signature 3/6/09
Name: S. S. Pathak
(Member of the DCS)

Signature 3.6.'09
Name: D. SARKAR
(Member of the DCS)

Signature R. Garg 3.6
Name: R. GARG
(Member of the DCS)

Signature D. Datta 03.06.09
Name:
(Supervisor)

Signature Saswat Chakrabarti 03.06.
Name:
(Supervisor)

Signature
Name:
(External Examiner)

Signature 3/6/09
Name:
(Head of the Department)

Professor & Head
E & E.C.E. Dept.
I.I.T., Kharagpur

INSTITUTE OF
TECHNOLOGY
KHARAGPUR-721302

PARTMENT OF ELECTRONICS AND ELECTRICAL
MMUNICATION ENGINEERING

संस्थ
खड़ग

CERTIFICATE

This is to certify that the thesis entitled "**Studies on MAC Protocols and Transmission Impairments in WDM-Based Optical Access Networks**" submitted by **Jayashree Ratnam** to **Indian Institute of Technology, Kharagpur**, is a record of bona fide research work carried out by her under our supervision and is worthy of consideration of the degree of **Doctor of Philosophy** of this institute.

Saswat Chakrabarti
(Saswat Chakrabarti)
Professor and Chairman, GSSST

D. Datta
(Debasish Datta)
Professor, Dept. of E & ECE

Date: 02 June, 2009

Dedicated in loving memory of
my parents
Sri. N. Jaya Ram and Smt. N. Eswari

ॐ असतो मा सद् गमय ।

तमसो मा ज्योतिर्गमय ।

मृत्योर्माऽमृतम् गमय ॥

"Om! Asatoma Sadgamaya
Thamaso Maa Jyothir Gamaya
Mrithyor Maa Amrutham Gamaya
Aum Shanti Shanti Shantihi"

- Brhadaranyaka Upanishad

Om! Lead me from the unreal to the real; from the darkness (ignorance) to the light (knowledge): and from the death to immortality.

Let there be Peace, Peace, Peace

Acknowledgements

My father's constant advice, "to target for higher goals" has always been a guiding light for my academic pursuit. I acknowledge my sincere thanks to my research advisors, Prof. D. Datta and Prof. S. Chakrabarti, for the moral support they have given me all throughout. Their firm belief that good research can be done only with a free mind, allowed me to work in a stress-free environment. I profusely thank Prof. D. Datta for motivating me to take up research and for suggesting live problems in the area of Optical Networks. This thesis would not have taken the present shape, if not for his meticulous approach to look into finer details.

I am grateful for the kind gesture from Prof. A. Ghosh, ex-Director of IIT Kharagpur, permitting me to pursue Ph.D programme, while working as a Scientific Officer in the Institute. My special thanks to Prof. S. Chakrabarti, Chairman G. S. Sanyal School of Telecommunications for being very supportive, while I carried on my research work as an employee of the School. I also thank Prof. R. Garg (Dept. of E&ECE), Prof. S. L. Maskara (Retd.), Prof. T. S. Lamba (Retd.) for their encouragement and support. I acknowledge my thanks to Prof. S. S. Pathak (Dept. of E&ECE) and Prof. D. Sarkar (Dept. of CSE) for their valuable advice as members of my Doctoral Scrutiny Committee. Thanks are due to all my co-scholars and colleagues in GSSST for the warm cordiality that I received from each one of them.

My family gave me a lot of support at various stages. My husband, Prof. R. V. Raja Kumar's quality-conscious approach towards his students motivated me to work harder. I feel proud of my daughter, Shruti for helping me finalize a mathematical formulation. I consider myself fortunate that my son, Vishnu managed himself very well away from home, allowing me to concentrate on my work. I am grateful indeed to my extended family, Smt. Bharathi, Smt. Lakshmi, Capt. Sreenivas and Smt. Harika, for taking good care of my children during a part of the research period. I take this opportunity to thank all my friends and elders for their well wishes and blessings. My mother's memories and affection from my siblings Smt. Padma Shree and Dr. Suresh kept me in good stead during difficult times. I am grateful to almighty for blessing me with the determination to fulfill my father Sri. N. Jaya Ram's dream by taking a "doctoral degree".

R. Jayashree
2.06.09

CONTENTS

List of Abbreviations

S. No.	Abbreviation	Description
1.	AN	Access node
2.	APON	ATM PON
3.	AWG	Arrayed-waveguide grating
4.	BER	Bit-error rates
5.	BPON	Broadband PON
6.	CD	Collection and distribution
7.	CO	Central office
8.	DFB	Distributed feedback
9.	DWDM	Dense WDM
10.	EDFA	Erbium-doped fiber amplifier
11.	FBG	Fiber Bragg grating
12.	FP laser	Fabry-Perot laser
13.	FPR	Free propagation region
14.	FSAN	Full service access network
15.	FSR	Free spectral range
16.	FTTx	Fiber-to-the-x
17.	GQ	Global queue
18.	GPON	Gigabit PON
19.	HG	Header generator
20.	IM-DD	Intensity-modulated direct-detection
21.	MAC	Medium-access control
22.	MUI	Multiple user interference
23.	OCDMA	Optical code division multiple access
24.	ODN	Optical distribution network
25.	O-E-O	Optical/electronic/optical
26.	OOC	Optical orthogonal codes
27.	OLT	Optical Line Terminal
28.	ONT	Optical network terminal
29.	ONU	Optical network unit
30.	PON	Passive optical network
31	PSC	Passive star coupler
32.	RN	Remote node
33.	RSOA	Reflective semiconductor optical amplifiers
34.	RT/NRT	Real time/ Non-real time
35.	SCM	Sub-carrier multiplexing
36.	SSFBG	Super-structured Fiber Bragg grating
37.	TDM/TDMA	Time-division multiplexing/multiple access
38.	VCSEL	Vertical cavity surface emitting laser
39.	WDM	Wavelength-division multiplexing
40.	WDMOAN	WDM-based optical access network
41.	WDMPON	WDM-based passive optical network

List of Figures and Tables

ABSTRACT

Wavelength-division-multiplexing-based optical access networks (WDMOANs) have the potential to address the "last-mile" connectivity issues through passive architectures and to support quality-ensured telecommunication services. Over the years WDM-based passive optical networks (WDMPONs) with tree topology are evolving as one class of WDMOANs with a promise towards a cost-effective and flexible broadband access solution. In the present thesis, we investigated some of the relevant MAC-layer and physical-layer issues for such networks for three different network configurations.

First we investigate the performance of medium access control (MAC) protocols in a WDMOAN with two-level hierarchical topology, consisting of a backbone ring interconnecting several passive-star-based clusters of optical networking units (ONUs) at customer premises. Each cluster is connected to the backbone through an access node (AN). A scheduler located in each AN, executes two MAC protocols, one for the intracluster traffic and the other for the intercluster traffic. The performance of MAC protocol for intracluster traffic is evaluated through event-driven simulation. The delay performance of the intracluster MAC protocol is found to improve on increasing the number of control channels but with an early take-off of the delay curves. Further, incorporating a few more control channels using subcarrier multiplexing (SCM) on a single control wavelength proved useful in improving the overall delay performance, without reducing the number of wavelengths needed for data traffic, albeit at the cost of increased hardware for SCM. The performance of MAC protocol for intercluster traffic is evaluated through analytical modeling of the queuing system employing two dynamic bandwidth management schemes. A comparative study of the two intercluster schemes in terms of end-to-end delay is carried out in terms of end-to-end delay, to understand the effect of priority queuing on the real-time and non-real-time service packets.

Next we consider the resource provisioning aspects in a WDMPON which employs WDM along with optical code division multiple access (OCDMA) technique for better bandwidth utilization. First, we adopt a heuristic approach for allocating optical codes to the ONUs which takes into consideration the traffic asymmetry between the upstream and downstream transmissions. Thereafter we improvise the heuristic provisioning towards an optimal design by using our observations on PON throughput and thereby drifting from the heuristic estimate incrementally. For this purpose we develop an analytical model for system

throughput taking into consideration the effects of interference and code contention in the upstream channels which helps in understanding the behavior of a network with asymmetric traffic. Using the throughput models, we examine the under-provisioned and the over-provisioned (with reference to the heuristic solution) cases using open-search mode of optical code allocation to arrive at an optimum resource (code) provisioning for the network.

Finally, we consider a WDMPON, which employs an arrayed-waveguide grating (AWG) at the remote node (RN) and examine the bit-error rate (BER) performance of routed optical channels at various AWG ports. The AWG-based RN demultiplexes the incoming (downstream) WDM signal to distinct output port locations, through static wavelength routing mechanism. An analytical model is developed for the routed optical signals, which takes into consideration finite laser linewidth, spatial dispersion and far-field intensity profile in the AWG. A novel spectral-to-spatial domain transformation technique is used to determine the amount of optical signal power captured at the various output port locations with due considerations to signal impairments like interchannel crosstalk and the consequent interferometric beat noise at the receiving end. It is observed that for increasing linewidths, beat noise effects on the optical signal at the receiver are strong enough to deteriorate the BER values by 2-3 orders at the outer ports and by 3-4 orders at the inner ones.

CHAPTER 1

Introduction

1.1 Fiber in the Last Mile

Broadband access networks using optical fibers have emerged as the high-bandwidth "last mile" wired-solution for this information-era. In near future, a customer would expect the subscribed network to be capable of delivering services like HDTV, video-on-demand, VoIP, video-conferencing, etc. Copper-based access, whether it is through twisted pair wire or coaxial cable, in spite of employing digital subscriber loop-modem technologies, falls short of addressing the bandwidth demands of such emerging services. In view of this, many incumbent local exchange carriers and multiple system operators in North America, Asia-Pacific and Europe are gearing up for a migration to fiber-based access infrastructure. The fiber-to-the-x (FTTx: x being any one the Curb/ Premises/ Building/ Home) architecture, can employ either point-to-point or point-to-multipoint type of connectivity, between the central office (CO) and customer premise terminations [FPSB89].

In a point-to-point system, a source-destination pair enjoys exclusive usage of an optical link and is justified for a business house or an organization. On the other hand, in a point-to-multipoint system, the candidate topology could be a passive star or a tree connecting a cluster of users and, such clusters may be interconnected using ring or other suitable intercluster backbone (feeder) topology using optical fibers. For the local cluster formation, the passive star topology would need a central access node (AN) placed on a local hub on the fiber backbone, while for tree topology each cluster would need a feeder fiber from the AN or the hub to a point called remote node (RN). From the RN, service traffic would be distributed through appropriate passive device on individual distribution fibers to the users. Such networks are in general termed as passive optical networks (PONs). Typically, such a PON would consist of an optical line terminal (OLT) located at the hub, with multipoint connectivity to optical network units (ONUs) or optical network terminals (ONTs) located near or in the user premises. For PONs with tree topology, depending upon the geographical distribution of the users, RN can have either a single-stage or a multi-stage configuration employing power splitters (using star couplers) and/or wavelength-routing devices, such as arrayed-waveguide grating (AWG).

FTTx is the outcome of an earlier initiative taken by Full Service Access Network (FSAN) consortium, consisting of several global service providers, manufacturers and equipment vendors, with the objective to bring out a common interoperable access solution for delivering integrated broadband services. FSAN's proposal was ratified by ITU-T in 1998 and became the first PON standard under G.983 recommendation [MaOF01]. Systems based on this standard were called ATM PONs (APONs), which operated on 1490/1310 nm wavelength for downstream/upstream transmissions. As the name implies, this access solution is based on ATM data encapsulation and has the capability to handle the QoS requirements of triple play services at 622/155 Mbps transmission rates. The basic APON was improved upon with an "analog video" overlay at 1550 nm along with a higher downstream speed of upto 1.2 Gbps which came to be popularly known as Broadband PON (BPON). Dominance of data traffic over voice traffic and ubiquitous presence of Ethernet-based networks created also the need for an access standard to carry data services efficiently. In 2004 IEEE's drive to bring Ethernet to the last mile (later identified as the "first mile") led to the emergence of EPON or GEPON which offers symmetric data rates of 1.25Gbps. All these standards are based on time-division multiplexing/multiple access (TDM/TDMA) for their transmissions. Subsequently, optical technology became mature enough to bring down the network cost, so much so that increasing number of last mile installations found it necessary to upgrade their systems to FTTx architectures. In order to enable all proprietary networks (TDM and non-TDM) to seamlessly communicate with each other, ITU-T came up with a new standard G.984, called Gigabit PON (GPON), which supports ATM, Ethernet, IP and SONET payloads through a gigabit encapsulation method (GEM) and can also stream video-over-IP at 2.5Gbps symmetric rates.

In July 2007, regional FTTH councils in various parts of the world published a global ranking of economies, with "greater than 1% FTTx penetration" as the qualifying factor. Fiber roll-outs are being prioritized in countries like US, Japan, South Korea, Hong Kong and which would soon set a path for other countries to follow. This momentum will further give rise to a variety of media-rich interactive services demanding more scalability and higher utilization of the optical links in PONs. In this aspect, a TDMPON needs an overhauling of the entire network in order to accommodate new services and subscribers. This sets an upper limit to the maximum bandwidth a subscriber can be offered. Further as the customer-base grows in size, access control mechanisms for upstream traffic and multiplexing techniques for downstream traffic need to be enhanced with more powerful technologies [KSGW07], [Mukh00] like wavelength-division multiplexing (WDM). At this stage, design considerations other than cost become important to future-proof the existing TDM-based PON deployments. A WDM-based optical access network (WDMOAN) offers virtual point-to-point connections to the end-users on a shared infrastructure with either active (AONs) or passive architectures (PONs) and leverages all the benefits of a shared network making them suitable for cost-sensitive access segment [Koon06], [KSGW07].

1.2 WDM-based Optical Access Networks

WDM is already an established networking technology in the wide area and metropolitan area segments. There is a growing awareness in the world communities, regarding the benefits of having high bandwidth connection with the information highway. This changed the attitude of a prospective customer, who is now willing to pay more for the quality of service connection. In such a scenario, deploying WDM in the access segment, not only brings several benefits for the subscribers, but also makes the network reconfigurable according to traffic dynamics. In spite of the need, WDM penetration in the local loop is in want of mature devices. In recent years, WDM device technology has made remarkable progress and a variety of optical transmitters and receivers of both fixed and tuned type, are now readily available [Zirn98], [Tong98], [ElMo00]. Similarly tunable optical filters for WDM networks have undergone considerable progress [SaBo98]. Tunable transceivers are relatively more expensive, making them suitable for OLTs. However, for ONUs located in business premises or large research and development units, the transceiver cost might be negotiated for the bandwidth advantage. As mentioned earlier, such WDMOANs typically used ring-on-star topology, where the passive-star-configured ONU clusters are connected to a ring-configured feeder fiber. Traffic distribution within the cluster was carried through power splitters whereas the aggregated cluster-traffic on the feeder ring employed wavelength routing using active subsystems (with optical-electronic-optical conversion). Scheduling and other MAC-layer related functionalities were carried out centrally at the access node (where OLT is co-located).

Subsequently, in order to reach the network services to all sections of customers, the distribution nodes were moved closer to the user-premises with a completely passive distribution between the OLT and ONUs leading to a tree topology. These access networks are called WDM-based passive optical networks (WDMPONs). They can be power-splitting (broadcast-select services) type, wavelength-routed (switched services) type or a combination of both, depending upon the local telecom needs. An optical channel in a wavelength-routed PON experiences low splitting loss and is transparent to the line rate, data format and transmission protocols, lending itself to a smooth up-gradation path. Arrayed waveguide grating (AWG) devices which feature low insertion loss, periodic routing and spatial wavelength reuse, play a pivotal role in realizing efficient wavelength-routed WDMPONs. WDMPONs are emerging as the next evolutionary step towards realizing FTTx technology in the service-driven access network segment.

In order to support large customer-base whose per-user bandwidth requirements are nominal, PONs employing hybrid technologies prove to be more cost-effective. Hybrid PONs with TDM and subcarrier multiplexing (SCM) techniques along with WDM, viz., WDM-TDM [SJSS05] and WDM-SCM [KaHa06] configurations have been investigated in several experimental studies. However the scalability of the network is limited in the former (TDM) due to the high operating (aggregate) speed requirements by the ONUs and beat noise effects amongst the RF carriers, in the latter (SCM) case. In this regard, a relatively new multiple access technique, optical code division multiple access (OCDMA) is also being considered as a possible solution for the PON segment [KiWW06]. OCDMA systems are suitable for carrying bursty data traffic with asynchronous communication, obviating the need for either synchronization (as in TDMPONs) or tunability (as in WDMPONs) of the ONU transceivers. Further, it has the potential to maintain the service quality of heterogeneous services (expected in future PON traffic) through multi-rate coding [MaVi98]. OCDMA-based PONs can be realized with the help of passive devices, like Fiber Bragg Grating (FBG) for encoding/decoding the information bits. FBGs are more amenable for mass fabrication compared to the fiber delay-line based codecs that were used earlier. However interference from simultaneous users limits the scalability of OCDMA-based PONs. Hence, a more useful way to exploit the inherent advantages of OCDMA is to use it in conjunction with WDM (called W-OCDM PONs). Such realizations of W-OCDM PONs offer secure (in-built due to encoding process) connections with modular (in terms of optical code size) scalability.

1.3 Some Major Issues and Motivation for Research

Like any promising technology, WDMOAN too has its own share of challenges to be overcome before its intrinsic benefits are harnessed for the needs of a true FTTx solution. In order to utilize the benefit of WDM, WDMOANs need appropriate MAC protocols with suitable network and AN configurations. Furthermore, as mentioned earlier clusters of users belonging to passive stars or trees need to communicate amongst themselves through fiber backbone for intercluster traffic.

In our first research problem, we investigate the MAC protocols for a WDMOAN with passive-star based clusters interconnected by fiber ring as backbone (feeder). We investigate some methods of reducing contention in the control channel to improve throughput in data channels. Further, we incorporate priority queuing in the MAC protocol for handling multi-service (real-time and non-real-time) traffic in the feeder network and carry out delay analysis for two different priority queuing methods.

With growing subscriber population, a network designer has to find improved ways of multiplexing downstream channels as well as use novel access mechanisms for upstream transmissions. In future the upstream traffic will gradually grow and upstream-to-downstream traffic ratios exceeding 1:2 (eg., 1: 0.75 and 1:0.9) may not be uncommon. Thus, in our next research problem we carry out investigations on the problem of resource provisioning in W-OCDM PON. We propose a hybrid architecture which utilizes WDM/WDMA and OCDM/OCDMA in an integrated way to support a large number of bidirectional transmissions. An analytical formulation for evaluating upstream and downstream data throughputs, using a heuristic estimate for code allocation is carried out. Based on the analysis, we attempt to reach an optimum resource allocation for a user-cluster, in terms of appropriate figures of merit for PON performance.

Service transparency and link upgradeability can be effectively realized only on WDMPONs employing wavelength routing. However the cost-effectiveness of such a WDM PONs depends on optimization of link power budget, which needs a systematic study of various factors affecting the routed WDM channels through AWG used in the RN. In our next problem, we take up a WDMPON configuration, which uses an AWG to perform channel distribution at the remote node using wavelength routing. AWG being a passive routing device is particularly preferred in RNs with either high fan-out, single-stage distribution or with multiple-stage distribution. We develop an analytical model to study the impact of impairments resulting from non-ideal nature of the laser spectrum, routing device, co-channel interference on physical-layer performance of the receivers, viz., crosstalk power, beat noise, non-uniform power distribution in AWG and their manifestation as bit-error rates (BER) at various AWG output ports.

1.4 Thesis Contributions

As discussed in the foregoing, the following investigations have been carried out in the present thesis:

- Investigations on MAC protocols to implement in a WDMOAN with ring-on-stars topology, wherein passive stars form the local cluster of ONUs and the clusters are interconnected using a WDM ring.
  - Proposed a scheduler-based access node configuration, which centrally coordinates intra/inter-cluster transmissions using two separate MAC protocols
  - Performance analysis of the proposed intra-cluster MAC protocols using pre-transmission coordination through event-driven computer simulation
  - Performance analysis of the proposed inter-cluster communication protocols using queuing models
- Studies on resource provisioning in W-OCDM PONs with asymmetric traffic distribution for upstream/downstream communications
  - Analytical modeling of upstream and downstream data throughput for a given traffic asymmetry with and without contention for shared codes in the upstream channels
  - Performance analysis of upstream and downstream communications of aggregate throughput rate using the developed analytical models
  - Studies on the methodologies for scalable resource provisioning (optical codes per wavelength as the resource divided between upstream and downstream communication) in a W-OCDM PON, based on the overall throughput estimates for the PON using the developed throughput models.
- Studies on transmission impairments in AWG-based WDMPONs
  - Development of a novel analytical model to estimate the signal and interchannel crosstalk power levels at AWG output ports using a frequency-to-spatial domain transformation of non-ideal laser spectrum

- Studies on BER performance for downstream communication through AWG and evaluation of BER variation across the AWG ports leading to the assessment of scalability of AWG-based RNs in WDMPONs

1.5 Thesis Organization

The rest of the thesis is organized in the following manner. Chapter2 provides background for WDMOANs with a brief account of the related studies and developments reported in the literature. Chapter 3 deals with the studies on MAC protocols for a employing ring-on-stars topology for intracluster as well as intercluster communications. Chapter 4 presents the studies on resource provisioning using throughput analysis in a W-OCDM PON for asymmetric traffic distribution for upstream/downstream communication. Chapter 5 deals with physical-layer performance in a wavelength-routed WDMPON employing an AWG as its RN. Finally Chapter 6 presents the concluding remarks on our investigations followed by some discussion on the possible future scope of the work.

References

[Brack90] C. A. Brackett, "Dense wavelength division multiplexing networks: principles and applications," *IEEE Journal of Selected Areas of Communications*, vol. 8, no. 6, pp. 948-964, Aug. 1990.

[ElMo00] J. M. H. Elmirghani and H. T. Mouftah, "Technologies and architectures for scalable dynamic dense WDM networks," *IEEE Communications Magazine*, pp.58-66, Feb. 2000.

[FPSB89] D. W. Faulkner, D. B. Payne, J. R. Stern and J. W. Balance, "Optical networks for local loop applications," *IEEE/OSA Journal of Lightwave Technology*, vol. 7, no.11, pp. 1741-1751, Nov. 1989.

[Koon06] T. Koonen, "Fiber to the Home/ Fiber to the Premises: What, Where, and When?" *Proceedings of the IEEE*, vol. 94, no. 5, May 2006.

[KSGW07]L. G. Kazovsky, W. T. Shaw, D. Gutierrez, N. Cheng and S. W. Wong, "Next-generation optical access networks," *IEEE/OSA Journal of Lightwave Technology*, vol. 25, no. 11, pp. 3428-3442, Nov. 2007.

[MaOF01] Y. Marda, K. Okada and D. Faulkner, "FSAN OAN-WG and future issues for broadband optical access networks," *IEEE Communications Magazine*, pp 126-132, Dec. 2001.

[Mukh00] B. Mukherjee, "WDM optical communication networks: progress and challenges," *IEEE Journal of Selected Areas of Communications*, vol. 18, no. 10, pp. 948-964, Oct. 2000.

[SaBo98] D. Sadot and B. Gurion, "Tunable optical filter for dense WDM networks," *IEEE Communications Magazine*, pp 50-55, Dec. 1998.

[Tong98] F. Tong, "Multiwavelength receivers for WDM systems," *IEEE Communications Magazine*, pp 42-49, Dec. 1998.

[Zirn98] M. Zirngibl, "Multifrequency lasers and applications in WDM networks," *IEEE Communications Magazine*, pp 39-41, Dec. 1998.

CHAPTER 2

WDM-Based Optical Access Networks – An Overview

2.1 Introduction

Over the last two decades, several configurations for WDMOANs have emerged, uncovering various issues involved in deriving the benefits of a dedicated wavelength per ONU. Most of the early studies on access networks focused more on the traffic aggregation issues of the feeder segment compared to the distribution segment [SaSi99] and mainly targeted corporate user premises [MoBa99]. One of the early WDMOAN architectures which supported dedicated wavelengths per every ONU was proposed by Modiano et. al. [MoBa00] which employed a ring-on-stars topology with the ONUs equipped with elaborate transceiver units. The distribution segment was configured generally in a star topology with the hub located in the AN collocated with the CO as shown in Fig.2.1. The AN was designed to handle data traffic within the local cluster all-optically through a passive star coupler (PSC) and the inter-cluster (between clusters) traffic through OEO conversion mechanisms. In fact way back in 1989, Wagner *et al.* conducted an experimental demonstration on passive photonic loop architectures using 16-channel AWG-router in a double-star configuration [WaLe89]. Their study established the fact that a significant amount of cost-reduction can be achieved as compared to the dedicated fiber connectivity to a residential user or a small business customer.

In subsequently proposed WDMOAN[1] configurations, the distribution node was separated from the AN, brought closer to the user premises and was called RN. The ONUs had a point-to-multipoint connectivity to the RN with either a star or more suitably a tree topology. The main objective driving this change has been presumably to enable WDM-based access network deployments as cost-effective as possible through passive

[1] Thus WDMOAN and WDMPON became eventually synonymous with WDMPONs referred more popularly to imply the passive tree topologies.

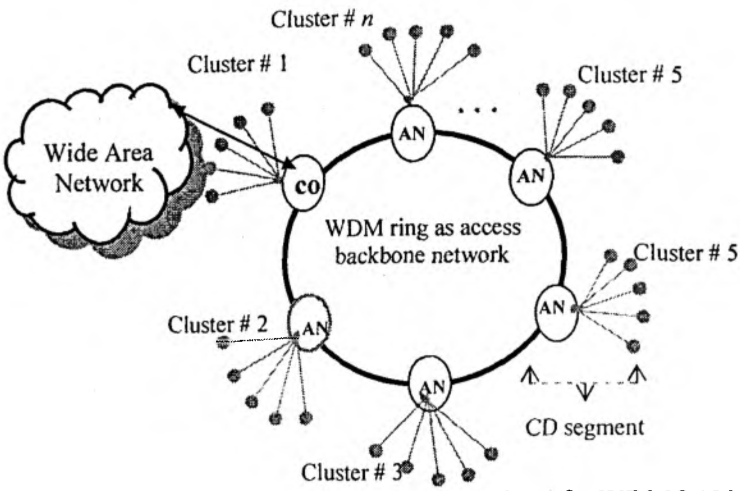

Fig. 2.1. Typical Network Configuration of a WDMOAN

distribution and increased sharing with branched connectivity. Thus topologically the ring-on-star based architecture gave way to the tree-based configurations so that more and more users can be connected with minimal fiber laying overhead per user. As a consequence, the transceiver and MAC units (of erstwhile AN) constituted the OLT which along with the distribution portion between OLT and ONUs came to be known as a WDM passive optical network (WDMPON). With time, the distribution segment in a PON grew in size and the attendant implementation issues drew considerable attention from the research community [FMDP94] and [ZJSK95]. Accordingly several WDMPON architectures were proposed and studied experimentally as well as analytically for their cost effectiveness, efficiency and scalability. In our subsequent discussion, we consider some important aspects of WDMPONs and mention briefly the reported work on each aspect as evident through recent literature.

Deployment point of view, the intervening portion between the OLT and the ONUs also called the optical distribution network (ODN), is crucial for a WDMPON. An ODN fabric consists of a branching device whose input port is joined to the OLT through a relatively long and shared fiber segment and output ports are connected to the ONUs through distribution fibers. The branching device accomplishes channel separation using either power splitters and/or wavelength routing devices. For small split-ratios (<16), power-splitter based RNs are adequate whereas for higher split-ratios, router based remote nodes [BaFM98] offer better technical advantages. Thus we have two categories of WDMPONs, based on the type of ODN employed.

Power Splitter-based WDMPONs

Typically a power splitter-based PON (PSPON) employs 1 × *N* transmissive passive star coupler (PSC) in the RN to distribute the signal power entering the input port into *N* output ports. Thus the RN distributes/collects the data channels in a broadcast-select mode. Most of the early PSPON configurations were coarse WDMPONs, which employed WDM only to distinguish upstream and downstream transmissions with widely separated transmission windows as shown in Fig. 2.2a. Such coarse WDMPONs used TDM/TDMA transmission to distinguish the data channels. For instance in APONs and BPONs the desired channel is identified and selected through either ATM cell header or the time-slot depending upon the type of protocol used [Itut98].

On the other hand, in regular WDMPONs [MoBa00], the channels are identified by their carrier wavelengths and selected through tunable transceivers. This mechanism might make upstream transmission expensive for the ONUs. For this reason, more economical PSPON configurations employ single carrier transmitters in the ONUs and burst-mode receivers in the OLT while using a TDMA protocol for the upstream. Main advantage of a PSPON is that, depending upon the communication requirements, an ONU can dynamically

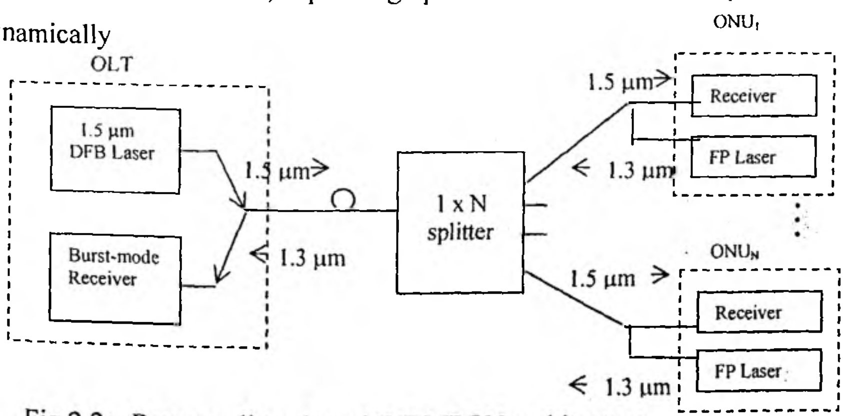

Fig.2.2a. Power splitter-based WDMPON architecture

vary its share of bandwidth on a upstream/downstream channel simply by increasing its usage slots without the need for any allocation algorithm. As long as no single ONU grabs unduly large portions of bandwidth, this feature helps in increasing the provisioning aspect of a PON. Further PSPONs offer service providers, the flexibility to determine the split ratio at a particular deployment site without affecting the ONU transceiver design [FHJZ98]. However since the line rate is shared amongst the ONUs, scalability of such configurations is limited in terms of user-bandwidth and power budget (due to splitting loss).

Hybrid PONs based on WDM/SCM, WDM/TDM and WDM/OCDM employ PSCs along with routing devices in multi-stage RN configurations. In such networks relatively high overall user-counts are achieved, by operating each PSC (with low port-counts) on a different optical carrier, which are multiplexed/demultiplexed through a wavelength router. The broadcast nature of PSPONs is not only ideal for delivering community services in downstream channels, but can also be used for sending control channel information to coordinate the upstream transmissions [MoBa99] .

Wavelength Router-based WDMPONs

Switched type of service distribution can be implemented by employing wavelength router-based PONs. Dispersive devices like AWG are most extensively used in the RN configurations of such PONs, as evident from the literature [FMDP94], [ZJSK95]. AWGs have many desirable attributes of a distribution node like fixed insertion loss (~6 dB) and good crosstalk performance (35 to30 dB) irrespective of port count. In such PONs two important properties of an AWG viz., free spectral range (FSR) and coarseness, are extensively exploited for enhancing the network connectivity pattern. FSR is the periodicity with which higher order frequencies on the WDM grid are routed to the same output port.

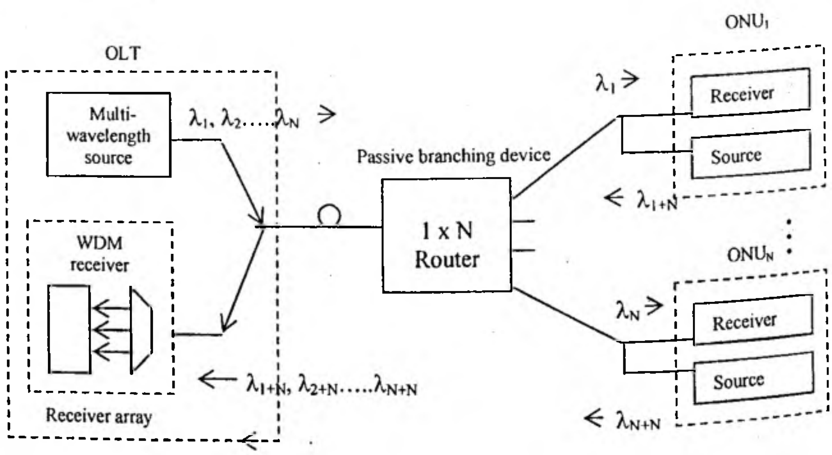

Fig.2.2b. Routed-based WDMPON architecture

Coarseness of an AWG determines the number of contiguously routed channels to an output port.

With appropriately chosen value of coarseness, desired number of channels can dropped at each output port and the rest passed on to the next stage of distribution.

Similarly, FSR of an AWG can be used to separate upstream and downstream transmissions on a single distribution fiber between an OLT-ONU pair, as shown in Fig.2.2b. FSR and coarseness have also been usefully exploited in multi-stage PON configurations to study the optimum connectivity pattern between a large number of users with an overall utilization of optical bandwidth [MMPS01]. Multiple FSRs have been successfully utilized in realizing multiple cascaded stages of AWG-based RNs which can serve a very large number of ONUs with reduced mean delay and increased throughput [MaRW03]. Parker *et al.* exploited the cyclic properties (FSR) of AWG in a three stage PON through active and passive coarse AWGs to offer bidirectional addressing to up to 6912 customers using only 24 wavelengths [PaFW98].

Kazovsky *et al.*, proposed and examined some network architectures which can support the existing TDM-based PON services [AKGK04] while being readily upgradeable to WDM-based PON configurations. WDM techniques are used to separate the upgraded and the prevalent signal traffic with sufficient guard band to avoid crosstalk. The RN is a combination of AWG and PSC which seamlessly connects the users to all available network services. In yet another study, as reported by Fan *et al.*, both AWG and PSC can be deployed in a parallel combination to achieve improved throughput-delay performance and protection against single point failures (as in the RN) [FaMR04]. In order to save on wavelength resources which are divided between upstream and downstream directions, same set of wavelengths have been spatially reused on separate fibers in some PONs like RITENET. Though this significantly reduces the inventory problem for the transceivers and very little additional loss due to doubled port-count, this approach incurs fiber-laying costs and fault-diagnosis problems in the outside plant.

2.2 Subsystems and Devices

Next, we consider the building blocks of WDMPONs, viz., the subsystems and the devices that are employed in the end terminals. We briefly discuss their salient features and review the relevant technology developments. A comprehensive report on the system requirements, device and manufacturing technologies for state-of the-art FTTx solutions was given by Huang *et al.* in [HLXL07].

Remote Nodes

We focus our discussion more on AWG-based RNs as they are very popular choice for WDMPONs. Wavelength granularity in the distribution segment of wavelength-routed networks was made possible with the advent of AWG. AWG is advantageous for high channel counts (>16), amenable to monolithic integration (both Si-based and InP based) and is currently available in planar lightwave circuit form. Major network configurations based on AWG-routers have been extensively reviewed by Banerjee *et al.* in [BaFM98].

Several experimental and theoretical studies were carried out since Smit's work on AWG functionality [Smit88]. AWGs were continuously worked upon by various R&D groups world over, for improved frequency response in pass bands, minimal polarization

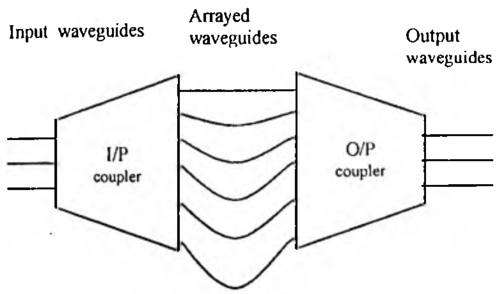

Fig. 2.3. Arrayed Waveguide Grating

mode dispersion loss, temperature independence etc. [KGYO99]. Temperature-controlled athermal AWGs eliminate the necessity for monitoring wavelength shift in the RN (which is located outdoors) and make the distribution system very reliable. There are several component manufacturers, offering athermal AWGs with 40 channels and 6 dB insertion losses as off-the-shelf products [Ligh07]. Parker, *et al.*, carried out studies on transform techniques which help in the designing flat pass bands (over 30% of the FSR) for AWG-based routers [PaWa99]. AWGs are amenable to monolithic integration using silica waveguide technology to realize planar lightwave circuits (PLCs). However the birefringence of the waveguides in PLCs makes the AWG polarization sensitive. Experimental studies were carried out to overcome this problem through a compensation technique in the etching process, which improves mutual coupling of array waveguides [NWLM99]. This technique enabled them to realize polarization insensitive, low-loss (4.5 dB) and adiabatic (temperature independent) AWGs with cross-talk levels as low as 40 dB. Other efforts directed towards crosstalk reduction suggested the use of cascade-connection of integrated band-pass AWGs to the original AWG, to implement AWGs with extremely low crosstalk levels of < 80 dB [KKIH05]. InP-based AWGs have good potential to integrate with other active devices (like detector and lasers) in the chip fabrication process, but are subject to coupling losses. Zirngibl *et al.*, demonstrated a 15 × 15 AWG on InP with an FSR of 10.5 nm and channel spacing of 0.7 nm in the 1550 nm region. The on-chip insertion loss was only 2-4 dB and the residual cross talk better than 25 dB [ZiDJ92].

PSCs have traditionally been used in most of the early RN implementations, as they were low-cost and readily available. In spite of their splitting losses, PSC-based RNs do not as yet have a clear alternative for carrying broadcast and select based transmissions in PONs. They are used in combination with AWGs to realize hybrid RNs to support WDM-TDM PON, wherein the individual strengths of both the devices are appropriately utilized [SJSS05].

Optical Transceivers

Transmitter/receiver (or transceiver) sections are crucial for the design of any communication link, as they ultimately determine the link power budget. Typically Class-B PONs (which are most common), have a power budget of 20-25 dB. Transceivers have the ability to compensate for signal impairments accumulated in the fiber channel by proper choice of system parameters (transmitter power and receiver sensitivity). On the other side, non-ideal nature of the same transceiver alone can cause power penalties apart from other impairments like laser relative intensity noise (RIN), group velocity dispersion, multi path interference, mode partition noise, modal noise and modal dispersion [HLXL07]. Non-linearity effects will surface mostly for analog video channels via self-phase and cross-phase modulation. Depending on the geographical distance of the link involved (from OLT to ONU), the effect of each of these factors will be different on the relevant channel quality. When burst-mode operation is considered in the upstream channels, the laser bias and modulation current must be adjusted with care. Here sensitivity, dynamic range and response time of the receiver are of paramount importance, for high speed data transfer.

Tunable transmitters and receivers are more appropriate for the OLT compared to ONU due to cost concerns. Traditional tuning mechanisms like external cavity tuning and multi-section tuning [WoLA07] have their respective limitations related to tuning speeds (msec range in external cavity) and tuning ranges (a few nm in multi-section DFB lasers). Vertical cavity surface emitting lasers (VCSELs) are gaining popularity for their tuning speeds of a few μs and tuning range of 10-20 nm. The tuning mechanism is based on a micro-electromechanical system structure and can be operated in both 1.3 μm and 1.5 μm wavelength regions. Tunable receivers are generally realized using a tunable optical filter in front of a broadband photodetector. New integrated CMOS devices based on metal-oxide semiconductor have also been reported, which offer nanosecond speed receivers for both 1550- and 850-nm systems [CCMH05].

2.3 MAC Protocols and Scheduling

The role of MAC layer has been predominantly arbitration of access amongst several simultaneous users in the upstream with minimal contention. With the advent of EPON standard, research efforts were intensified for improving the bandwidth efficiency of IP-traffic-carrying TDM PONs. In this direction, Kramer *et al.* employed interleaved polling to introduce dynamic bandwidth allocation (DBA) amongst the ONUs. While DBA issue is limited to scheduling upstream transmissions on a single wavelength in TDMPONs, in a WDMPON, it should take into account different wavelengths allocated for upstream transmissions. Recently online scheduling methods were suggested for the WDM upgrade of EPON to achieve lower delays at higher loads [McRe06]. In WDMPONs, since each ONU's transmissions are on distinct wavelength channels, MAC protocols and scheduling algorithms are employed mostly for either addressing scalability aspects or incorporating QoS issues. For instance, a scheduler-based access node in [MoBa00] coordinates the inbound and outbound traffic to support unsynchronized communication. Further the MAC protocol includes 'look-ahead' feature in the scheduling algorithm, to overcome receiver contention. Kamiyama incorporated collision avoidance schemes in the MAC layer to contain packet collisions in PSCs, which are deployed between the AWGs and the user nodes for a scalable configuration [Kami05]. For AWG-based wavelength-routed WDMPONs, Spencer *et al.*, proposed a MAC protocol which does not need a centralized controller at the OLT [SpSo00]. Every ONU operates on WDM request/allocate protocol called WRAP, through in-band signaling. They studied and compared the performance of different allocation algorithms under the protocol for finding the suitability of each under heavy to light loads of data traffic.

In order to guarantee fairness between upstream and downstream traffic and provide efficient communication between OLT and ONUs, scheduling algorithms were executed based on time-bound batch frames, so that the data frame with earliest departure time is scheduled first [KKIH05]. This improved the operational efficiency of the centrally tunable sources at the OLT. In their study [BoJK05], the authors proposed a MAC protocol for AWG-based networks which used OEO conversion to prioritize virtual output queues to realize QoS. Spatial wavelength reuse property of AWG is utilized to send both control channel and data channel information simultaneously to all ONUs. Wide-area network (WAN) technology like optical burst switching was investigated for handling high-speed, bursty, IP traffic in PONs in a recent study [SeVP07]. By aggregating the data frames into bursts, provides ample scope for the OLT to carry on scheduling exercise with less number of constraints. This also indicates the possibility of the transparent integration of WANs with PONs in near future through optical packet switching.

2.4 Resource Management

Operational efficiency of a WDMPON deployment depends on the way available resources are managed, without sacrificing the service quality. According to one study, 80% of a customer's bill is determined by the ONU cost. For this reason, most of the research efforts in WDMPON have been towards reducing the cost of ONU, especially the transmitter section. In the downstream, WDMPON systems used either simultaneous (multi-wavelength source) transmission or bit-interleaved (chirped pulse source) transmission.

One of the earliest WDMPON configurations to address the resource management issue was, RITENET which employed re-modulation techniques on continuous optical bursts, sent from the OLT on downstream channels. However this arrangement increased the RIN due to lower laser extinction ratio and beat noise, both of which affect the signal quality of the existing downstream transmissions. Further an external modulator at each ONU cannot be a cost-effective solution until the relevant device technology becomes more matured.

Research efforts were oriented towards making the transceiver simpler and low-cost by developing colorless or wavelength-selection free ONUs in order to overcome the inventory problem. Several techniques have been demonstrated, such as, spectral-sliced broadband light source, injection-locked FP lasers and reflective semiconductor optical amplifiers (RSOA). These devices were utilized to generate the optical carrier power from a centralized site (either OLT or RN) whose cost can be shared. Since the device can be wavelength-tuned by external means through injected signals, resources can be optimally provisioned.

Another attempt came from Jung *et al.* [JSLC98], who employed spectral-sliced broadband spectrum of an 1.5 μm LED for upstream transmissions and spectral-sliced amplified spontaneous emission from a fiber amplifier for downstream transmissions. Bandpass filters and Erbium-doped fiber amplifier (EDFA) were deployed in the OLT, to ensure that the passband is within the FSR of the AWG and also to compensate for the optical power loss due to slicing (about 10 dB). However crosstalk and loss in spectral-sliced signals were found to be too high for access systems, unless power equalization of received signals is done [Feld97].

In [CCTC02], each ONU used a low-cost Fabry-Perot (FP) laser which was injection-locked with the downstream wavelength and then directly modulated with upstream data. Under certain operating conditions, the original data on the downstream wavelength is largely suppressed so that a single wavelength manages the up-link and down-link traffic in a half-duplex mode. Another way of isolating the bidirectional traffic was to employ different modulation formats like optical frequency shift keying in downstream and ON-OFF keying in the upstream channels as reported in [DCCT03].

Subsequently RSOAs were deployed in the ONUs which played the role of both a modulator and an amplifier for upstream transmissions, on wavelength seeding them with spectral slices generated at the OLT [HTFM01]. Recently Wong *et al.*, reported the feasibility of a self-seeding RSOA which receives the seeding light from a reflected spectrum off an FBG device located at the RN [WoLA07] as shown in the block schematic of Fig.2.4. This arrangement not only relieves the hardware burden on the OLT, but also incurs less reflective path losses compared to the OLT-generated seeded

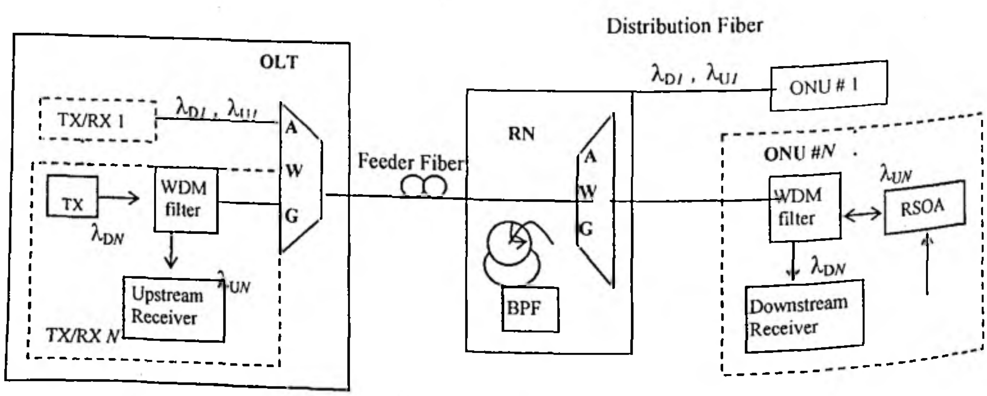

Fig.2.4. WDMPON architectures with colorless ONUs [WoLA07]

scheme, due to the relative proximity of the ONU. However, losses due to Rayleigh back-scatter have to be contained through circulators and isolators at the entry/exit points of the RN and ONUs. By using identical devices in user premises, the production costs reduce considerably. In another study as reported in [KaHa06], the RSOA remodulates the downstream light with a radio frequency sub-carrier, obviating the need for a separate seeding source from either OLT or RN. This results in a hybrid WDM/SCM PON which offers resources in both optical and microwave domain. We next consider some of the landmark testbed studies and field trials which took place in various parts of the globe in an attempt to find viability for WDMPON technology and systems.

2.5 Testbed Studies and Field Trials

Feasibility studies and field trials are indicative of the demand and acceptability for the technology in question. Several organizations and universities in different parts of the world participated in this development activity by forming various consortia and initiating research projects. Most of them employed purely passive architectures while some more ambitious projects included active configurations. We briefly discuss about the salient aspects of some such major studies.

LARNET

LARNET is an acronym for local access router network (mentioned earlier briefly) and is one of the first few model- architectures for WDMPON, which were proposed from AT&T labs. It employs broadband edge-emitting LED sources in the ONUs and multi-frequency laser in the OLT as shown in Fig.2.5. Upstream and downstream signals are separated by 1.3/1.5 μm WDM couplers. The downstream WDM signal carries the

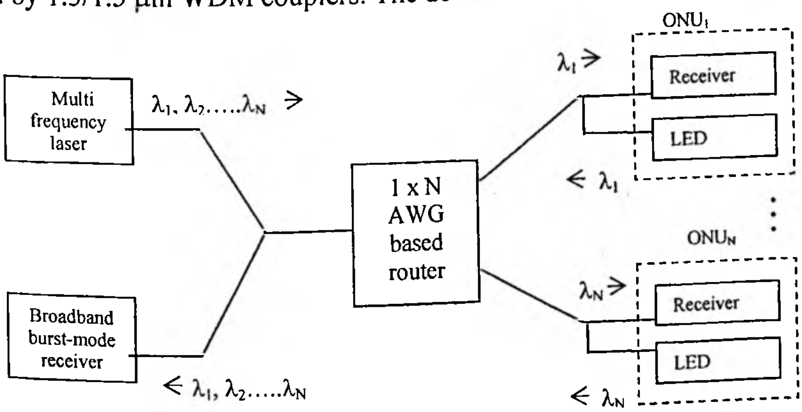

Fig.2.5. LARNET Architecture [ZJSK95]

information for the ONUs on N distinct wavelengths. In the upstream direction, modulated LED output spectrum is spliced at the AWG-RN ports. As a result the data generated at each ONU, reaches the OLT in distinct spectral portions of the 1.3 μm wavelength-window. The spectral slices arriving at the CO are demultiplexed with a second AWG and recovered by the receiver. Upstream channels are shared using a TDMA scheme and a burst-mode receiver at the OLT. The architecture is cost effective for moderate line rates with no serious beat noise effects between spliced spectral portions. However for longer distances (>15 Km), power budget for upstream transmissions becomes constrained due to accumulated spectral losses in two AWGs.

RITENet

RITENet or remote interrogation of terminal network avoids a separate transmitter at the ONU altogether [FMDP94]. The OLT consists of a tunable laser which uses the same optical carrier for generating downstream signal as well as for sending a burst of carrier power to the ONU for upstream transmission in a time-multiplexed manner. The ONU receivers are fixed-tuned photo-detectors to extract distinct downstream transmissions. Every ONU taps the optical burst from the incoming signal and utilizes it for generating its upstream transmission through a modulator. Since both upstream and downstream signals are on the same wavelength, their propagation paths are separated through fibers, as shown in Fig.2.6. As a result the RN split ratio is doubled but does not incur any significant additional loss due to AWG. A tunable receiver at the ONU is set to receive the upstream

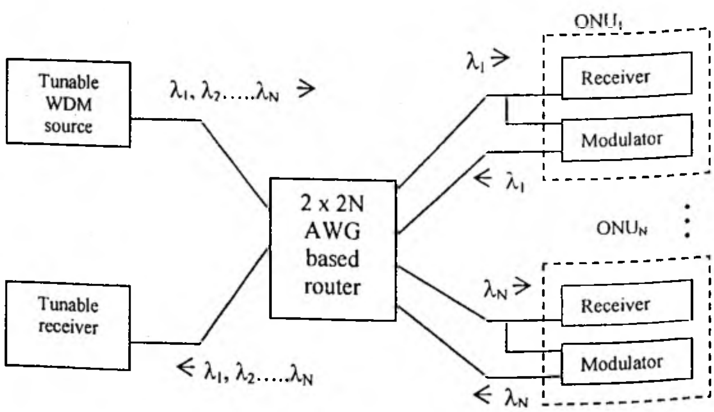

Fig.2.6. RITENET Architecture [FMDP94]

transmissions in a TDMA mode. With this architecture RITENET reduces the ONU costs considerably but is limited in scalability due to the round-trip power losses for the upstream signal. Further the overhead due to additional fiber-laying costs cannot be neglected in evaluating the overall network cost.

SuperPON:

SuperPON [VMVQ00] system was initiated under the auspices of European ACTS (advanced communication technology and services) project PLANET (photonic loop access network) with the intention to extend the capabilities of standard APON (ITU-T G.983). It supports a bit rate of 2.5 Gbps/311 Mbps (down/up), over a range of 100 km with a spitting factor of 1:2048.The downstream and upstream transmission speeds are shared by the ONUs in TDM-mode. EDFA in the downstream and gain-switchable semiconductor optical amplifiers (SOA) in the upstream are employed in the feeder and splitter junctions to boost the signal power as shown in Fig.2.8.

The scheduling and arbitrating functionalities of the OLT consist of maintaining virtual output queues for the access requests (from the ONUs) and sending permits to the ONUs. The MAC protocol uses cell scheduling algorithm to prioritize the queues and thus incorporates QoS for the TDM-based network. In this context, synchronization of the ONU transmissions becomes a challenging task for the Super PON. Further burst-mode transmission in the upstream direction becomes equally daunting and requires OLT receivers to support large dynamic range, high sensitivity and dynamic threshold setting (due to DC

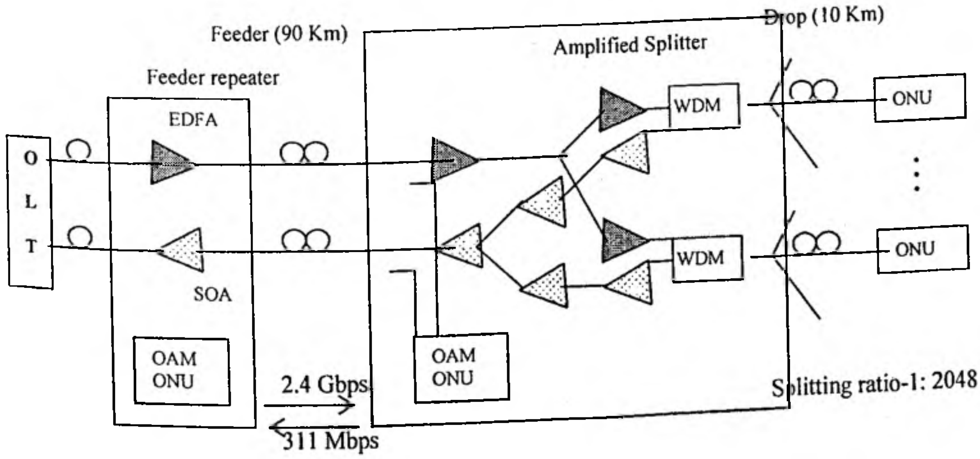

Fig.2.7 . The Super PON architecture [VMVQ00]

level variation). The demonstrator was presented in a European conference (ECOC'99) and connected to an all-optical core network (PELICAN–pan European lightwave core and access network) between Paris and Brussels for a successful feasibility study. It was learnt from the study that, in spite of overall reduction in operational and maintenance cost due to larger sharing, the component cost was still high and needed more mature technology to make the prototype widely acceptable for deployment.

SONATA

Another testbed study, called SONATA, was underway, which employed wavelength routers for service distribution, unlike the power splitter-based SuperPON. The project was under European Union's ACTS program and conducted studies on the access portion of a nation-wide network, employing static wavelength-routed PONs connected in a mesh topology [BLMN00].

It employed a combination of TDMA and WDMA mechanisms based on reservations to connect 400 PONs with 50,000 terminals per PON and 622 Mbps maximum rate per terminal. A passive wavelength-routing node supported 801 × 801 ports with an estimated throughput of 200 Tbps over a 1000 Km range. It allocated a specific timeslot-wavelength combination to the terminals (ONUs) upon their request. Every network terminal was equipped with a tunable transmitter/ receiver pair for data traffic and a fixed transmitter/

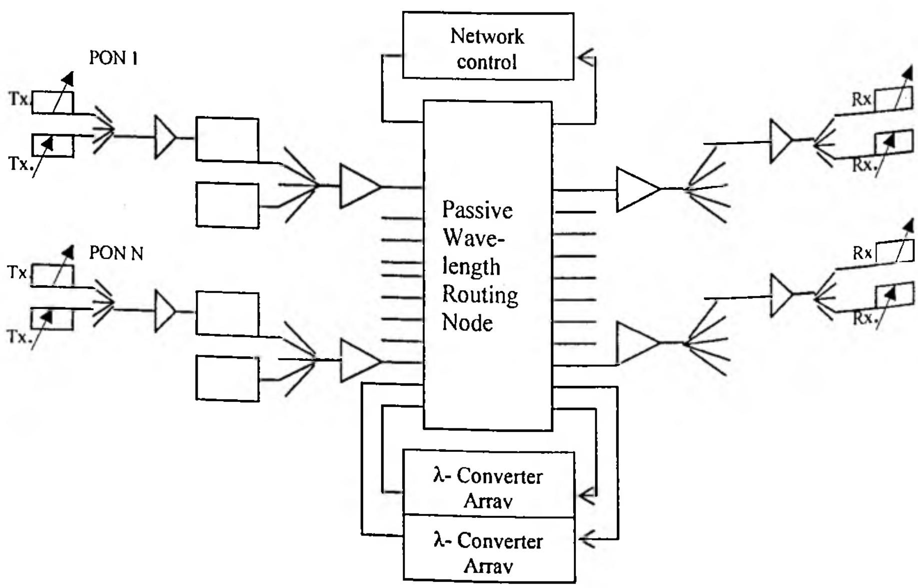

Fig. 2.8. SONATA network architecture [BLMN00]

receiver pair for signaling. Each PON shared the same wavelength for all its ONUs and so multicasting was possible within a PON. SONATA was an ambitious project with a centralized network controller managing the resource allocation procedures. Additional ports were available on the router for allocating capacity dynamically with actively controlled wavelength converter trays as shown in the figure. The centralized network controller employs exhaustive resource allocation algorithms and logical topology design models to carry the stupendous task. This project established the feasibility of passive network structure on a huge scale by incorporating both static and programmable components in a passive wavelength router.

NGI-ONRAMP

One of the first major initiatives to explore the viability of WDM OANs supporting the fast emerging IP-based traffic was taken by NGI-ONRAMP (next generation internet-optical network for regional access with multi-protocols) program through DARPA (defense advanced research projects agency) of USA. Its mission was to develop a reconfigurable WDM testbed and carry out the study of physical and network layer architectures for efficient traffic management. The architecture consisted of a feeder ring connecting several distribution segments through ANs. The testbed deployed reconfigurable ANs capable of

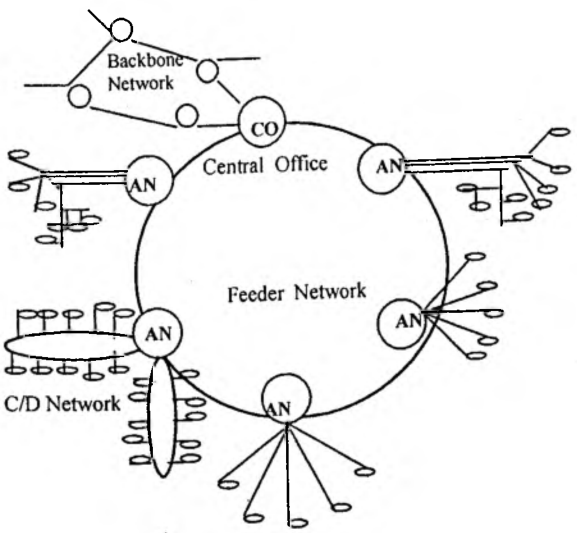

Fig.2.9. ONRAMP Architecture [FHRK00]

both all-optical and opaque switching to transport the IP traffic. The research focus in ONRAMP was more on exploiting the networking features of WDM through the AN than optimizing the cost of the distribution segment. The network incorporated several advanced features, like, logical topology reconfiguration, optical by-pass, protection switching and service restoration to support heterogeneous traffic formats through WDM-aware IP layer. Further, each node had a local network management station to control its components. With this set up the feeder covered 100 to 1000 square miles of geographical area with 10 to 20 nodes. Distribution network connected 100 or more business premises each with about 1 Gbps user data rate.

SUCCESS

In recent past, a testbed study was reported from Stanford University Access program (SUCCESS), which was developed to provide a smooth migratory path for existing PON configurations based on TDM towards futuristic architecture of a WDMPON. SUCCESS allows a user to be backward compatible with other users attached to TDMPONs while providing services on a dense WDMPON (DWDM PON). For this reason, the system incorporates both star couplers and AWGs in the RNs as shown in Fig.2.10. The network employs ring-on-stars topology like ONRAMP with the collector ring running through the RNs which are the centre of the stars. If RN is a PSC, one dedicated wavelength on DWDM grid is used for downstream transmissions from OLT and ONUs use a wavelength on the coarse-WDM (CWDM) grid for upstream transmissions. On the other hand, when RN employs an AWG, each ONU has a dedicated wavelength on the DWDM grid to communicate with OLT. The architecture employs fast tunable transmitters and receivers at the OLT which are shared by the ONUs. The OLT in addition to generating downstream data traffic, also provides continuous bursts of optical carrier power to the ONUs for upstream transmission, in a half-duplex mode [AKGK04]. The network achieves traffic balancing by integrating CWDM/TDM-based PONs serving about a 100 residential users and DWDM TDM-based stars serving about 60 corporations on single infrastructure. Data packet transmissions at a line rate of 1.25Gbps over a 22.5 km range were supported. Further, a MAC protocol based on batch scheduling algorithm was employed which allowed for priority queuing by scheduling the packet transmissions over multiple frames. This algorithm

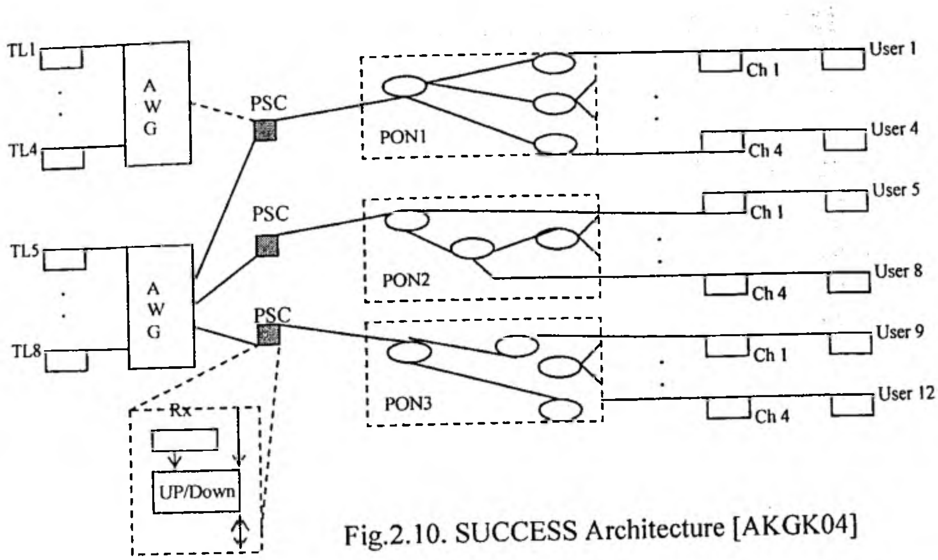

Fig.2.10. SUCCESS Architecture [AKGK04]

achieved efficient coordination of bidirectional transmissions between the OLT and ONUs, with relatively small number of transmitters and receivers. For example as shown in Fig. 2.10, 12 user transmissions can be scheduled using only 4 wavelengths through AWG/PSC RNs with the help of the algorithm.

2.6 Summary

In this chapter, we presented a comprehensive review of various research activities and technological developments in the area of WDMOANs/WDMPONs as reported from different parts of the world. We considered various aspects of its network architecture viz., network configurations, subsystems, resource management, MAC protocols etc., and outlined the state-of-art in each category. Finally we selected a few landmark testbed studies on WDMPONs and highlighted their salient features.

References

[AKGK04] F. T. An, K. S. Kim, D. Gutierrez, S. Yam, E. Hu, K. Shrikhande and L. G. Kazovsky, "SUCCESS: a next generation hybrid WDM/TDM optical access network architecture, *IEEE/OSA Journal of Lightwave Technology*, vol. 22, no. 11, Nov. 2004.

[BaFM98] D. Banerjee, J. Frank and B. Mukherjee, "Passive optical network architecture based on waveguide grating routers," *IEEE Journal on Selected Areas in Communications,* vol. 16, no. 7, Sept. 1998.

[BLMN00] A. Bianco, E. Leonardi, M. Mellia and F. Neri, "Network controller design for SONATA-A large-scale all-optical passive network," *IEEE Journal of*

Selected Areas in Communications, vol. 18, no. 10, pp. 2017–2028, Oct. 2000.

[BoJK05] A. Bohm, M. Johnson and K. Kunert, "AWG-based optoelectronic router with QoS support," Proceedings of *IEEE Conference, 2005.*

[BPCM05] A. Banerjee, Y. Park, F. Clarke, H. Song, S. Yang, G. Kramer K. Kim and B. Mukherjee, "Wavelength-division-multiplexed passive optical network (WDM-PON) technologies for broadband access: A Review," *OSA Journal of Optical Networking*, vol. 4, no.11, pp. 737–758, Nov. 2005.

[CCMH05] R. Chen, H. Chin, D. A. B. Miller, K. Ma and J. S. Harris Jr., "MSM-based integrated CMOS wavelength-tunable optical receiver," *IEEE Photonics Technology Letters*, vol.17, no. 6, 1271-1273, Jun. 2005.

[CCTC02] L. Y. Chan, C. K. Chan, D. T. K. Tong, F. Tong and L. K. Chen, "Upstream traffic transmitter using injection-locked Fabry Perot diode as modulator for WDM access networks," *Electronics Letters,* vol. 38, no. 1, Jan. 2002.

[Chan00] C. J. Chang-Hasnian, "Tunable VCSEL," *IEEE Journal of Selected Topics in Quantum Electronics*, vol. 6, no. 6, pp. 978-987, Nov./Dec. 2000

[DCCT03] N. Deng, C. K. Chan, C. K. Chan and F. Tong, "Data remodulation on downstream OFSK signal for upstream transmission in WDM passive optical network," *Electronics Letters*, vol. 39, no. 24, pp. 1741-1743, 2003.

[Feld97] R. D. Feldman, "Crosstalk and loss in wavelength division multiplexed systems employing spectral slicing," *IEEE/OSA Journal of Lightwave Technology*, vol.15, no.11, Nov. 1997.

[FHJZ98] R. D. Feldman, E. E. Harstead, S. Jiang, T. H. Wood and M. Zirngibl , "An Evaluation of architectures incorporating wavelength division multiplexing for broad-band fiber access," *IEEE/OSA Journal of Lightwave Technology*, vol. 16, no. 9, pp. 1546-1559, Sept. 1998.

[FHRK00] N. M. Froberg, S. R. Henio, H. G. Rao, B. K. Hazzard, S. Parikh, B. R. Romkey and M. Kuznetsov, "The NGI ONRAMP Test Bed: Reconfigurable WDM technology for next generation regional access networks," *IEEE/OSA Journal of Lightwave Technology*, vol.18, no.12, pp. 1697-1708, Dec. 2000.

[FMDP94] N. J. Frigo, P. D. Magill, T. E. Darcie, P. P. Iannone, M. M. Downs, B. N. Desai, U. Koren, T. L. Koch, C. Dragone and H. M. Presby, "RITENET: a passive optical network architecture based on the remote interrogation of terminal equipment," *Optical Fiber Communication Conference* (OFC'94) 1994.

[HTFM01] P. Healey, P. Townsend, C. Ford, L. Johnston, P, Townley, I. Lealman, L. Rivers, S. Perrin and R. Moore, "Spectral slicing WDM-PON using wavelength-seeded reflective SOAs," *Electronics Letters*, vol. 37, no. 19, Sept. 2001.

[HLXL07] W. P. Huang, X. Li, C-Q. Xu, X. Hong, C. Xu and W. Liang, "Optical transceivers for fiber-to-the-premises applications: System requirements and enabling technologies," *IEEE/OSA Journal of Lightwave Technology*, vol.25, no.1, Jan. 2007.

[Itut98] ITU-T Rec. G.983, Draft D, Feb. 1988.

[JSLC98] D. K. Jung, S. K. Shin, C. H. Lee, and Y. C. Chung, "Wavelength-division-multiplexed passive optical network based on spectrum slicing techniques," *IEEE Photonics Technology Letters*, vol.10, no. 9, 1334-1336, Sept. 1998.

[KaHa06] J. M. Kang and S. K. Han, "A novel hybrid WDM/SCM-PON sharing wavelength for up- and down-link using reflective semiconductor optical amplifier," *IEEE Photonics Technology Letters*, vol. 18, no. 3, 502-504, Feb. 2006.

[KFHC00] M. Kuznetzov, N. M. Froberg, S. R. Henion, H. G. Rao, J. Korn, K. A. Rauschenbach, E. H. Modiano and W. S. Chan, "Next-generation optical access networks," *IEEE Communications Magazine*, pp.66-72, Jan. 2000.

[KGTK05] K. S. Kim, D. Gutierrez, F. Tai and L. G. Kazovsky, "Design and performance analysis of scheduling algorithms for WDMPON under SUCCESS-HPON architecture," *IEEE/OSA Journal of Lightwave Technology*, vol. 23, no. 11, pp. 3716-3731, Nov. 2005.

[KGYO99] A. Kaneko, T. Goh, H. Yamada, T. Tanaka and I. Ogawa, "Design and applications of silica-based planar lightwave circuits," *IEEE Journal of Selected Topics in Quantum Electronics*, vol.5, no. 5, pp. 1227-1236, Sept./Oct. 1999.

[KITF01] J. Kani, K. Iwatsuki, N. Takachio and N. Fujii, " A simple broad-band coherence multiplexed optical access network and its scalability," *IEEE/OSA Journal of Lightwave Technology*, vol. 19, no. 4, pp. 456-464, Nov. 2001.

[KKIH05] S. Kamei, A. Kaneko, M. Ishii, T. Shibata, y. Inoue and Y. Hibino, "Crosstalk reduction in arrayed waveguide grating multiplexer/demultiplexer using cascade connection," *IEEE/*OSA *Journal of Lightwave Technology*, vol.23, no. 5, pp.1929-1938, May 2005.

[Ligh07] http://www.lightwave.com/

[MaRW03] M. Maier, M. Reisslen, Adam Wolisz, "A hybrid MAC protocol for a metro WDM network using multiple free spectral ranges of an arrayed wave guide grating," *Computer Networks*, 41 (2003) 407-433.

[McRe06] M. P. McGarry and M. Reisslein, "WDM Ethernet passive optical networks," IEEE Optical Communications, pp. s18-S24, Feb. 2006.

[MoBa99] E. Modiano and R. Barry, "Architectural considerations in the design of WDM-based optical access networks, *Computer Networks*, vol.31, pp. 327-341, Feb. 1999

[MMPS01] G. Maier, M. Martinelli, A. Pattavina and E. Salvadori, "Design and cost performance of the multistage WDM-PON access networks," *IEEE/*OSA Journal of Lightwave Technology, vol. 18, no.2, pp. 125-143, Feb. 2000.

[NWLM99]C. K. Nadler, E. K. Wildermuth, M. Lanker, W. Hunziker and H. Melchior, "Polarization sensitive, low-loss,low-crosstalk wavelength multiplexer modules," *IEEE Journal of Selected Topics in Quantum Electronics*, vol.5, no. 5, pp. 1379-1384, Sept./Oct. 1999.

[PaWa99] M. C. Parker and S. D. Walker, "Design of arrayed-waveguide gratings using hybrid Fourier-Fresnel transform techniques," *IEEE Journal of Selected Topics in Quantum Electronics*, vol.5, no. 5, pp. 1379-1384, Sept./Oct. 1999.

[PLJS04] S. J. Park, C. H. Lee, K. T. Jeong, H. J. Park, J. G. Ahn and K. H. Song, "Fiber-to-the-home services based on wavelength-division-multiplexing passive optical network," *IEEE/OSA Journal of Lightwave Technology*, vol. 22, no.11, pp. 2582-2591, Nov. 2004.

[PaFW98] M. C. Parker, F. Farjady and S. D. Walker, "Wavelength-tolerant optical access architectures featuring N-dimensional addressing and cascaded arrayed waveguide gratings," *IEEE/OSA Journal of Lightwave Technology*, vol. 16, no. 12, pp. 2296-2302, Dec. 1998.

[RaSi98] R. Ramaswami and K. N. Sivarajan, "*Optical Networks- A practical perspective*," Morgan and Kaufmann Inc., 1998 edition.

[SaSi99] A. A. M. Saleh and J. M. Simmons, Architectural principles of optical regional and metropolitan access networks, *IEEE/OSA Journal of Lightwave Technology*, vol. 17, no. 12, pp. 2431-2448, Dec. 1999.

[SeSP07] J. Segarra, V. Sales and J. Prat, "All optical-access metro interface for hybrid WDM\TDM PON based on OBS," *IEEE/OSA Journal of Lightwave Technology*, vol. 25, no.4, pp. 1002-1016, Apr. 2007.

[SeVP07] J. Segarra, V. Sales and J. Prat, "An all-optical access-metro interface for hybrid WDM/TDM PON based on OBS," *IEEE*/OSA Journal of Lightwave Technology,
vol. 25, no.4, pp. 1002-1016, Apr. 2007.

[SJSS05] D. J. Shin, D. K. Jung, H. S. Shin, J. W. Kwon, S. Hwang, Y. Oh and C. Shim, "Hybrid WDM/TDM PON with wavelength-selection-free transmitters," *IEEE*/OSA Journal of Lightwave Technology, vol. 23, no.1, pp. 187-195, Jan. 2005.

[SpSo00] M. J. Spencer and M. A. Sommerfield, "WRAP: a medium access control protocol for wavelength-routed passive optical networks," *IEEE*/OSA *Journal of Lightwave Technology*, vol.18, no. 12, pp.1657-1676, Dec. 2000.

[VMVQ00] I. V. Voorde, C.M. Martin, J. Vandewege and X. Z. Qiu, "The Super PON demonstrator: An exploration of possible evolution paths for Optical Access Networks," *IEEE Communication Magazine*, pp.74-82, Feb. 2000.

[WaLe89] S. S. Wagner and H. L. Lemberg, "Technology and system issues for a WDM-based fiber loop architecture," *IEEE/OSA Journal of Lightwave Technology*, vol. 7, no. 11, pp. 1759-1768, Nov. 1989.

[WoLA07]E. Wong, K. L. Lee and T. B. Anderson, "Directly modulated self-seeding reflective semiconductor optical amplifiers as colorless transmitters in wavelength division multiplexed passive optical network," *IEEE/OSA Journal of Lightwave Technology*, vol. 15, no. 1, pp. 67-74, Jan.2007.

[ZiDJ92] M. Zirngibl, C. Dragone and C. H. Joyner, "Demonstration of a 15 x 15 arrayed waveguide multiplexer on InP," *IEEE Photonics Technology Letters*, 4, 1250-1253, Nov. 1992.

[ZJSK95] M. Zirngibl, C. H. Joyner, L. W. Stulz, C. Dragone, H. M. Presby and I. P. Kaminow, "LARNET, a local access router network," *IEEE Photonics Technology Letters*, 7, 215-217 (1995).

CHAPTER 3

MAC Protocols for a WDMOAN with Ring-on-Stars Topology

3.1 Introduction

WDMOANs have the capability to support high-bandwidth services such as videoconferencing, video-on-demand, high-definition TV, graphics-intensive interactive games and distributed computing which in turn have the potential to generate sizable revenues for the network operators and service providers. The targeted user-premises for such applications generally consists of either a multi-storey dwelling, a commercial complex, a campus LAN or a business house who can share the associated cost of rather high-end WDM transceivers located in the ONUs. In order to keep the revenues flowing in, present day telecom service sector needs to introduce flexible service provisioning and dynamic resource-allocation schemes with QoS guarantees in the OANs. WDMOANs are capable of taking this challenge, while serving as fault tolerant future network-upgrades for "last mile" solutions. In order to provide QoS-aware services, they need to employ suitable coordination schemes and scheduling algorithms in the MAC layer, to meet the demands of a particular application.

MAC protocols play a very important role in WDMOANs, where the available wavelengths have to be optimally utilized for carrying both data transmissions as well as control information for proper coordination between the OLT and the ONUs. In order to increase the throughput in data channels, the contention in control channels needs to be minimized. This might require more wavelengths for handling the access requests from the ONUs. At the same time any amount of reduction in wavelength count for data channels can affect the network scalability at the cost of improved network performance. Further, in order to differentiate between real time (voice and video) and non-real time (data) services, appropriate scheduling algorithms should be incorporated in the MAC protocol. Several studies were reported on access protocols in high-speed optical LANs using passive star topology [HaKS87], [JiMu92] and [Mehr90]. They mainly focused on contention reduction aspects in the control channels and receivers for data traffic. One of the first studies to address the multicast issues in a broadcast-and-select WDMOAN was from [Modi98] for an asynchronous communication. Over a short span OANs adopted router-based architectures which have different issues to deal at the MAC layer, a brief review for which we provided in Chapter 2.

A WDMOAN might employ, in general, a hierarchical connectivity consisting of several collection and distribution (CD) segments interconnected by an access backbone (called feeder segment). As the name implies, a CD segment is a cluster of several ONUs, and usually interconnected with a star or a tree topology to an OLT. Thus, each OLT would provide services to (through the respective ONUs) several clusters of closely located subscribers who have high bandwidth requirements. In the early configurations of OAN, AN was in the place of OLT with some additional functionality to coordinate all the transmissions into and out of the OAN. In this chapter, we consider some additional functionality for the node and hence use the earlier terminology (i.e., AN) for OLT.

The access backbone network may connect the individual CD clusters using a bus/ring topology through their respective ANs to the regional servers/databases and to higher levels of network hierarchy. A star-based architecture employing passive power-splitters is optimum for an access network of moderate size (10-20 ONUs) with short spans (a few kms, typically), in which distribution of downstream (video distribution, typically) channels to a small group of ONUs is the main objective. For larger size CD segments, with medium- to long-reach spans (10-20 km), tree topology would prove more cost effective. Such realization of OANs with tree topology usually employs a remote node (RN) in between AN and the cluster of ONUs, wherein an RN uses a passive star coupler for collection/distribution of upstream/downstream traffic. Power budget of such OANs can be further trimmed by using arrayed-waveguide grating (AWG) as passive wavelength router in an RN. In both cases (i.e., star or tree topology) the passive transmission portion of the CD segment between the OLT/ AN and the ONUs is called PON, which is cheaper and easier to maintain. The ONUs in a CD segment might use various multiplexing techniques, viz., TDM, WDM, SCM, as well as several medium-access control (MAC) techniques, viz., TDMA, WDMA and OCDMA on their downstream/upstream transmissions. In this chapter, we consider only star-coupler based distribution segment for OAN employing WDM/WDMA techniques. Router-based PONs are considered in subsequent chapters.

When an access network has to support interactive services while carrying considerable upstream TPS (triple play service) traffic, the ANs need to be active, with optical/electronic/optical (O-E-O) conversion. This ensures QoS-based bandwidth management with priorities for real-time service traffic. The requisite signal processing and buffer management functions have to be carried out in the electronic domain. Generally a MAC

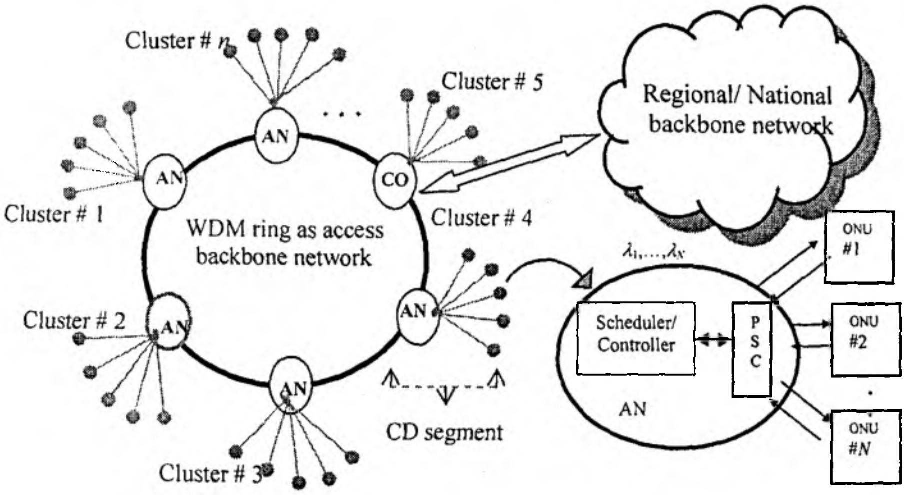

Fig.3.1. A WDM-based optical access network with stars as local clusters inter connected by a backbone ring (AN: Access Node; CO: Central Office; PSC: Passive Star Coupler; ONU: Optical Network Unit)

scheduler unit collocated with the access node, addresses these functionalities [MoBa00]. The cost of multiple transceivers and additional processing and memory requirements of the active node is shared not only by the ONUs in the local cluster but also by ONUs of other clusters that are connected to the feeder backbone for carrying intercluster traffic.

In this chapter, we consider a two-level hierarchical WDMOAN as shown in Fig.3.1. Each CD segment is a star-configured WDMPON operating with a broadcast-and-select mechanism, where the ONUs belonging to the local cluster are connected to a star-coupler-based AN. The AN has a hybrid functionality. It employs passive communication (all optical) for intra-cluster data packets and active (O-E-O) communication for control packets. For intercluster traffic, communication is active for both data and control packets. A scheduler serves as an interface between CD and the feeder segments. It coordinates the intra-cluster traffic without any need for the user terminals to synchronize their transmissions. The scheduler is also responsible for carrying out priority queuing mechanisms while handling the inter-cluster traffic. The access backbone segment in this network is a wavelength-routed WDM ring which uses dedicated set of wavelengths for transporting the intercluster data streams.

The rest of the chapter is organized as follows. Section 3.2 describes the hierarchical network architecture and the proposed access node configuration. Section 3.3 deals with two modified MAC protocols for intracluster (within a CD-cluster) and intercluster communication (among the clusters). In Section 3.3, we describe and present the results on the performance of the two MAC protocols obtained through simulation and analytical modeling. Finally, Section 3.4 presents the summary of the work.

3.2 Network Configuration

We have considered a WDM-based optical access network with a two-level hierarchical topology comprising of a feeder ring at a higher level and several passive-star-based CD clusters at a lower level, as shown in Fig. 3.1. Each passive star-based AN can support a moderately-sized network (in terms of ONUs and link span). The power budget for some typical cases have been estimated and shown in Table.3.1. We have considered an average AN/OLT-ONU link span of 10 km, a fiber attenuation of 0.25 dB/km and PIN detectors in the ONU transceivers. The maximum number of ONUs that each star coupler-based AN can support at different data rates along with the available power budget (excluding attenuation and power splitting losses) has been evaluated. It is found that, for typical laser transmit powers between -2 to 0 dBm the maximum number of ONUs that can be supported varies between 17-27 at 155 Mbps and 7-11 at 622 Mbps for a power budget of 20 dB. For data rates beyond 1Gbps, both the link span and the power budget are reduced by about 50% with pin-FET receivers. Thus a cluster size of 25 ONUs at 155 Mbps and of 10 ONUs at 622 Mbps can be easily supported over the proposed OAN. For instance, if each ONU connects to about 10 users, the total number of users served by the CD cluster would be 250 and 100 for the two examples respectively.

It may be noted that, there are two types of traffic flow through the AN, viz., intracluster traffic (i.e., from one ONU at a user interface to another within a cluster) and intercluster traffic (i.e., between ONUs of different clusters through the access backbone). Intercluster traffic is further classified into two types: incoming and outgoing. As depicted in the figure, the scheduler located in the AN schedules both intracluster and intercluster traffic.

Proposed AN Configuration

In order to establish an efficient communication for broadband services in such a hierarchical access network, one needs to design an appropriate AN, which will oversee the communications within and between the clusters of the given access network. In view of this, we propose a configuration for the AN connected to each one of the clusters as shown in Fig. 3.3.

Each ONU is equipped with a fixed tuned transmitter (FT) at λ_C for issuing upstream control packets (access requests), and a fixed tuned receiver (FR) at λ_C', for receiving downstream control packets (access grants). In addition, the ONU has a tunable transmitter (TT) operating in the range $(\lambda_1,\ldots,\lambda_M,\ldots,\lambda_{M\cdot K})$ to send data and a tunable receiver (TR) to

Table.3.1. Power Budget Calculations for Various Data Rates and Cluster Sizes

S. No	Data Rate	OLT Transmit Power, P_{Tx}	Max. ONUs N_{ONU}	Power budget, dB ($P_{Tx} - P_{Rx}$ -10log$_{10}N_{ONU}$)
	155 Mbps (pinFET Rx Sens. P_{Rx}: -36dBm; 10 km)	-10 dBm	3	21.23
		-5 dBm	8	22.00
		-2 dBm	17	21.70
		0 dBm	27	21.69
2.	622 Mbps (pinFET Rx Sens. P_{Rx}: -32 dBm; 10 km)	-10 dBm	1	22.00
		-5 dBm	3	22.23
		-2 dBm	7	21.55
		0 dBm	11	21.59
3.	1.25 Gbps (pinFET Rx Sens. P_{Rx}: -26 dBm; 5 km)	-10 dBm	3	11.23
		-5 dBm	10	11.00
		-2 dBm	21	10.78
		0 dBm	33	10.81

receive data on wavelengths $(\lambda_1,\ldots,\lambda_M)$. The wavelengths $(\lambda_1,\ldots,\lambda_M)$ are assigned for intracluster data channels and can be broadcast directly (i.e., all-optical transmission) through the passive star-coupler, but only the destined ONU will select and receive the data. Acousto-optically and electro-optically tuned lasers provide typically 20 nm range with tuning times of tens of μs and are available at affordable price range. Further each ONU has a dual-fiber connectivity (to the AN), whose installation cost would be shared by several users for which the ONU serves as a concentration point.

For intracluster communication, control packets are converted into electrical domain and stored in the request queues $(Q_1,\ldots,Q_N)$ allocated for their respective source ONUs which are subsequently transmitted on a separate wavelength λ_C' at the appropriate time instants as governed by the synchronization process (ranging) for the respective ONUs (discussed later in Section 3.3.1). Furthermore, for the intracluster communication, although control packets undergo O-E-O conversion at AN, data packets reach from source ONU to destination ONU via AN with end-to-end all-optical transmission at an appropriate wavelength from the pool of data wavelengths ($\lambda_1,...,\lambda_M$). For intercluster communication, control packets enter a separate global queue (GQ) in the scheduler, and data packets undergo OEO conversion at

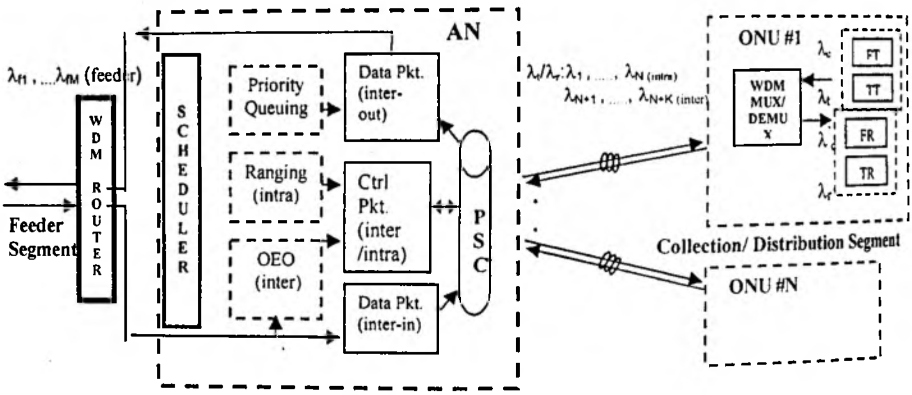

Fig. 3. 2. Block Schematic of Functional Blocks in WDMOAN
(FT/FR: Fixed tuned transmitter/ receiver; TT/TR: Tunable transmitter/ receiver)

the ANs of both source and destination CD clusters. As shown in Fig. 3.2, the module, termed as "scheduler" performs these functionalities with appropriate functional blocks.

The wavelengths ($\lambda_{M+1},...,\lambda_{M+K}$) are assigned to outgoing intercluster data packets for reaching the AN, of the local cluster. Subsequently, using the information in the control packets of the global queue, separate headers are generated for the outgoing traffic by header generator (HG), which are attached to their corresponding O/E converted data packets, as shown in the Fig. 3.3. It may be noted that the end-to-end delay for intercluster packets may be significantly more than that of intracluster traffic due to the access contentions experienced in local and destination clusters and also because of the queuing delays in buffers kept for intercluster scheduling. In view of this, we propose to divide the intercluster packets into real-time (RT) and non-real-time (NRT) categories with some judicious priority awarded to the RT category of intercluster packets. These packets are sorted into RT and NRT queues belonging to respective source ONUs, realizing QoS-based bandwidth management with priorities for RT services. The scheduler employs priority schemes (discussed in section 3.3.2) to order the RT/NRT

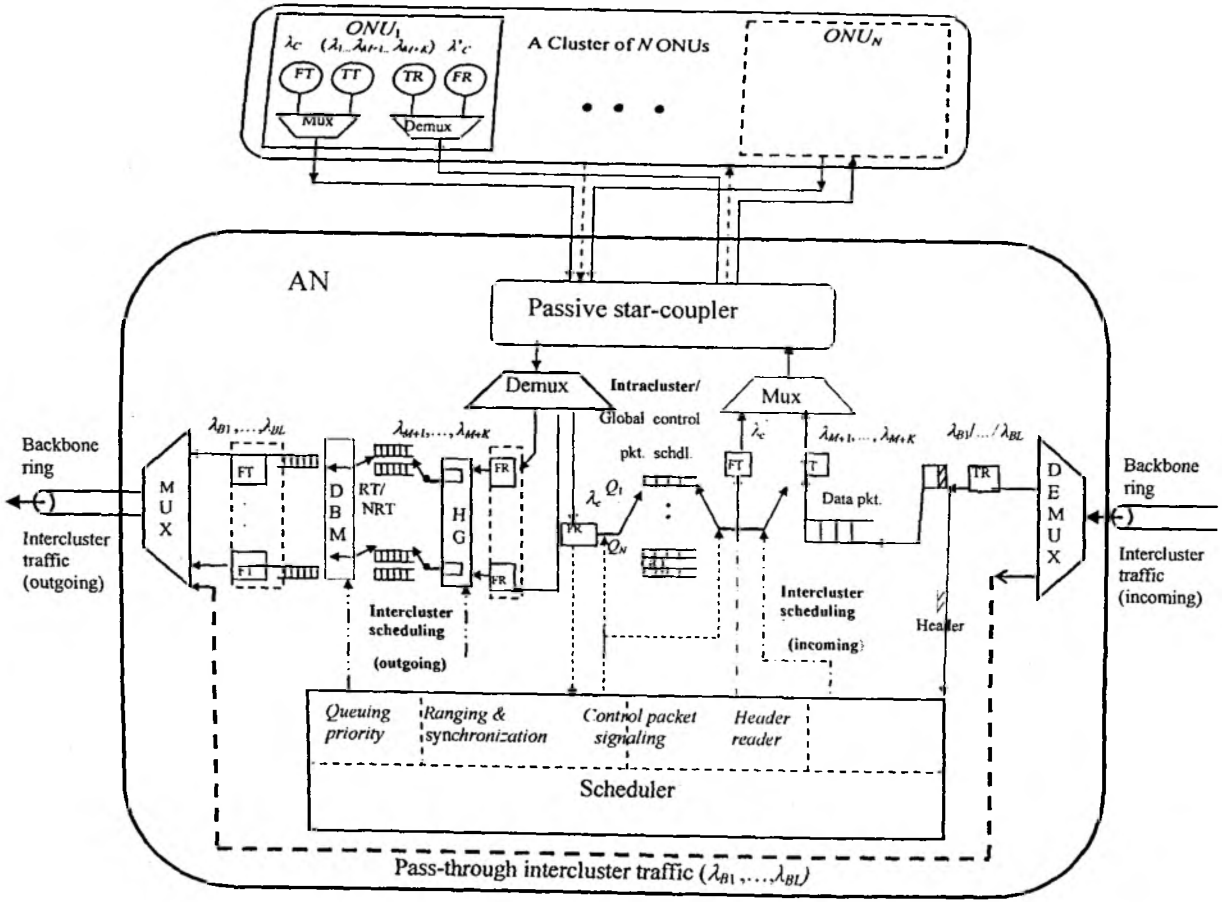

Fig. 3.3. Optical access node configuration (DBM: Dynamic bandwidth management; HG: Header generator; GQ: Global queue; Q: Cluster Queue RT:Real time; NRT: Non-real time) ——▶ Data path - - - -▶ Control path

packets and finally transmit them to the AN of the destined cluster on predetermined backbone wavelengths ($\lambda_{B1},...,\lambda_{BL}$), unique for a source-destination AN pair. The incoming traffic on rest of the wavelengths in the pool ($\lambda_{B1}, ...,\lambda_{BL}$), constitute the pass-through traffic meant for other destination ANs and are not processed at the intermediate ANs.

The incoming intercluster packet at the respective destination AN is stripped off its header (which goes into the header-reader block of the scheduler) and the payload packets are queued up as shown in Fig. 3.3. The scheduler uses the information from the header reader and signals for the issue of access grants on λ'_C for these packets. Subsequently queued data packets are mapped into wavelengths ($\lambda_{M+1},...,\lambda_{M+K}$) through OEO conversion and broadcast through the star-coupler into the local cluster following similar synchronization process as used for intracluster packets.

3.3 MAC Protocols and their Performance Evaluation

In this section, we consider two protocols for assessing the channels for intracluster and intercluster communication in the proposed access network. Performance of the MAC protocol employed within the CD network (intracluster) is examined using computer simulation and the one employed in the access backbone (intercluster) network is examined using an analytical model.

3.3.1 *Intracluster Communication*

We have adopted a MAC protocol for intracluster communication from an earlier work [MoBa00] and modified the same for further improvisation. The protocol under consideration is based on a scheduler as indicated in Fig. 3.2. All ONUs send their requests to the scheduler, which is assumed to schedule (using ranging process) the requests and inform the ONUs when and on which wavelength to transmit. Upon receiving their assignments (access grants), the source ONUs immediately tune to their particular wavelength and transmit. Hence they need not maintain any local synchronization subsystem and timing information. Simultaneously the destination ONUs tune their transceivers to the wavelength as indicated in the access grant packet and start receiving data. We describe the protocol by addressing some of its major features as described in the following.

Ranging:

The ranging process is able to overcome the effects of non uniform propagation delays between ONUs and AN, by measuring the round-trip delay of each ONU to the AN, and using that information to inform ONUs of their turn to transmit in a timely manner. In this way the transmissions of different terminals can be scheduled back-to-back, with some idle (guard) times between consecutive data packet transmissions. Unlike other systems where terminals need to range themselves to their ANs, only the AN needs to know this information.

Access Protocol:

For transmission of control packets by ONUs, one needs to employ an appropriate MAC protocol. The control packet lengths (access requests/ access grants) are much smaller than the data packet lengths (typically 100:1) and their collision probability is relatively low even after considering repeated transmissions. Further, at the data rates in the range of hundreds of Mbps to a few Gbps, the high latency of the network renders protocols like CSMA/CD unsuitable. TDM allocation for control channel would mean that the ONUs should be synchronized whereas in our architecture we keep them asynchronous for simpler coordination. Hence we use pure (unslotted) ALOHA protocol for the control channel access. An ONU access request, contains the source- and destination-ONU addresses, state of its buffer queue (last request that was scheduled) and the duration for which it wishes to transmit (length of the queue). An ONU sends the access request again if an "access grant" is not received within a random time-out. Since access requests are sent on the control channel λ_c at random, it is possible for two or more terminals to send their requests during overlapping time intervals. In such a case the transmissions would collide and not be received by the scheduler. However, since the reservation request messages are sent repeatedly, the scheduler will eventually receive all requests. As the scheduler answers the requests, ONUs update their requests to reflect the changes in their request-queue and overcome receiver contention.

Scheduling:

In order to simplify the design of the scheduler, a slotted scheme is used where requests are made for fixed-size time slots and the scheduler maintains a slotted reservation system. However, it is important to note that the transmission timings of ONUs remain unslotted and unsynchronized. As stated earlier, ranging technique used by scheduler controls all the timing. The scheduling algorithm works by maintaining N request queues, each containing the transmission requests from one of the N ONUs in the CD network. The algorithm is implemented on slot-by-slot basis, where requests are served on a first-come first-serve (FCFS) queuing model. In each slot, a given ONU can be scheduled for at the most one transmission and one reception. The algorithm visits every ONU in random order (in order to maintain fairness among the ONUs) and starting with the first request in the queue, it searches for the request that can be scheduled. The optimum slot time is chosen, taking into consideration the number of ONUs, network activity and the control packet size so that the slot utilization is maximized.

Look-Ahead:

In practice the number of requests served by the scheduler is limited by the wavelengths, M and head-of-line (HOL) blocking due to receiver contention. HOL blocking would result when the requests at the head of any two successive queues have the same destination ONU (receiver) address. Having scheduled an ONU to receive transmissions, the scheduler cannot serve the first request of the next queue, if it contends for the same ONU. In such situations the scheduler with look-ahead feature, will neither serve another queue nor wait for the contended receiver to get free, but instead look ahead into each input queue and schedule requests that are not necessarily at the head of the same queue. HOL blocking is reported [MoBa99] to limit the throughput of a FCFS input-queued switch to 58.5% (under uniform traffic conditions) even when the numbers of ONUs and channels are equal (without look-ahead) whereas the throughput can reach up to 81% with look-ahead. Interestingly, the throughput can be increased to 99% when the number of ONUs is higher than the data channels at relatively smaller values of look-ahead. This is because the probability that multiple ONUs have a packet at the HOL to the same destination is now reduced and also the algorithm has more requests to schedule the data transmissions from. Thus, an attempt to improve throughput using look-ahead becomes more effective when the system suffers from high congestion with number of ONUs less than the number of available data wavelengths (channels).

Improved Access to Control Channel:

As the number of active ONUs increases, so does the chance of collision on the control channel, resulting in an increase in delay in refreshing the queue status at the AN. This bottleneck problem in the control channel can be alleviated with the increase in control channels. Thus both the collision on control channel and the pre-transmission coordination delay would be reduced. But at the same time the effective service rate would be decreased due to the reduction in the number of channels available for data transmission. In order to overcome this problem, SCM is introduced in the protocol, albeit with some additional hardware [Fon93]. In this scheme, control packets of each ONU are same optical carrier (λ_C) in the passive star topology. Thus, each ONU used to modulate a unique microwave sub carrier, which is subsequently broadcast and will have a unique control channel and the hardware requirement for such SCM implementation would be as shown in Fig. 3.5. With this arrangement one can expect good performance at low and moderate loads. However at high loads, the performance will eventually degrade, because with the avoidance of collision in the control channel, there will be far too many requests than can be accommodated with the limited number of data channels. Hence at high loads, a packet is likely to face longer

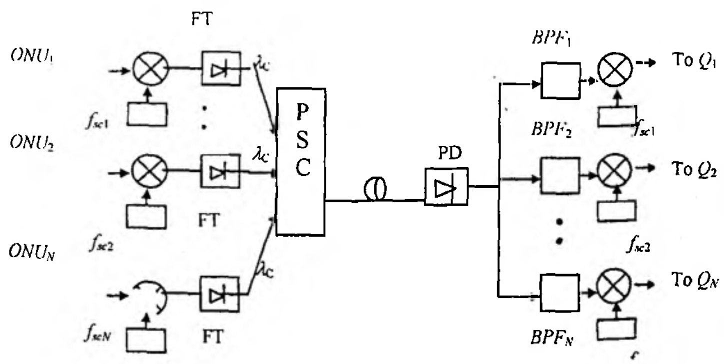

f_{scN} : N^{th} RF carrier λ_C: Optical carrier PSC: Star coupler
PD: Photo detector BPF_N : Nth band pass filter Q_N: Nth control packet queue

Fig. 3.4. Control packet transmission employing SCM

delay than previous cases. However several issues need further attention in this respect. First, the complexity of the ONU transceiver is increased with SCM brought in. Secondly, it may bring in a physical-layer problem, as the total signal power in the control wavelength will be increased very much, thereby increasing the signal dependent shot noise at the receiver. Transmitting control packets at a reduced bit rate might alleviate this problem. Since the control packet length is a small fraction of that of a data packet, a little dilation of the control-packet duration (when applied with SCM) is not expected to affect the control channel throughput significantly. Since the size of the network is not going to be large (10-25 ONUs), and the number of ONUs is not too large as compared to the number of wavelengths, practically SCM would be operating below the saturation limit. By computer simulation, the delay characteristics of this MAC protocol are evaluated and discussed in Section 3.4.

3.3.2 *Intercluster Communication*

For the intercluster communication, in order to differentiate real-time services from non-real time services, we adopt a MAC protocol which is based priority queuing. As mentioned earlier, the intercluster traffic between ANs on the backbone ring is classified into two categories: incoming intercluster traffic at an AN arriving from another AN via backbone ring and, outgoing intercluster traffic at an AN arriving from the ONUs in the local cluster. An outgoing intercluster packet arrives from its source ONU at the source AN (on $\lambda_{M+1},...,\lambda_{M+K}$) after going through the ALOHA-based contention process (using control packet on λ_{C}), in the same way as the intracluster packets. The outgoing data packet is scheduled in the local AN (with RT/NRT based priority) and transmitted thereafter on appropriate backbone wavelengths and subsequently considered as an incoming intercluster packet at the destination AN. In an access network setting with fewer wavelengths as compared to long-haul backbones, instead of wavelength conversion it would be easier to make use of optical-electronic-optical conversion (more easily realizable) for mapping inter-cluster packets on one wavelength into the intra-cluster packets on another. O-E-O conversion is used for inter-cluster traffic to map the outgoing data packets on λ_{M+1} .... λ_{M+K} onto source-destination specific backbone/feeder wavelengths λ_{B1} ..... λ_{BL} (and vice versa for the incoming data packets). Thus an incoming data packet at the destination AN, is first converted into electronic domain for further processing. Each of these intercluster packets, after being received from the source ONUs in the source ANs and scheduled at the source AN, is transmitted towards the destination AN with a special header, which plays the role of a control packet after reaching the destination AN. This header of an intercluster packet, which is added at source AN, is stripped off at the destination AN and sent to the header reader (HR). The scheduler uses the information from the header reader and generates control packets on λ_{C} (after O/E/O conversion) and stores them in a separate queue referred to as cluster queue (CQ). Similarly the data packets (after removal of headers) are queued up for scheduling as shown in Fig. 3.3. The scheduler uses the information in the control packet to issue access grants on λ_{C} and transmit the data packets on ($\lambda_{M+1},...,\lambda_{M+K}$) to the destination ONUs.

Dynamic Bandwidth Management

At the source AN, along with the intracluster control packet queues, there will be a separate queue for the control packets for outgoing intercluster traffic referred to as global queue (as mentioned earlier GQ). The scheduler will follow the same procedure as it does for intracluster traffic, but the data packets for different services are treated in a different manner for intercluster traffic. Having received from the scheduler about the wavelength and timing allocation on λ'_C, outgoing intercluster packets in the source cluster will be broadcast from ONUs (on $\lambda_{M+1},\ldots,\lambda_{M\cdot K}$) towards the local source AN. As mentioned earlier upon receiving these packets, the source AN converts them into electrical domain and queue them up (with necessary sorting for RT and NRT services) for onward transmission on appropriate backbone wavelength ($\lambda_{B1},\ldots,\lambda_{BL}$). For distinguishing the quality of service for different types of packets, we consider here RT and NRT data packets with different priorities. Thus by employing this configuration, one can implement an AN, that can employ dynamic bandwidth management scheme on fixed wavelengths for intercluster communication.

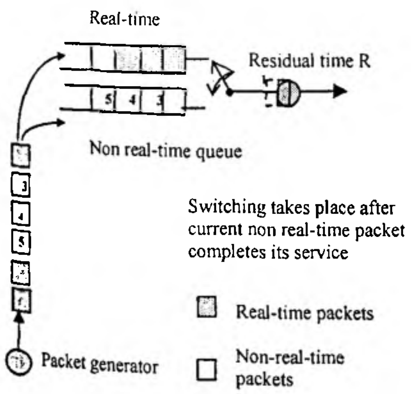

Fig. 3.5. Nonpreemptive resume priority

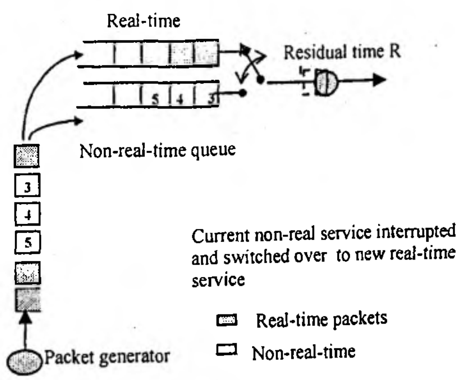

Fig. 3.6. Preemptive resume priority

Analytical Model for Queuing Delay

In the following we consider an analytical model for studying two different dynamic bandwidth management (DBM) schemes [BeGa97] viz., preemptive resume priority and nonpreemptive resume priority schemes. The model is developed for estimating the queuing delay of prioritized/non-prioritized traffic streams and hence in principle accounts for the entire inter-cluster traffic carried by any given channel or wavelength. The model makes distinction only between real-time and non-real-time data queues with the scheduled packets in each queue, from practically any of the active ONUs (and hence any λ) in the access network. We consider a M/G/1 system to model the single-server queuing system which employs priority schemes in scheduling the intercluster traffic. In such a system, the packets arrive according to a Poisson process, and the packet service times have a general distribution. The arrival processes of all classes are assumed independent, Poisson-distributed, and independent of the service times. The system differentiates between two priority classes of the outgoing intercluster traffic viz., RT and NRT. With λ_1 and λ_2 as the arrival rates, μ_1 and μ_2 as the service rates for RT and NRT packets respectively, the average service times $\overline{X_1}$ and $\overline{X_2}$ and traffic intensities ρ_1 and ρ_2 for RT and NRT packets are expressed respectively as, $\overline{X_1} = \frac{1}{\mu_1}$; $\overline{X_2} = \frac{1}{\mu_1}$; $\rho_1 = \frac{\lambda_1}{\mu_1}$ and $\rho_2 = \frac{\lambda_2}{\mu_2}$

Here λ_1 and λ_2 are the arrival rates, μ_1 and μ_2 are the service rates and ρ_1 and ρ_2 are the traffic intensities for RT and NRT packets respectively.

Nonpreemptive Resume Priority:

Next, for evaluation of non-preemptive resume priority scheme, we determine the total waiting times (T_1 for RT and T_2 for NRT) for the data packets in terms of their salient statistical parameters. The average delay T, a data packet experiences in the system, is the sum of its average waiting time in the queue W and the average service time $1/\mu$ is given by

$$T = W + \frac{1}{\mu}$$

It may be noted that a given RT/NRT data packet at the head of the queue may still have to wait for a finite time R, to get the service as the server might remain busy with the packet from another queue. This is called mean residual service time R and is the remaining time for completion of the data packet already in service. In nonpreemptive priority scheme (Fig. 3.5), the service of a lower-priority packet (i.e., NRT data packet) is allowed to complete without interruption even if a higher-priority packet (RT data packet) arrives in the meantime. However, service is transferred to RT data packets immediately after completing the ongoing service of that particular NRT packet. Figure 3.5 illustrates that even though the RT packet 2 is waiting and arrived later than NRT packet 1, the server (scheduler) is allowed to complete the service of the NRT packet before transferring control to the RT data packets. For these reasons, in a nonpreemptive case, residual service time has to account for both RT and NRT packets. Also given the fact that in an ergodic process (which we assume) time average is equal to ensemble average, the mean residual time, R is given by [Ber97],

$$R = \frac{\lambda_1 \overline{X_1^2}}{2} + \frac{\lambda_2 \overline{X_2^2}}{2} \quad (3.1)$$

where, X_1^2 and X_2^2 are the second moments of the service times of RT and NRT data packets. As shown in Fig. 3.3, a separate queue is maintained for each priority class. Average total waiting time in the queue W for each class of data packets is given by the sum of average total residual time R and the average total service time at the queue N_Q/μ, where N_Q is the average number of packets waiting in the queue.

The waiting time for RT packets W_1 depends only on RT packets, but the waiting time for NRT packets, W_2 has to count the delay due to RT packets already in the queue as well as the additional delay due to arrival of higher-priority RT packets while the NRT packets are waiting in the queue. By using Little's theorem ($N_Q = \lambda W$) to eliminate N_Q, we arrive at the following expressions for the expected values of waiting times in the queue for RT packets (W_1) and NRT packets (W_2) respectively as,

$$W_1 = \frac{R}{1-\rho_1} \text{ and } W_2 = \frac{R}{(1-\rho_1)(1-\rho_1-\rho_2)} \quad (3.2)$$

The total time delay for RT data packets (T_1) is given by,

$$T_1 = \frac{1}{\mu_1} + \frac{R}{1-\rho_1} \quad (3.3)$$

The total time delay for NRT data packets (T_2) is given by,

$$T_2 = \frac{1}{\mu_2} + \frac{R}{(1-\rho_1)(1-\rho_1-\rho_2)} \quad (3.4)$$

From the above expressions the delay for RT data packets and NRT data packets for a given channel allocation can be found out for the nonpreemptive priority scheme.

Preemptive Resume Priority:

In preemptive resume priority, whenever higher-priority RT data packet arrives, the service of a lower-priority NRT data packet is interrupted immediately and is resumed from the point of interruption once all packets, with higher-priority have been served. Hence, in this case we can expect less delay for the RT data packets as compared to the NRT data packets. As shown in Fig. 3.6, in this case RT packets are served first rather than NRT packets. While a packet 1 (NRT) is being served as soon as a RT packet arrives, the NRT packet 1 is interrupted and then queued up with the remaining NRT data packets. The service for the remaining bits of NRT data packet 1 is resumed immediately after the transmission of all the

RT data packets 2, 6 and 7. Thus, the RT data packets are served with higher-priority as compared to the NRT data packets (3, 4 and 5).

In this case, the residual time R is different for RT and NRT data. In particular, the mean residual time for RT packets R_1 is by no means dependent on NRT packets. But mean residual time R_2 for NRT packets certainly bears the impact of both RT and NRT packets, as an NRT packet might have to wait for the completion of a suddenly-arrived RT packet in the queue and also for the NRT packets ahead of it in the NRT queue. The mean residual times R_1 and R_2 are given by

$$R_1 = \frac{\lambda_1 \overline{x_1^2}}{2} \quad \text{and} \quad R_2 = \frac{\lambda_1 \overline{X_1^2} + \lambda_2 \overline{X_2^2}}{2} \tag{3.5}$$

The total waiting time (in queue and in service) for RT data packets is given by

$$T_1 = \frac{\left(\frac{1}{\mu_1}\right)(1-\rho_1) + R_1}{(1-\rho_1)} \tag{3.6}$$

Similarly the total waiting time for NRT data packets is given by

$$T_2 = \frac{\left(\frac{1}{\mu_2}\right)(1-\rho_1-\rho_2) + R_2}{(1-\rho_1)(1-\rho_1-\rho_2)} \tag{3.7}$$

From the above analysis one can examine the delay variation with respect to the traffic intensities (ρ_1 and ρ_2) and estimate the maximum number of RT/NRT transmissions to be allowed on a single wavelength at minimum allowable delay. The numerical results for the delay characteristics obtained using this analytical model for the above mentioned two schemes are discussed in the following section.

3.4 Results and Discussion

In this section we present the results of our investigation on the performance of intracluster (Fig.3.7 through Fig. 3.10) and intercluster (Fig. 3.11 through Fig. 3.18) communications. The proposed MAC protocol for the intracluster traffic has been examined using event-driven simulation, wherein the packet arrival process has been modeled after Poisson distribution and the data traffic is assumed to be uniformly distributed among all ONUs. As the delay analysis plays an important role in performance evaluation of any QoS-aware access network, we examine the delay characteristics of the proposed MAC protocols.

Figure 3.7 illustrates the delay characteristics for varying amounts of load per ONU with control channels as the parameter for the intracluster traffic. In these plots, the load per ONU represents the total average load per ONU, including the control packets for both intracluster and intercluster communications (in $Q_1,\ldots,Q_N$ and GQ) generated from each ONU. As the load per ONU increases, so does the length of the queue and in turn, the delay. When the aggregate packet arrival rate (i.e., for all ONUs together) increases beyond the

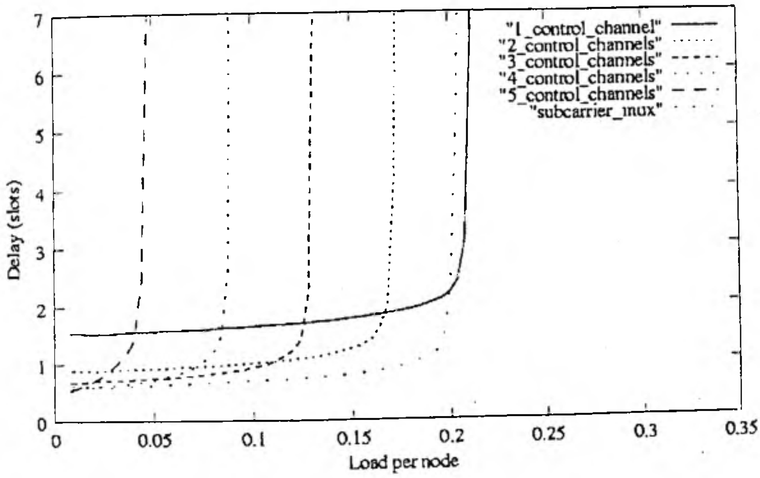

Fig. 3.7. Delay for 21 ONUs and 6 intracluster wavelengths

service rate (which is one packet per slot per data wavelength) the delay increases with a sharp takeoff, which is explicitly revealed in Fig.3.7. For example, in this case with 1 control channel, there are 5 data channels and the "knee" of the delay plot takes place at a load (per ONU) ~ 0.215. At this load, the total network load per each data channel = 0.215×21/5 ~ 0.903. This implies that the network load per channel at this point approaches unity, thereby causing the takeoff. As the control channels increase in number, there is less control-packet

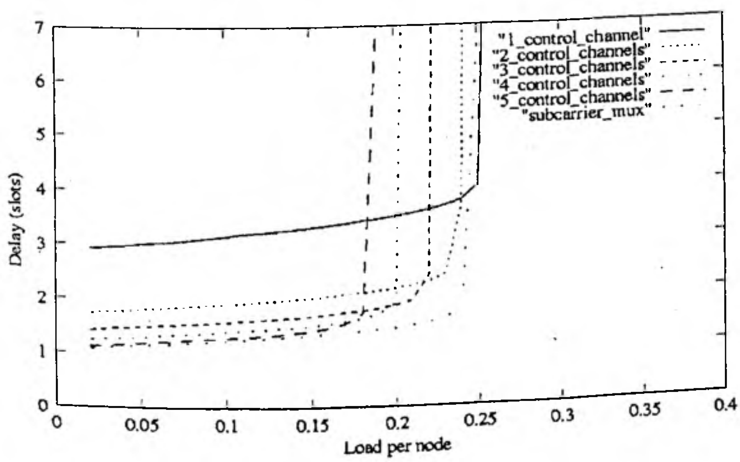

Fig. 3.8. Delay for 50 ONUs and 12 intracluster wavelengths

collision and hence less delay at lower traffic values. However take-off points in the delay curves occur at lower load-per-ONU values due to the relatively lower number of data channels. Thus, more control channels can improve the network performance until the load per ONU approaches the takeoff point. Furthermore increase in number of ONUs as in Fig. 3.8, causes more control channel collisions and hence increases the delay. In order to reduce the control channel collisions, we consider SCM of the ONU, in which probability of

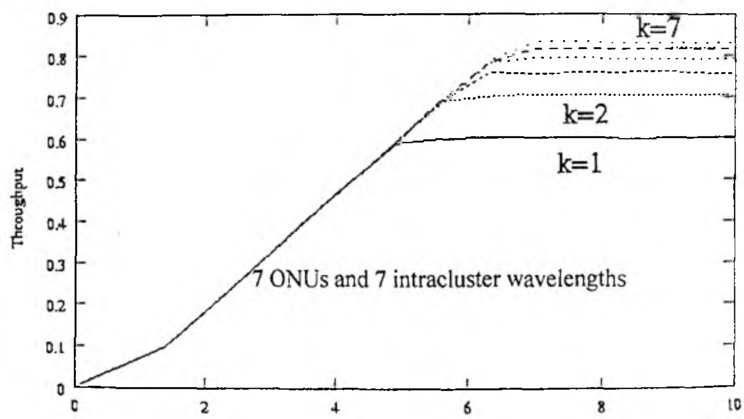

Fig. 3.9. System throughput with look-ahead, k

collision is far less and this in turn decreases the access delay. Thus the results from Fig. 3.7 and 3.8 reveal that, the proposed method with SCM outperforms all the previous cases.

We find in Fig. 3.9, for a system with 7 ONUs and 7 data channels, the throughput is limited to 58% with no look-ahead i.e., k=1. With increasing values of k=1 to 7, the effect of

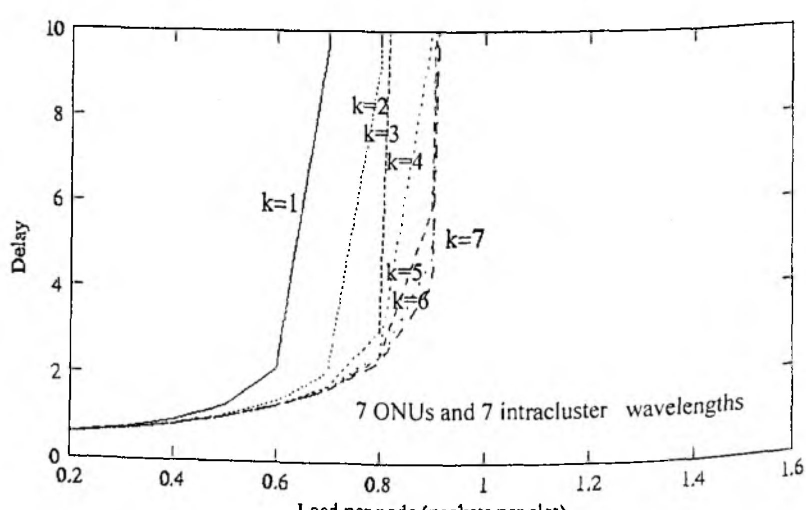

Fig. 3.10. Delay characteristics with look-ahead, k

receiver contention is gradually overcome, resulting in improvement in the system throughput. However even with k=7, the maximum achieved throughput is only 86% and saturates thereafter. This is so because the choice for scheduling data transmissions (at higher traffic loads) is low for ONU-to-channel ratio of 1. It may also be observed that the difference in the performance narrows down for increasing values of look-ahead. In the case of delay (Fig. 3.10), we observe a similar phenomenon where there is improvement in delay performance with increasing values of k. The take-off points occur at higher values of load-per-ONU and thus increase traffic transport capability of the cluster with look-ahead option.

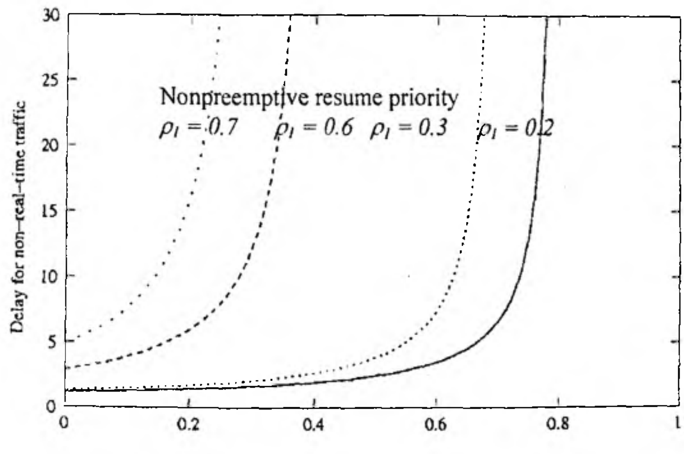

Fig.3.11. Delay vs. traffic intensity for NRT data with nonpreemptive resume priority queuing

Next we examine the performance of the MAC protocol for intercluster traffic based on the given analytical model, for different traffic intensities of RT (ρ_1) and NRT (ρ_2) data packets, while maintaining the packet size fixed. Figure 3.11 shows the plots of delay (in number of packets) for NRT packets under nonpreemptive priority queuing scheme, with RT traffic intensity (ρ_1) as a varying parameter. It is evident from Fig. 3.11 that, as the traffic (ρ_1) increases, delay for NRT data packets increases and the delay profile is highly sensitive to the RT traffic. In particular, it is worthwhile to note that the take-off points of the delay curves takes place in the vicinity of $\rho_2 = 1 - \rho_1$. This applies to all the curves and is expected as well, because in those regions the total traffic approaches unity making the delay unacceptably large. Figure 3.12 shows the plots of delay for NRT data packets in case of preemptive resume priority scheme. Here the delay curves resemble the previous plot in Fig.3.11, but the delay for NRT packets is relatively high compared to that of the nonpreemptive case. The major reason behind this is that the queue for NRT data packets builds up faster as higher-priority is given to RT data packets due to the preemptive nature of the MAC.

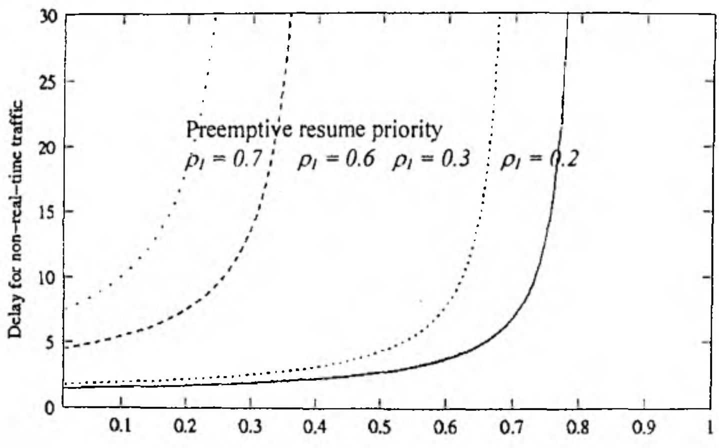

Fig.3.12. Delay vs. traffic intensity for NRT data with preemptive resume priority queuing

Figures 3.13 and 3.14 illustrate the plots of delay for RT data packets versus NRT traffic in nonpreemptive priority and in preemptive priority schemes respectively, with RT traffic intensity, as a varying parameter. It is evident from these figures, that in preemptive resume priority scheme, the NRT traffic shows lesser impact on the RT packet delay as compared to the nonpreemptive case. The reason is that, in nonpreemptive priority, the ongoing NRT data

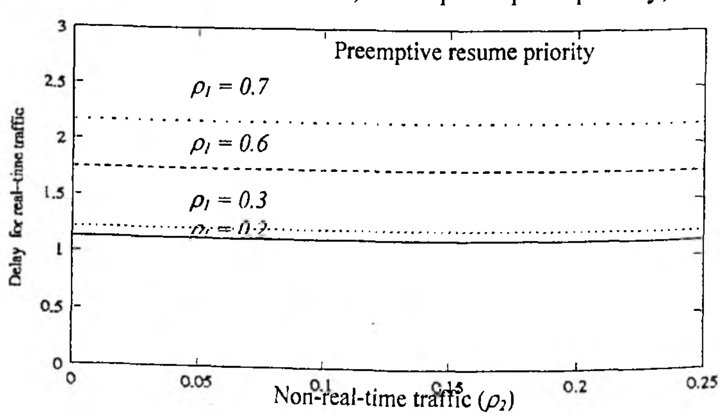

Fig. 3.14. Delay for RT traffic vs. NRT traffic with preemptive resume priority queuing

packet is allowed to be served even if there is a RT packet arrival. But in case of preemptive resume priority the delay for RT data packets is independent of arrival of NRT packets.

In Fig. 3.15 and Fig. 3.16, NRT traffic intensity is held constant for a given RT traffic variation over a typical range. Figure 3.15 depicts the delay characteristics for RT data packets by varying NRT traffic intensity in the nonpreemptive case. It is observed that there is only slight impact of the NRT traffic on the delay profile whereas in the case of preemptive resume priority scheme as shown in Fig. 3.16, the delay for RT packets is almost independent of NRT traffic.

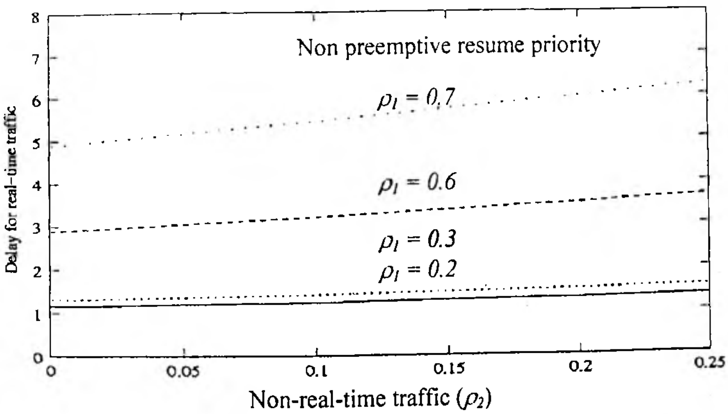

Fig.3.13. Delay for RT traffic vs. NRT traffic with nonpreemptive resume priority queuing

Figure 3.17 shows the plots of delay difference (for RT and NRT packets) between preemptive and nonpreemptive priority queuing schemes vs. RT traffic, for a fixed NRT

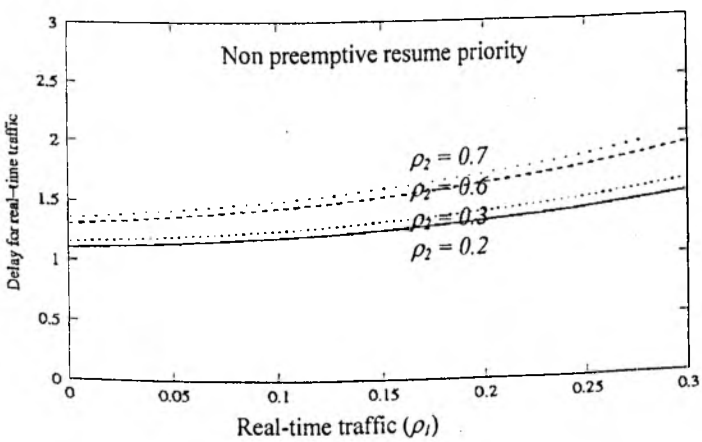

Fig. 3.15. Delay for RT traffic with non preemptive resume priority queuing

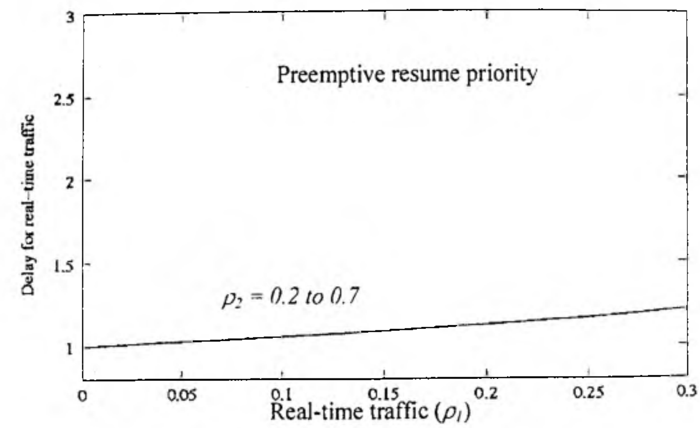

Fig.3.16. Delay for RT traffic with preemptive resume priority queuing

traffic intensity (0.2). From the figure it is evident that, the delay difference for NRT data packets increases with increase in RT traffic, whereas for RT data packets, the delay difference decreases by significant amount. This happens because, in case of preemptive scheme, the delay for NRT packets is more significantly affected (as compared to RT packets) as the ongoing service of NRT packets is interrupted immediately to give way to RT packets. Thus as the RT traffic increases, these interruptions for NRT packets further increase leading to more queuing delay for NRT packets. But in case of nonpreemptive scheme, the delay for NRT packets is less affected by increase in RT traffic as the ongoing service of the

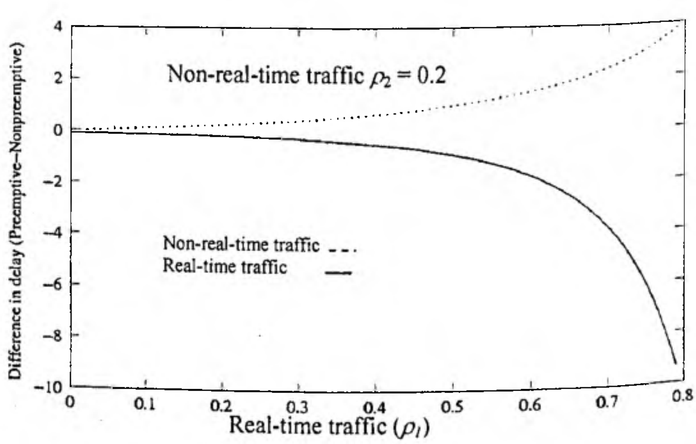

Fig. 3.17. Delay difference between the two schemes for RT and NRT traffic as a function of RT traffic

NRT packet is allowed to continue without interruption. Hence the delay difference between the preemptive and nonpreemptive priority for RT packets decreases with increase of RT traffic (i.e., nonpreemptive scheme shows degraded performance with respect to preemptive scheme). On the other hand, as mentioned earlier, the delay difference between the preemptive and nonpreemptive schemes for NRT packets increases with increase of RT traffic.

Figure 3.18 shows the plots of delay difference (for RT and NRT packets) between preemptive and nonpreemptive priority queuing schemes vs. NRT traffic. Even if the delay for NRT packets is more in case of preemptive resume priority, it is found that the delay difference for NRT packets remains constant with varying NRT traffic. This happens because in case of increasing NRT packets, preemptive and nonpreemptive schemes do not

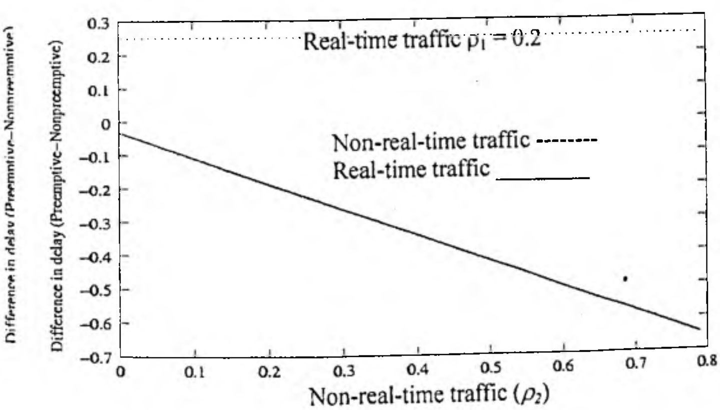

Fig. 3.18. Delay difference between the two schemes for RT and NRT traffic as a function of NRT traffic

experience any difference in respect of their queuing delays. But for RT traffic, difference in delay decreases (i.e., nonpreemptive scheme experience more delay as compared to preemptive scheme) with increase in NRT traffic. This is expected because impact of NRT packets on RT packets is insignificant in preemptive scheme and hence the delay for RT traffic is hardly affected by increase in NRT traffic.

3.5 Summary

In this work we have examined an optical access network comprising of a backbone-ring connecting several passive-star-based clusters of ONUs at the customer premises. In particular, we have proposed an AN configuration that handles both intracluster and intercluster communications through appropriate scheduling functionalities. We have studied the performance of the MAC protocols, that are employed in the scheduler-based AN to manage the transport of data packets. For intracluster traffic, the MAC protocol incorporates pre-transmission co-ordination based scheduling, whose performance has been evaluated through computer simulation. The delay performance has been found to improve on increasing the number of control channels but with an early take-off of the delay curves. Further, our results indicate that, incorporating a few SCM (subcarrier) channels on a single control wavelength reduces the number of collisions between the control packets, without reducing the number of wavelengths needed for data traffic. This in turn improves the delay performance albeit, with some additional hardware complexity at ONUs as well as ANs. For intercluster traffic, we have examined a MAC protocol employing priority-based queuing to differentiate between RT and NRT packets. An analytical model was developed for evaluating the network performance for intercluster communication. Based on our analysis, comparative evaluation of the priority queuing schemes has been made by examining their delay difference for both RT and NRT data. Thus, our study is expected to serve as a useful tool for designing a WDM-based optical access network with two-level hierarchical topology.

References

[BeGa97] D. Bertsekas and R. Gallager, *Data Networks*, Prentice Hall Inc., USA, Second Ed., 1997.

[FoOl93] S. Fong Su and R. Olshansky, Performance of multiple access WDM networks with sub-carrier multiplexed control channels," *IEEE*/OSA *Journal of Lightwave Technology*, vol.11, no. 5/6, pp.1028-1033, May/ June 1993

[HaKS87] K. M. I. Habib, M. Kavehrad and C. E. W. Sundberg, "Protocols for very high-speed optical fiber local area networks using a passive star topology," *IEEE/OSA Journal of Lightwave Technology*, vol. 15, Dec. 1987.

[JiMu92] F. Jia and B. Mukherjee, "The receiver avoidance collision (RCA) protocols for single hop WDM lightwave networks," Proceedings ICC'92, Jun. 1992.

[Mehr90] N. Mehravari, "Performance and protocol improvements for very high-speed optical fiber local area networks using a passive star topology," *IEEE/OSA Journal of Lightwave Technology*, vol. 8, Apr. 1990.

[MoBa99] E. Modiano and R. Barry, "Design and Analysis of AN Asynchronous WDM local area network using a master/slave scheduler," *IEEE Proceedings of INFOCOM* 1999.

[MoBa00] E. Modiano and R. Barry, "A novel medium access control protocol for WDM-based LAN's and access networks using a master/slave scheduler," *IEEE/OSA Journal of Lightwave Technology*, vol. 18, no. 4, pp. 461-468, Apr. 2000.

CHAPTER 4

Resource Provisioning in a Hybrid PON Employing OCDMA over WDM

4.1 Introduction

Resource provisioning is an important aspect of any network segment, which has a prospect of foreseeable growth, like that of a PON. It deals with the methodologies adopted for preparing the network for futuristic demands, in terms of size or service quality. While allocating the available resources to support user services, a complete assessment of the network performance under different traffic conditions helps in minimizing the overhead expenses. An exhaustive study in this respect can give useful insight regarding optimal deployment of available resources during network expansion. In the near future, the data traffic volumes generated by the subscribers are bound to increase with more and more interactive services entering the customer premises. A PON should be able to distribute not only a wide range of data, voice and video based services from the CO, but also carry considerable amount of multi-media traffic originating from the customer end to the CO. As a result, a service provider is required to mobilize and appropriately distribute the available resources in either direction in order to abide by the service level agreements with the customers. However the directional asymmetry of the traffic will remain for some time, and this aspect can be usefully exploited while provisioning the PON.

In order to keep up with the expected growth in subscriber density, PONs should adopt scalable configurations, which would allow them to smoothly support increased number of bidirectional transmissions. Such scalability, in a cost-sensitive setting like PON, is difficult to maintain through a single type of multiplexing/multi-access technique. For instance, in order to scale up, a WDM-based PON will need agile transceivers with a wide tuning range and good response time while a TDM-based PON requires transceivers operating at the aggregate speed, in addition to addressing end-to-end (OLT to ONU) synchronization issues. A possible way to circumvent these operational constraints is to combine different access schemes through a multistage RN employing both AWGs and passive star couplers. This approach to network connectivity generates a much larger resource-pool, which can be utilized for smooth provisioning of the PON. In addition, the end user enjoys the benefit from all the constituent access schemes, with the ONU hardware needing no elaborate upgradation. Further, the scope of provisioning also improves with an enhanced pool of resources. For example, in a hybrid WDM-TDM PON every subscriber is addressed by a unique wavelength-time-slot combination, allowing a much larger subscriber-base. Here WDM gives an additional dimension to the network size while the speed requirements of the transceivers remaining unchanged.

In this context, it is worth considering the merits of OCDMA in hybrid PONs. OCDMA-based systems support asynchronous communication and have been extensively studied for their suitability in local area networks and later in access networks [Sale89], [Jaya00] and [StSa02]. Other studies on systems, employing multi-rate codes [MaVi98], indicate the possibility of OCDMA systems supporting heterogeneous services (as in an access segment) with differing service quality. Due to its fair, flexible and inherently secure mechanism of providing asynchronous multi-access, OCDMA technology can ease out connectivity problems in a distribution segment. However network deployments based on OCDMA systems have so far been confined to research test-beds and laboratory experiments for want of mass-fabricated, off-the-shelf encoding/decoding devices. The emergence of FBG, a passive encoding/decoding device [ToCY99] has increased the prospects of OCDMA for cost sensitive PON segment. Recently Kitayama et al suggested employing OCDMA over WDMPON to realize gigabit-speed services for FTTH solutions [KiWW06].

In this chapter, we consider a hybrid PON configuration based on WDM and OCDMA techniques. In the PON under consideration, our resource pool consists of wavelengths and optical codes. The performance of a network mostly depends on the way the limited resources are put to use. We address this issue by adopting some resource allocation strategies, while keeping the resources limited. Further, we examine the implications of possible under- and over-provisioned situations with varying code allocations.

4.2 Proposed Hybrid PON Configuration

In this section, we propose a PON configuration which employs WDM as well as OCDMA techniques (and hereafter called as W-OCDM PON) to realize a hybrid PON. This functionality is realized using two separate RNs at different stages with an AWG in the first stage and one or more PSCs in the second stage, with the latter placed nearer to the cluster centre of the ONUs. The configuration is modular and scalable, where wavelengths provide coarse granularity and optical codes provide finer granularity. An OLT, which is generally collocated with a central office, connects the PON with higher levels of telecom infrastructure. The fiber link between OLT and the first-stage RN configuration constitutes the feeder section covering about 15-20 km distance. This is followed by the distribution segment comprising of the two-stage RN reaching out to ONUs over a range of 10-15 kms. With lesser traffic, for upstream transmission, the number of codes is kept fewer than number of users and hence the access in upstream, takes resort to multiple access rather than circuit-switched (dedicated) resources for downstream transmission. Thus through hybrid multiplexing (WDM-OCDM) for downstream transmissions and hybrid multiple access

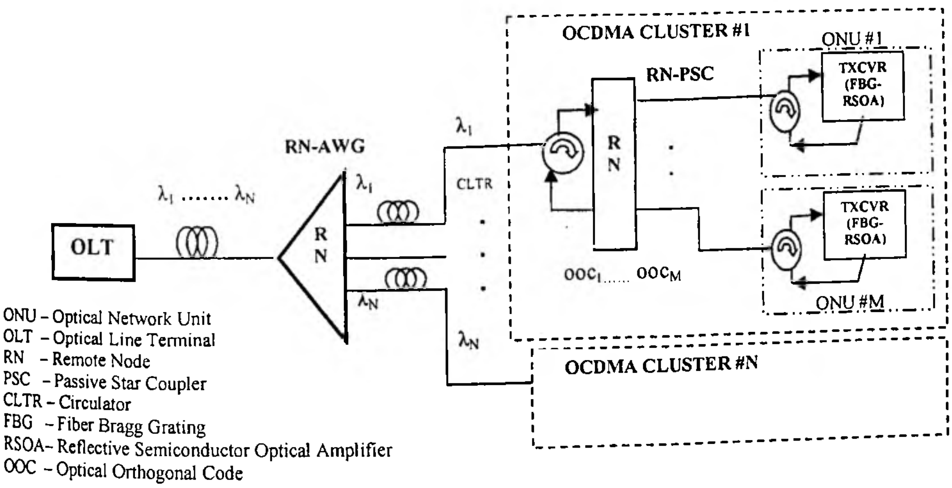

Fig.4.1. Block Schematic of a W-OCDM PON

(WDMA-OCDMA) for upstream transmission, every channel transmission is uniquely defined by a wavelength-optical code combination. As seen from Fig.4.1, ONUs under each OCDMA-cluster, are provided with M optical codes (OOC_1.....OOC_M) for their transmissions (including upstream and downstream). N such OCDMA-clusters, each on a distinct wavelength, can provide a total of $N \times M$ wavelength-code channels. A brief description of the subsystems follows, with our major focus on the provisioning aspect.

RN-AWG and RN-PSC: Two Stages of RN

As shown in the block schematic, the RN configuration comprises of an AWG-based remote node in the first stage followed by a PSC-based RN in the second stage. Thus channel distribution is carried out through routers (using AWG) and power splitters (using PSC). Each output port of a $1 \times N$ AWG connects to a PSC of size $1 \times M$. With this set-up, M

optical codes in each code-cluster are reused on N wavelengths enabling the PON to support $M \times N$ bidirectional transmissions. As mentioned in Chapter 2, AWG works on a static wavelength routing mechanism which enables it to spatially separate and combine optical channels as a function of their operating wavelengths and port locations (an elaborate study on the physical layer issues of the demultiplexing device is covered in the following chapter). On the other hand a PSC is a widely used power-coupling device which carries out the function of combining/splitting through its M input/output ports. It is particularly suitable in multi-access environment supporting asynchronous transmissions like an OCDMA-based ONU-cluster.

OLT and ONU

OLT is considered the resource-centre for the distribution segment. It is equipped with arrayed or tunable multi-wavelength light sources/detectors to generate/receive simultaneous data transmissions for/from the ONUs. These are followed by arrays of FBG-based codecs needed for optically encoding and decoding the data signals. Since the cost of OLT is shared amongst all the PON subscribers, it can afford to use a post–amplifier to compensate for the losses in the distribution segment. In our proposed setting, OLT supplies optical carrier power to the ONUs, for their upstream transmission which we discuss subsequently.

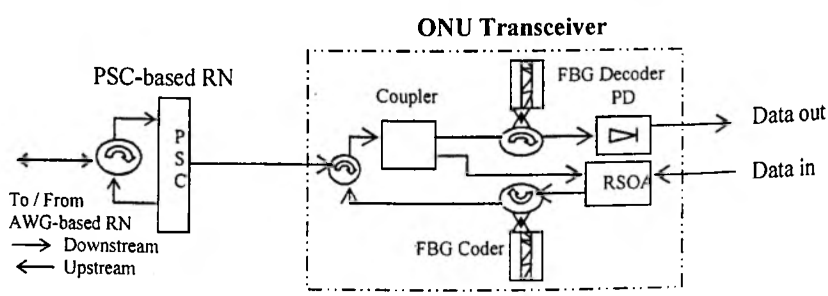

Fig.4.2. Fiber Bragg Grating-based ONU Transceiver

As shown in the Fig.4.2, an ONU transceiver would consist of a receiver section comprising of a FBG decoder followed by a PIN photo-detector while the transmitter section consists of a RSOA and an FBG coder. The downstream channels are first decoded in the FBG section and later photo-detected. A 3-dB coupler taps the optical carrier power from the downstream channels and supplies the seed carrier power to be modulated by the RSOA with upstream data. The RSOA works as a modulator, when operated in the saturation region [KaHa06] supporting data rates of 100's of Mbps. The modulated data stream is then encoded through the FBG to be transmitted in the upstream via PSC-based RN. Both upstream and downstream channels use a common fiber link.

FBG-based Optical Coding

Several encoding/decoding schemes based on fiber Bragg grating technology have been proposed and developed [TPIR01]. The operating principle is that an incident data bit is imparted a unique coding pattern onto its reflection profile as it emerges from the FBG encoder. As shown in Fig. 4.3, the incident and encoded signals are isolated by a circulator in the transmitting section of the ONU. In the receiving section of the ONU, the encoded bit enters an FBG decoder which has a conjugate coding pattern. This gives a despreading effect to the encoded signal and the original bit is reconstructed after reflection. Coding patterns are etched into the fiber section of the device by modulating its refractive index profile, through the use of spatial mask and holographic techniques. Super-structured FBGs (SSFBG) have been tried in test-bed studies [HWWK06] which can generate 511-chip code sequences employing coherent coding method.

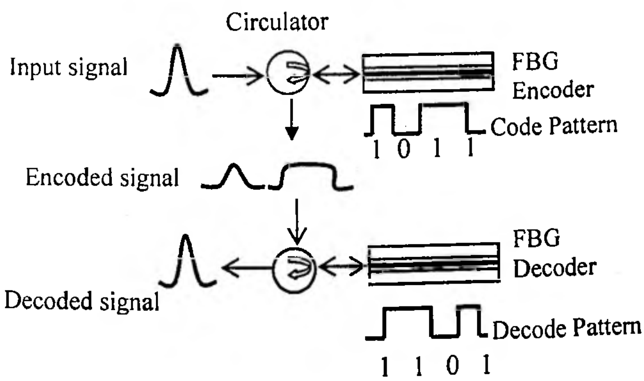

Fig. 4.3. FBG-based Encoding/Decoding

Optical orthogonal codes (OOCs) are unipolar code sequences represented by the n-tuple (n, w, λ_a, λ_c) where n is the code length, w is the code weight, λ_a is the autocorrelation constraint and λ_c is the cross correlation constraint [ChSa89]. They are sparse codes, designed to have very low w/n values which ensure low interference amongst the "ON" chip pulses and thus minimizes the multiple user interference (MUI). They also have constraint values equal to 'unity' (near ideal) i.e., $\lambda_a = \lambda_c = 1$. However, long sequences (value of n), reduce the spectral utilization of the codes. They are suitable for a PON setting where the required bit rates are not very high but user-count is high. We would consider a set of OOCs which are characterized by (364, 4, 1) giving a code size of 30.

4.3 Traffic Asymmetry and Resource Provisioning

The data traffic in an access network is bidirectional in nature, comprising both upstream and downstream packet transmissions. However in general, there is relatively more traffic on the downstream channels, due to bandwidth-hungry streaming multimedia services. The upstream transmissions are low both in spectral content (bandwidth) and rate of information generation. This brings about a traffic asymmetry which can be profitably utilized by the PON designer for allocating resources. For instance, users in a code-cluster (supported by each PSC) may be allocated dedicated optical codes (OOC) to receive messages on the downstream channels (due to higher traffic) whereas on the upstream channels, the users can share a common set of codes (with more than one user per code) for transmitting. Consequently either more users can be accommodated within the given set of codes or some codes can be saved if the users are fewer in number. The codes thus saved can be used for future provisioning of the PON. However, it is important to examine the right approach used for code allocation, in order to enhance network performance for optimized resource utilization (in this case, optical codes used for each wavelength). In this context, we adopt a method of allocating resources and study its impact on the system throughput by means of an analytical model.

4.3.1 *Code Allocation using a Heuristic Approach*

In an OCDMA-based system, code allocation can be a straightforward exercise where each user gets a single distinct code for both transmitting and receiving in half-duplex mode. As a result, the maximum number of users that can be supported is determined by the code size. When the same system is deployed in an WDMOAN, where transmission and reception can take place simultaneously, a user has to be provided with two separate codes. However keeping in mind the inequality in the traffic intensities in either direction, we assign the codes for the upstream and downstream channels in proportion to the traffic they generate. The heuristic estimate of code count for the upstream and downstream channels using a code size of M is evaluated for a given code-cluster. We denote the total offered traffic due to coded packet transmissions in the code-cluster as G. If the average values of the offered traffic in upstream and downstream directions are G_{up} and G_{dn} respectively, we have $G = (G_{up} + G_{dn})$. This traffic is generated by using the codes supported by an OOC $(n, w, 1)$ whose code size is given by $C_d = (n-1)/[w(w-1)]$. Let the codes assigned for downstream and upstream transmission be N_{dn} and N_{up} and let the average ratio of upstream to downstream traffic be $\beta = (G_{up}/ G_{dn})$. Then the offered load in the upstream and downstream directions is G_{up} =

$G[\beta/(1+\beta)]$ and $G_{dn} = G[1/(1+\beta)]$. However in an OCDMA network, offered load is equal to the number of codes employed for packet transmission. At full load conditions, all the allocated codes C_d constitute the total offered traffic G. In our heuristic approach, we allocate upstream codes in proportion to the traffic ratio β and allocate the balance codes for downstream transmissions so that

$$N_{up} = \left|\left[C_d \frac{\beta}{(1+\beta)}\right]\right| \quad ; \quad N_{dn} = (C_d - N_{up}) \quad \text{and} \quad \beta \sim \left(\frac{N_{up}}{N_{dn}}\right) \qquad (4.1)$$

Thus the code allocation ratio is set equal to the traffic ratio β.

4.3.2 *Optimal Code Allocation based on Open Search around Heuristic Solution*

A proportionate code allocation may not necessarily be an optimum choice in general. The throughput and traffic are not necessarily related linearly and hence the proportional provisioning may not yield the best results. In an attempt to find an optimum code allocation, we therefore adopt a more general method of provisioning in which we examine the code allocations around the heuristic estimate naming it an "open search mode" however with the starting point set at the heuristic (proposed) solution.. There we select a limited range (say over a range of 10-15% of code size) around the heuristic estimate and assign values for upstream code count. The remaining codes are allocated to downstream channels, which effectively determine the cluster-size (users). Let Δ be the incremental deviation of the code allocation from the heuristic estimate. In this approach, for a given deviation Δ, the upstream code count N'_{up} becomes $(N_{up}+\Delta)$ and consequently downstream code count N'_{dn} becomes $(C_d - N'_{up})$. We subsequently examine the impact of this "open search mode" on network provisioning, for different levels of traffic asymmetry, through a throughput model. Next we define some parameters for the model using which we assess the overall PON performance and the effectiveness of the proposed method of code selection.

4.3.3 *Performance Measures for Provisioning Methodology*

While reducing the number of downstream codes (for better upstream contention resolution), one reduces the number of users for each code group and hence for each wavelength. Since the number of wavelengths is limited in a given network setting, this in turn reduces the maximum number of users over the entire network. Thus at the cost of higher upstream throughput one loses the number of users and hence compromise with the network-size. In order to examine this issue (and achieve an optimum trade-off), we define an overall performance measure Q = number of users-total throughput product, which helps in evaluating the overall impact of provisioning on the bidirectional throughput of the PON. Changes in the profile of the performance measure indicate a possible drift in the expected network behaviour. This may help the network designer to avoid certain code allocations while scaling up the network, while supporting a given traffic ratio. On the other hand, a high value for Q indicates quality-ensured provisioning for corresponding code allocation. We also evaluate both upstream and downstream performances separately by their respective aggregate throughputs as a function of code-allocation deviation Δ from the heuristic estimate.

4.4 Performance Evaluation of the Proposed Resource Provisioning Scheme

In this section we develop an analytical model to evaluate the performance of upstream and downstream data throughput. For this purpose, we need to estimate the aggregate throughput in each direction (upstream and downstream). As discussed earlier in our proposed hybrid PON, a channel is defined by a distinct wavelength-code combination. Individual channel performance of any of the $N \times M$ unidirectional channels is similar and is equally affected by simultaneous user interference. The overall throughput is then just N-fold that of a OCDMA-cluster consisting of M unidirectional channels or codes. This indicates that qualitatively the behaviour of PON will be similar to that of the individual code-clusters. Hence we consider the performance of a single OCDMA-based code cluster for a given wavelength, in our analytical model. It is assumed that M encoded data packet transmissions share the fiber medium using slotted ALOHA protocol. We consider two statistical distributions for modeling the network traffic. Further, we identify major factors determining the successful transfer of data streams and derive analytical expressions for each. With the help of these terms a complete throughput model is developed. We utilize this model to evaluate the code allocation schemes discussed in earlier sections.

The packet arrivals in a network under consideration can be reasonably characterized by binomial distribution for finite population and by Poisson distribution for infinite population. If M is the maximum number of transmissions (in this case equal to codes allocated) G in a given direction with an average offered traffic, then the probability of finding k packets in a packet slot is given by the following expressions for Poisson and Binomial cases respectively [Keis97].

$$P(k) = \frac{e^{-G} G^{k}}{k!} \quad \text{(Poisson Distribution)}$$

$$P_M(k) = \binom{M}{k} \left(\frac{G}{k}\right)^{M} \left(1 - \frac{G}{k}\right)^{M-k} \quad for\ k \le M \quad \text{(Binomial Distribution)}$$

$$= 0 \qquad for\ k > M \qquad (4.2)$$

At full load conditions, user transmissions M, allocated codes N and average traffic G all have the same value. Further in an asymmetric OCDMA PON, the values of M, G and N assume different values for each direction. As a result we have $G_{up}=N_{up}=M$ for upstream channels and $G_{dn} = N_{dn} = M$ for downstream channels.

In a multiple access network, the probability of data packets to be delivered successfully is determined by their arrival distribution, by the distinctness of the resource they share (if any) and by the impact of mutual interference to which they are subjected. Especially for upstream channels (which share optical codes) the probability of the code employed for transmission being distinct, decides the success of the data packets. We consider these issues in this section and arrive at a quantitative estimate for each of the above mentioned factors.

4.4.1 *Packet Arrival Probability*

We denote $f_{N_{up}}(k_{up})\ and\ f_{N_{dn}}(k_{dn})$ as the probabilities of arrival of k_{up} and k_{dn} packets on data channels from a code-cluster consisting of N_{up} and N_{dn} codes. We assume full load conditions in both directions, wherein all the allocated codes are used and direction-specific offered loads are given by eqn. 4.1. Making use of eqn. 4.2, the packet arrival probabilities in upstream and downstream directions can be expressed for a Poisson distributed traffic as

$$f_{N_{up}}(k_{up}) = \frac{e^{-N_{up}} (N_{up})^{k_{up}}}{k_{up}!} \qquad (4.3)$$

$$f_{N_{dn}}(k_{dn}) = \frac{e^{-N_{dn}} (N_{dn})^{k_{dn}}}{k_{dn}!} \qquad (4.4)$$

where k_{up} varies from 1 to N_{up} and k_{dn} varies from 1 to N_{dn}. For binomial traffic, the term (G/k) in eqn. 4.2 signifies the average traffic per user which is different for upstream and downstream users. In other words it is the transmission probability of a packet under a given traffic load and we denote it as $p(k_{up})$ for upstream users. The packet arrival probability is given by

$$f_{N_{up}}(k_{up}) = \binom{N_{up}}{k}\left\{(p(k_{up}))^{k_{up}}\right\}\left\{(1-p(k_{up}))^{N_{up}-k_{up}}\right\}$$

In upstream channels, N_{up} packet transmissions are generated from N_{dn} users on an average in each cluster. Thus the transmission probability per upstream user is N_{up} / N_{dn}.

By substituting $p(k_{up}) = N_{up} / N_{dn}$ ($\sim \beta_{trf}$)

$$f_{N_{up}}(k_{up}) = \binom{N_{up}}{k_{up}}\left\{\left(\frac{N_{up}}{N_{dn}}\right)^{k_{up}}\right\}\left\{\left(1-\frac{N_{up}}{N_{dn}}\right)^{N_{up}-k_{up}}\right\} \tag{4.5}$$

For downstream channels, the average traffic per user is unity and in full load condition, there are N_{dn} packets in every slot. The packet arrival probability in the downstream channel is given by

$$f_{N_{dn}}(k_{dn}) = \binom{N_{dn}}{k_{dn}}\left\{\left(\frac{N_{dn}}{N_{dn}}\right)^{k_{dn}}\right\}\left\{\left(1-\frac{N_{dn}}{N_{dn}}\right)^{N_{dn}-k_{dn}}\right\} \tag{4.6}$$

4.4.2 *Probability of Distinct Code Usage*

As mentioned earlier, code allocation for upstream transmission can take advantage of the inherent traffic asymmetry in a PON. This brings in the concept of sharing limited codes amongst a user group judiciously. Our heuristic approach for allocating upstream (shared) codes takes care of the traffic-dependent code contention to some extent. Just the same, since OCDMA PON employs S-ALOHA protocol where the transmissions are un-coordinated, there is a finite probability of two or more users using the same optical code in the same time-slot. We estimate the probability of distinct code usage of k_{up} packet transmissions, denoted by $P_d(k_{up})$ and expressed as a ratio, given by

$$P_d(k_{up}) = \frac{\text{Number of } k_{up} \text{ distinct code transmissions } Q(k_{up})}{\text{Number of combinations } k_{up} - \text{code transmissions } P(k_{up})}$$

wherein the numerator represents total number of possible transmissions which are encoded with k_{up} distinct codes and the denominator represents the total number of k_{up}-transmission attempts. The number of users in a code-cluster willing to participate in upstream transmission is equal to N_{dn}. Then the number of ways k_{up}-transmissions can take place from them is given by $P(k_{up}) = \binom{N_{dn}}{k_{up}}$. These combinations include redundant as well as distinct codes from k_{up} users. Further k_{up} upstream code-transmissions might have been generated from any of the g ($=N_{up}$) code groups where each code group is shared by g_m ($= N_{dn}/g$ approx.) members, contending for the same code. Since there are g distinct code groups, combinations of k_{up}-transmissions (with distinct codes) are given by $\binom{g}{k_{up}}$. Again in every such combination, each code could be from any one of the g_m possible users, giving us $(g_m)^{kup}$ possible user-combinations per every k_{up}-transmissions. Thus we get an overall $\binom{N_{up}}{k_{up}}\{(g_m)^{k_{up}}\}$ number of distinct code combinations which gives $Q(k_{up}) = \binom{N_{up}}{k_{up}}\{(g_m)^{k_{up}}\}$.

Using the expressions for $P(k_{up})$ and $Q(k_{up})$ we get the probability of distinct code usage as

$$P_d(k_{up}) = \frac{\left[\binom{N_{up}}{k_{up}}\{(g_m)^{k_{up}}\}\right]}{\binom{N_{dn}}{k_{up}}} \tag{4.7}$$

Since code allocation for downstream transmissions is done uniquely for each user,

$$P_d(k_{dn}) = 1 \tag{4.8}$$

Next we consider the bit error probability (BER) in data packets due to MUI.

4.4.3 *Probability of Correct Packet Transmission in presence of MUI*

MUI is more detrimental in an access setting where ONUs are capable of supporting bidirectional traffic with their transceivers simultaneously receiving and generating encoded data packets in a duplex mode. We estimate the packet error probability in presence of MUI in a given direction, by taking into account the BER resulting from chip co-incidences (in the code sequence) amongst packets from both directions. We assume that all transmissions are received with equal signal power and MUI is the dominant cause of errors. It is assumed that the codes are sufficiently random so that the bit errors are independent. An encoded data bit [using an OOC (n, w, 1)] experiences chip coincidence with a probability of w^2/n, from each one of i interfering codes (corresponding to simultaneous transmissions). It is the probability with which coincidences occur at w on-chip positions in the code sequence of n chips (the probability of chips being in 'on-state' is w/n). Coincidences translate into bit errors when i exceeds the detection threshold (= w) which sets the lower limit for i. Using these observations, we derive the packer error probability in upstream and downstream channels in the following.

Upstream Channels:

For upstream transmission, the total interference k_{int}, that an upstream data packet encounters is equal to $(k_{up}-1+k_{dn})$. Further while considering the interference from downstream users k_{dn} (which varies from 1 to N_{dn}), the corresponding arrival probability is also taken into consideration. We use the BER expression developed for our earlier work on multi-wavelength OCDMA systems [RaDa04], which expresses the BER of k_{up} transmissions as the sum of coincidence probabilities from all combinations of i interferers. Thus we get the expression for bit error probability for upstream channel as

$$P_{BER}=\left[\sum_{i=w}^{k_{int}} f_{N_{dn}}(k_{dn})\binom{k_{int}}{i}\left\{\left(\frac{w^2}{n}\right)\right\}^i\left\{\left(1-\frac{w^2}{n}\right)^{k_{int}-i}\right\}\right] \tag{4.9}$$

The probability of successful packet transmission $P_C(k_{up})$ for a data packet length of P_{len} is given by $P_c(k_{up})=(1-P_{len}\,P_{BER})$. Substituting for P_{BER} from eqn. (4.9) we obtain $P_c(k_{up})$ for Poisson and Binomial traffic models as

$$P_c(k_{up})=1-\left[P_{len}\left\{f_{N_{dn}}(k_{dn})\right\}\left[\sum_{i=w}^{k_{int}}\binom{k_{int}}{i}\left\{\left(\frac{w^2}{n}\right)\right\}\left\{\left(1-\frac{w^2}{n}\right)^{k_{int}-i}\right\}\right]\right] \tag{4.10}$$

where,

$$f_{N_{dn}}(k_{dn})=\frac{e^{-N_{dn}}(N_{dn})^{k_{dn}}}{k_{dn}!}\ \text{and}\ k_{int}=(k_{up}-1+k_{dn}) \qquad \text{(Poisson traffic)}$$

$$f_{N_{dn}}(k_{dn})=\binom{N_{dn}}{k_{dn}}\left\{\left(\frac{N_{dn}}{N_{dn}}\right)^{k_{dn}}\right\}\left\{\left(1-\frac{N_{dn}}{N_{dn}}\right)^{N_{dn}-k_{dn}}\right\}\ \text{and}\ k_{int}=(k_{up}-1+k_{dn})$$

(Binomial traffic)

Downstream Channels:

Similarly the expression for successful packet transmission in downstream channels is given by

$$P_c(k_{dn}) = 1 - \left[P_{len} \left\{ f_{N_{up}}(k_{up}) \right\} \left[\sum_{i=w}^{k_{int}} \binom{k_{int}}{i} \left\{ \left(\frac{w^2}{n} \right) \right\} \left\{ \left(1 - \frac{w^2}{n} \right)^{k_{int}-i} \right\} \right] \right] \qquad (4.11)$$

where,

$$f_{N_{up}}(k_{up}) = \left\{ \frac{e^{-N_{up}} (N_{up})^{k_{up}}}{k_{up}!} \right\} \text{ and } k_{int} = (k_{dn} - 1 + k_{up}) \text{ (Poisson)}$$

$$f_{N_{up}}(k_{up}) = \binom{N_{up}}{k_{up}} \left\{ \left(\frac{N_{up}}{N_{dn}} \right)^{k_{up}} \right\} \left\{ \left(1 - \frac{N_{up}}{N_{dn}} \right)^{N_{up}-k_{up}} \right\} \text{ and } k_{int} = (k_{dn} - 1 + k_{up}) \text{ (Binomial)}$$

4.4.4 *Data Throughput*

In the following, we finally construct the complete model for the system throughput in an OCDMA system. We assume that the bidirectional transmissions are completely independent of each other and that the data traffic is uniformly distributed in the ONU-cluster. The throughput probability for k_{up} packets $S(k_{up})$ is given by the product of the probability of packet arrival, the probability of distinctness of the codes used and the probability of successful packet transmission in the presence of MUI. Hence the throughput in the upstream channels is the sum total of success probabilities of all such k_{up} transmissions expressed as

$$S_{up} = \sum_{k_{up}=1}^{N_{up}} k_{up} \left\{ f_{N_{up}}(k_{up}) \right\} \left\{ P_d(k_{up}) \right\} \left\{ P_c(k_{up}) \right\} \qquad (4.12)$$

where, k_{up} is the number of upstream transmissions, $f_{Nup}(k_{up})$ is the probability of packet arrival, $P_d(k_{up})$ is the probability of distinct code usage and $P_c(k_{up})$ is the probability of successful packet transmission.

Using similar approach the throughput expression for downstream channels is given by

$$S_{dn} = \sum_{k_{dn}=1}^{N_{dn}} k_{dn} \left\{ f_{N_{dn}}(k_{dn}) \right\} \left\{ P_c(k_{dn}) \right\} \qquad (4.13)$$

Next we consider the two approaches for the shared upstream codes while evaluating the overall throughput.

Case 1: Shared Codes with Code Contention

Under this approach, upstream transmissions are un-coordinated, and hence if two or more users, desirous of sending data, might be contending for the same code. This results in failure of all the attempted transmission and in turn brings down the channel throughput. In section 4.4.2, we derived an expression for distinct code usage probability applicable to such situations. We also estimated the packet arrival probability, and packet error probability for unidirectional traffic. Substituting these expressions in eqns. 4.12 and 4.13, we get the overall throughput for upstream channels S^{up} for Poisson and Binomial traffic in the following. The overall upstream throughput S^{up} for each of the two traffic models is expressed as:

$$S^{up}_{poisson} = \sum_{k_{up}=1}^{N_{up}} k_{up} \left\{ \frac{e^{-N_{up}} (N_{up})^{k_{up}}}{k_{up}!} \right\} \cdot \left[\frac{\left[\binom{N_{up}}{k_{up}} \left\{ (g_m)^{k_{up}} \right\} \right]}{\binom{N_{dn}}{k_{up}}} \right] \cdot \left\{ 1 - \left[P_{len} \left\{ f_{N_{dn}}(k_{dn}) \right\} \sum_{i=w}^{k_{int}} \left\{ \binom{k_{int}}{i} \right\} \left\{ \left(\frac{w^2}{n} \right)^i \right\} \left\{ \left(1 - \frac{w^2}{n} \right)^{k_{int}-i} \right\} \right] \right\}$$

where,

$$f_{N_{dn}}(k_{dn}) = \frac{e^{-N_{dn}} (N_{dn})^{k_{dn}}}{k_{dn}!} \text{ and } k_{int} = (k_{up} - 1 + k_{dn}) \tag{4.14}$$

$$S^{up}_{binomial} = \left\{ \sum_{k_{up}=1}^{N_{up}} k_{up} \left[\binom{N_{up}}{k_{up}} \left(\frac{N_{up}}{N_{dn}} \right)^{k_{up}} \left(1 - \frac{N_{up}}{N_{dn}} \right)^{N_{up}-k_{up}} \right] \cdot \left\{ \frac{\left[\binom{N_{up}}{k_{up}} (g_m)^{k_{up}} \right]}{\binom{N_{dn}}{k_{up}}} \right\} \cdot \left\{ 1 - \left[P_{len} f_{N_{dn}}(N_{dn}) \sum_{i=w}^{k_{int}} \binom{k_{int}}{i} \left(\frac{w^2}{n} \right)^i \left(1 - \frac{w^2}{n} \right)^{k_{int}-i} \right] \right\} \right\}$$

where,

$$f_{N_{dn}}(k_{dn}) = \binom{N_{dn}}{k_{dn}} \left\{ \left(\frac{N_{dn}}{N_{dn}} \right)^{k_{dn}} \right\} \left\{ \left(1 - \frac{N_{dn}}{N_{dn}} \right)^{N_{dn}-k_{dn}} \right\} \text{ and } k_{int} = (k_{up} - 1 + N_{dn}) \tag{4.15}$$

Similarly overall throughput S^{dn} for downstream traffic can be obtained for the two traffic models as

$$S^{dn}_{poisson} = N_{dn} \cdot \left\{ 1 - \left[P_{len} \left\{ f_{N_{up}}(k_{up}) \right\} \left\{ \sum_{i=w}^{k_{int}} \left\{ \binom{k_{int}}{i} \left(\frac{w^2}{n} \right)^i \left(1 - \frac{w^2}{n} \right)^{k_{int}-i} \right\} \right\} \right] \right\} \tag{4.16}$$

where,

$$f_{N_{up}}(k_{up}) = \left\{ \frac{e^{-N_{up}} (N_{up})^{k_{up}}}{k_{up}!} \right\} \text{ and } k_{int} = (k_{dn} - 1 + k_{up})$$

$$S^{dn}_{binomial} = N_{dn}\left\{1-\left[\left\{P_{len}\left\{f_{N_{up}}(k_{up})\right\}\right\}\left\{\sum_{i=w}^{k_{int}}\binom{k_{int}}{i}\left(\frac{w^2}{n}\right)^i\left(1-\frac{w^2}{n}\right)^{k_{int}-i}\right\}\right]\right\} \quad (4.17)$$

where,

$$f_{N_{up}}(k_{up}) = \left[\binom{N_{up}}{k_{up}}\left\{\left(\frac{N_{up}}{N_{dn}}\right)^{k_{up}}\right\}\left\{\left(1-\frac{N_{up}}{N_{dn}}\right)^{N_{up}-k_{up}}\right\}\right] \text{ and } k_{int} = (k_{dn}-1+k_{up})$$

Case2: Shared Codes with Contention Avoidance

In order to improve the throughput performance in the upstream channels, pre- transmission coordination mechanisms can be employed by which code contention is avoided in the upstream broadcast channels. Through a separate control channel from the OLT, the ONUs can be informed of the status of the unused optical codes available for upstream transmission. With this information, new packet transmissions will refrain from contending for already acquired codes in the current time-slot. Instead they attempt after a finite duration as determined by the algorithm, the MAC protocol supports. This makes the distinct code usage probability for upstream channels, unity. The corresponding throughput expressions for upstream and downstream channels are given in the following.

Upstream throughput can be expressed as

$$S^{up}_{poisson} = \sum_{k_{up}=1}^{N_{up}} k_{up}\left\{\frac{e^{-N_{up}}(N_{up})^{k_{up}}}{k_{up}!}\right\}\left\{1-\left[P_{len}\left\{f_{N_{dn}}(k_{dn})\right\}\left\{\sum_{i=w}^{k_{int}}\binom{k_{int}}{i}\left\{\left(\frac{w^2}{n}\right)^i\right\}\left\{\left(1-\frac{w^2}{n}\right)^{k_{int}-i}\right\}\right\}\right]\right\} \quad (4.18)$$

where,

$$f_{N_{dn}}(k_{dn}) = \frac{e^{-N_{dn}}(N_{dn})^{k_{dn}}}{k_{dn}!} \text{ and } k_{int} = (k_{up}-1+k_{dn})$$

$$S^{up}_{binomial} = \sum_{k_{up}=1}^{N_{up}} k_{up}\left\{\binom{N_{up}}{k_{up}}\left\{\left(\frac{N_{up}}{N_{dn}}\right)^{k_{up}}\right\}\left\{\left(1-\frac{N_{up}}{N_{dn}}\right)^{N_{up}-k_{up}}\right\}\right\}\left\{1-\left[P_{len}\left\{f_{N_{dn}}(N_{dn})\right\}\left\{\sum_{i=w}^{k_{int}}\binom{k_{int}}{i}\left\{\left(\frac{w^2}{n}\right)^i\right\}\left\{\left(1-\frac{w^2}{n}\right)^{k_{int}-i}\right\}\right\}\right]\right\} \quad (4.19)$$

where,

$$f_{N_{dn}}(N_{dn}) = \binom{N_{dn}}{k_{dn}}\left\{\left(\frac{N_{dn}}{N_{dn}}\right)^{k_{dn}}\right\}\left\{\left(1-\frac{N_{dn}}{N_{dn}}\right)^{N_{dn}-k_{dn}}\right\} \text{ and } k_{int} = (k_{up}-1+k_{dn})$$

Since contention avoidance in the upstream channel does not affect the downstream channels, corresponding expressions for downstream throughput are given by eqn.s 4.16 and 4.17 in collision avoidance case too. Next using eqns. 4.16 and 4.19, we evaluate the data throughput for upstream and downstream channels for different values of code allocation around the heuristic solution in an "open search mode" as mentioned in Section 4.3.2.

4.5 Results and Discussion

We examine the role of the proposed resource provisioning scheme (through appropriate code allocation) in optimizing the performance of W-OCDM PON with asymmetric traffic. In this context, we choose an optical code (OOC: [364, 4, 1]) of size 30 to provision the bidirectional traffic in the code-cluster. Each cluster in the hybrid PON configuration operates on a separate wavelength with same data rate of 2.4/2.4 Gbps for downstream/upstream transmission. Thus, each of the 30 encoded data channels (including upstream and downstream) can effectively operate at 6.6Mbps (=2400/364) using the 2.4 Gbps link. We represent the channel throughput as the aggregate data rate as determined by the product of throughput S and operating channel data rate in Mbps, for a given direction. We consider a data packet length P_{len}= 75 Bytes for evaluating the throughput performance in the upstream and the downstream. However, we also show some results for different packet sizes, in order to illustrate certain aspects on the choice of packet length for the PON under consideration.

By using our heuristic approach, we first determine the codes to be allocated for a given traffic ratio β and evaluate the aggregate channel throughput (i.e., the total throughput for all the codes for a given wavelength or channel) in either directions. Next we vary this estimate for the number of upstream codes and leave the rest for downstream traffic. Thus the number of ONUs (or users) that can be supported by the PON becomes equal to the available number of downstream codes. The deviation Δ (defined earlier in Sec. 4.3.2) from the heuristic estimate (of upstream codes) is treated as an independent variable. Thus, positive values of Δ (on x-axis) in the following plots correspond to an increase in upstream code-allocation as compared to the heuristic value and a consequent decrease in the user count. On the other hand, negative values of code deviation correspond to an increase in user count at the cost of more code contention for upstream transmission. We chose four different traffic scenarios for the PON under consideration, based on the relative level of upstream traffic as compared to the downstream. Thus a low-level upstream traffic PON was assumed to have a traffic ratio β

= 0.25. Similarly, the other three cases considered for our studies are as follows: for a medium-level upstream traffic $\beta = 0.5$, for a high-level upstream traffic $\beta = 0.75$ and for a very high-level upstream traffic $\beta = 0.9$.

In the following, we present the results of our investigations in three parts:

- Upstream Performance (Case 1: Shared codes with code contention; Case 2: Shared codes with code contention avoidance)
- Downstream Performance
- Overall PON Performance

Upstream Performance

In this section, we present the PON performance of the upstream transmission for shared codes with and without code contention. We found that, in general, the plots of aggregate throughput versus Δ for various cases of traffic ratio β, exhibit a lower cut-off on Δ-axis which may extend beyond (above) the heusistic estimate (i.e., Δ = 0) into the over-provisioned region ($\Delta > 0$) depending upon the traffic ratio β. Basically this is the region over which an upstream data packet is unable to overcome the combined effect of code contention for shared codes as well as MUI from simultaneous transmissions, resulting in practically negligible output. Subsequently, as the number of allocated codes for upstream is increased (i.e., Δ is increased further), the situation improves with more successful transmissions contributing to the upstream throughput. We call the point at which throughput starts rising as "cut-off point" and the aggregate throughput corresponding to this cut-off point as "throughput threshold" (assumed to be about 2 Mbps in the present discussion). For example, with $\beta \geq 0.5$, cut-off point appears at $\Delta = +2$. Next we discuss the results in further details both with and without code contentions.

Case 1: Shared Codes with Code Contention

The plots in Fig. 4.4 present the throughput performance (aggregate throughput vs. Δ) in upstream channels in presence of code contention for $P_{len} = 75$ Bytes for binomial traffic. We also studied the throughput for a smaller packet size (of 20 Bytes) and a longer packet size (of 150 Bytes) in order to show the change in performance characteristics with packet length. However most of our observations are based on the packet size of 75Bytes.

It is observed that, in the PONs with $\beta = 0.25$, the cut-off point appears at $\Delta = +4$ and the aggregate upstream throughput remains rather low even beyond the cut-off point. In fact, the throughput remains low due to the overbearing effect of MUI from a relatively large number of downstream transmissions (at this traffic ratio). Since code contention is not a major issue for low β, there occurs very little improvement with additional codes allocated for upstream users. In PONs with $\beta \geq 0.5$, data packets experience relatively less interference from the opposite stream, but are subject to code contention which results in shorter cut-off value ($\Delta = +2$). Thereafter the situation improves markedly as the allocated code count exceeds the throughput threshold point, allowing the packets to recover from code contention and produce successful transmissions. The data throughput reaches a peak as seen

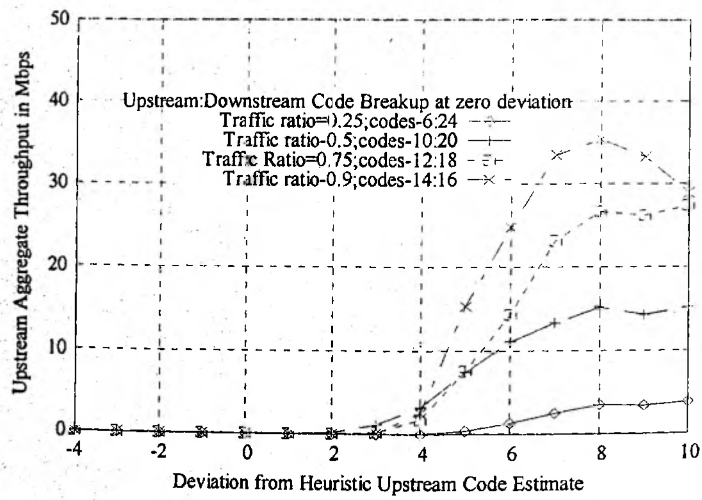

Fig. 4.4. Effect of code allocation on upstream aggregate throughput with symmetric speed of 2.4Gbps; Upstream bandwidth-per-user=6.6 Mbps; Binomial traffic; Shared codes with code contention; Packet Size=75B

in the plot and we find that increased allocation of upstream codes benefits PONs with $\beta \geq 0.75$ relatively more. Beyond this stage ($+8 \leq \Delta \geq +10$), the aggregate throughput either remains constant as for PONs with $\beta \leq 0.75$ or, gradually falls as in the case for PONs with higher upstream traffic ($\beta \leq 0.9$). The fall of aggregate throughput in the latter case takes place in spite of the increase in per-user throughput (due to larger number of codes) because, with increase in Δ, fewer codes can be allocated for downstream transmission implying thereby a decrease in the number of users in the network itself.

Next we assess the impact of decreasing the cluster size (say, over-provisioning by two codes beyond the peak throughput from $\Delta = +8$ to $+10$), under different traffic scenarios (β values). For instance, in the case of PONs with $\beta = 0.25$, it results in a decrease in the user-count (= downstream codes) from 16 to 14 (i.e., a 13% reduction in provisioned size) and a corresponding increase in per-user upstream throughput from 1.0Mbps (= upstream throughput at Δ / (reduced user count × traffic ratio) to 1.33Mbps i.e., a 33% increase. For a PONs with β = 0.5, a 17 % reduction in cluster size results in 20% increase in per-user upstream throughput. On the other hand for a high-level traffic PONs with β = 0.75, this provisioning results in a 20% reduction in cluster size for a corresponding 48% increase in per-user upstream throughput. For PONs with β = 0.9, a 25 % reduction in cluster size results in 16% increase in per-user upstream throughput.

At this stage it is also interesting to examine the corresponding change in code sharing ratio for the aforesaid over-provisioning. We find that for PONs with β = 0.25, code sharing ratio (codes: user) decreases from 14:16 at peak throughput to 16:14 (i.e., from 0.88 to 1.14). This is equivalent to a 30% decrease in code sharing for a corresponding 33% increase in per-user upstream rate for low-level traffic PONs. For PONs with β = 0.5, this results in a decrease in code-sharing, from 18:12 to 20:10 code/ user i.e., by 33% for a corresponding 20% increase in user rate. On the other hand for PONs with β = 0.75, this results in a decrease in code-sharing, from 20:10 to 22:8 code/ user i.e., by 38% for a corresponding 48% increase in user rate. On the other hand in PONs with β = 0.9, the code sharing decreases by 45% (22:8 to 24:6 of code/user ratio) for a 16% rise in per-user upstream rate. By and large, it is observed that in all cases, over-provisioning beyond the peak performance range results in wastage of resources in spite of the per-user-throughput advantage (codes in excess of users). On the other hand, over-provisioning within the peak region is expected to offer better resource utilization and upstream throughput as well.

In Fig.4.5 we present the plots of upstream aggregate throughput with P_{len}=150 Bytes, which exhibit similar behaviour as in Fig.4.4 but with extended cut-off points and lower

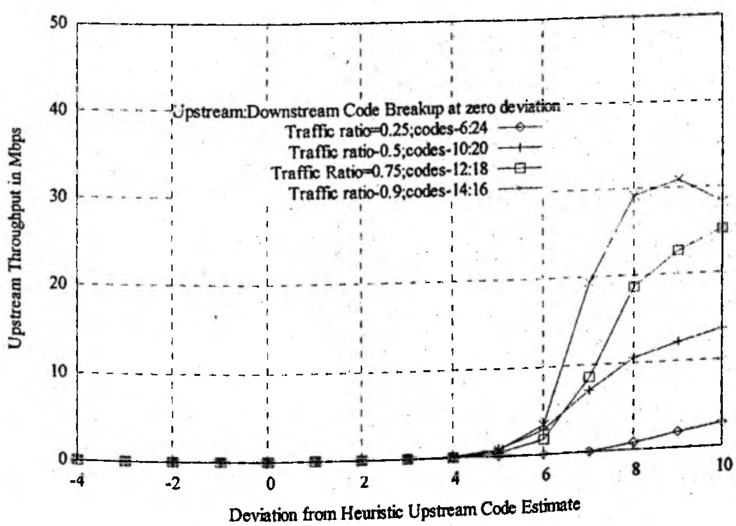

Fig. 4.5. Effect of packet length on upstream throughput with code contention; Upstream bandwidth-per-user=6.6 Mbps; Binomial traffic; Packet Size = 150B

Table 4.1. Some Optical Orthogonal Codes and their Characteristics

Code Weight Category	**Code Characteristic** $C=(n,w,\lambda)$	**Code Size** $\lvert C\rvert=[(n-1)/w(w-1)]$
(n,3,1)	(31,3,1)	5
	(63,3,1)	10
	(127,3,1)	21
	(255,3,1)	42
	(511,3,1)	85
	(1023,3,1)	170
	(2047,3,1)	341
	(4095,3,1)	682
(n,4,1)	(40,4,1)	3
	(121,4,1)	10
	(364,4,1)	30
	(1093,4,1)	91
	(3280,4,1)	273
(n,5,1)	(85,5,1)	4
	(341,5,1)	17
	(1365,5,1)	68
	(5461,5,1)	273
(n,6,1)	(156,6,1)	5
	(631,6,1)	21
	(3156,6,1)	105

throughput values. Thus the higher packet lengths may reduce the throughput for the specific optical code we have chosen due to more MUI and code contention. Since longer packets would need more upstream codes to overcome MUI, the supported size of the PON would also be lowered. Indeed longer packets can be used in the given network with a different set of OOCs characterized by longer code lengths and code weights in order to overcome the above problems. Table 4.1 gives the list of such OOCs with the corresponding code sizes, which were developed by Chung *et al.* [ChSa89]. However, we carried out our subsequent studies with P_{len}=75 Bytes as an example case study and would be exploring the longer packet sizes in our future studies.

Case 2: Shared Codes with Code Avoidance:

In this section, we examine the influence of contention avoidance scheme on the aggregate channel performance. Figure 4.6 illustrates the impact of contention avoidance on the aggregate upstream throughput for different data packet sizes. For both the β values we considered (0.25 and 0.5), smaller packet size reduces the cut-off point for Δ and thus throughput threshold appears for lower values of Δ than in the code contention case. For example, in a W-OCDM PON with $\beta = 0.5$, throughput threshold appears at $\Delta = +2$ for 75 Byte packets and at $\Delta = -4$ for 20 Byte packets. When $\beta = 0.25$, the impact of contention avoidance is slightly lower as expected, because of the reduced need for contention relief. It is also observed from Figs.4.4 and 4.6 that for a longer packet size (as for 75 Bytes) contention avoidance does not have any significant impact on the throughput. Thus, by using

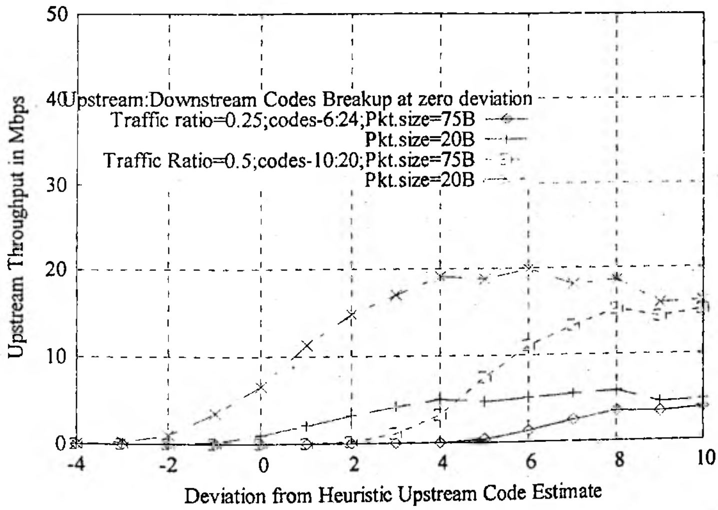

Fig. 4.6. Effect of code allocation on upstream throughput with varying packet size; Upstream bandwidth-per-user=6.6 Mbps; Binomial traffic; Shared codes with contention avoidance

the control channel information (regarding acquired codes) the network is able to overcome code contention and interference at an early stage with fewer number of shared codes (provided the packet size is not large for the chosen OOC). The early appearance of cut-off point suggests good prospects for scaling up the network. However for PONs with $\beta \geq 0.5$, the cut-off points get closer to our heuristic estimate with contention avoidance. Also the network recovers more gracefully from code contention as indicated by the smoother throughput curves as we increase the upstream codes (i.e., increasing Δ).

So far our results were based on Binomial traffic model of the hybrid PON. Figure 4.7 shows the throughput performance for a PON with Poisson traffic model with code contention. We find that, the throughput performance of Poisson traffic is observed to be better as compared to the Binomial traffic for PONs with low upstream traffic $\beta = 0.25$. On the other hand PONs with $\beta \geq 0.5$ show lower throughput as compared to those obtained with Binomial traffic (in Fig.4.4). It is further observed that the cut-off value of Δ corresponding to throughput threshold for $\beta \leq 0.5$ corresponds to our heuristic estimate for code allocation.

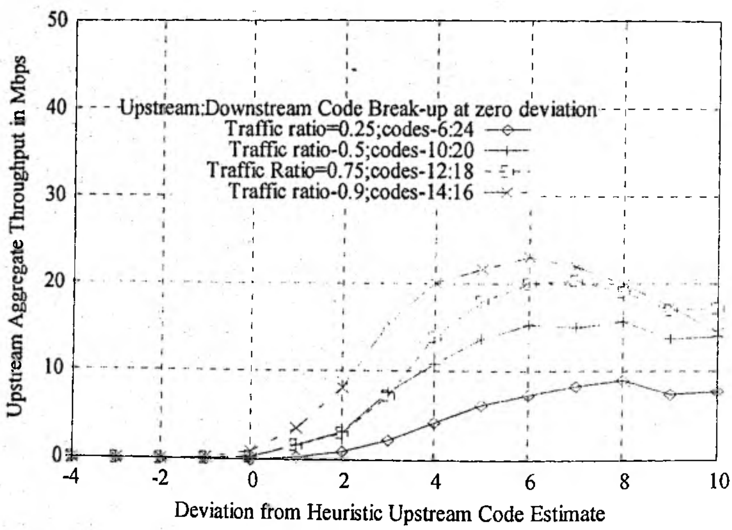

Fig.4.7. Effect of code allocation on upstream throughput; Upstream bandwidth-per-user= 6.6.Mbps; Poisson traffic model; Shared codes with code contention; Packet Size = 75B

Downstream Performance

Next we study the throughput performance of Binomial traffic in the downstream channels for different values of traffic ratio. It is observed from Fig. 4.8 that, the downstream channels exhibit a cut-off point similar to the upstream channels for a data packet size of 75 Bytes. We find that, throughput threshold for PONs with $\beta = 0.25$ appears to be same as the heuristic estimate, whereas higher upstream traffic needs increased upstream code allocation to recover from contention and MUI. Peak values of downstream throughput correspond to $\Delta = +8$ for all four traffic ratios. Thereafter PONs with $\beta > 0.5$ become more sensitive to code allocation showing rapid fall in their aggregate throughput levels as compared to the PONs with lower upstream traffic. This occurs because, at low β, the downstream throughput is from a major fraction of the user group, whose transmissions are minimally affected by those in the opposite (upstream) channels. By over-provisioning, downstream user number is reduced,

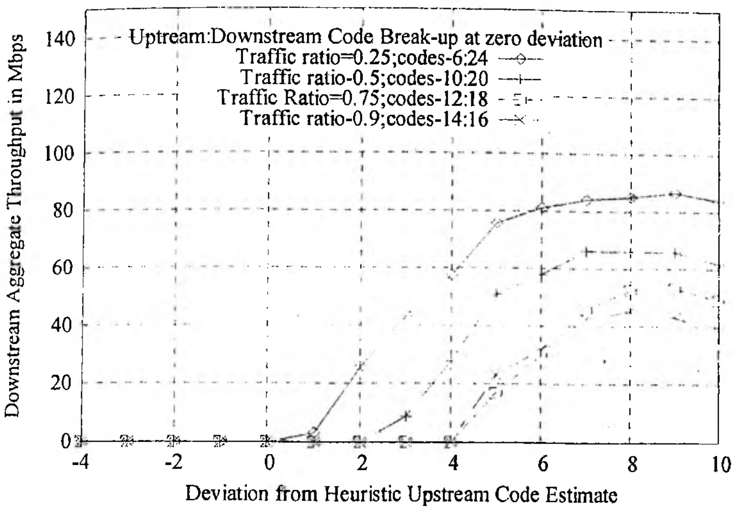

Fig. 4.8. Effect of code allocation on downstream throughput; Binomial traffic model; Downstream bandwidth-per-user=6.6 Mbps; Data packet size = 75 B

thereby lowering the aggregate values. But individual data rates are not much affected due to very low interference from the traffic in the opposite direction. It is also noticed that for the same value of Δ, aggregate data rates differ significantly with β. This is because the same value of code deviation leads to a different degree of provisioning for different data traffic ratios. However this difference reduces for β beyond 0.75 where the performance curves tend to converge.

Overall PON Performance

So far we examined the impact of both upstream and downstream transmissions on the performance of either upstream or downstream throughput, (i.e., one at a time for different traffic ratios and code allocations. In the following, we examine the code allocation scheme used for provisioning the entire W-OCDM PON, in terms of the overall network performance measure Q defined in Section 4.3.3.

Figure 4.9 presents the plots of Q vs. Δ for the four values of β, wherefrom we can assess the overall performance of the PON and arrive at an appropriate (optimum) resource provisioning. From Fig. 4.9, it is evident that, the PONs with lower upstream traffic β enjoy relatively better overall throughput performance in terms of Q. This is because they spare more number of codes to admit new users, who in turn incrementally increase the throughput in both upstream and downstream directions. This is indicated by higher values of Q for $\beta \leq$

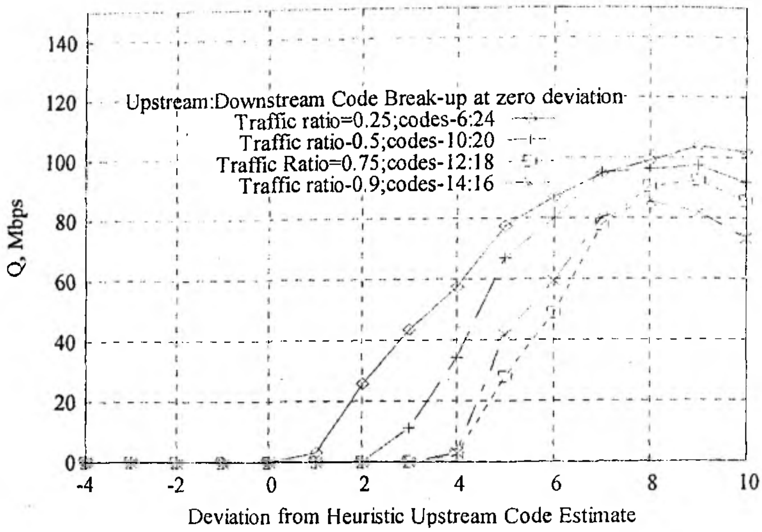

Fig.4.9. Total number of users- total throughput product Q2 versus code allocation deviation; Packet size=75B; Shared codes with contention; Binomial traffic

0.5 than for $\beta \geq 0.5$ at $\Delta = +7$. Further, it is understood from the plots that, the PONs with lower traffic ratios can support more number of users to obtain the same level of overall performance. Also we find that the performance of a W-OCDM PON becomes more sensitive with Δ for increasing upstream traffic which limits the scalability of the network for the corresponding traffic ratio.

4.6 Summary

In this chapter we examined the provisioning aspects in a hybrid PON which employs both WDM and OCDMA technologies. Provisioning in such a network essentially consists of allocating channels or resources for both improved throughput performance and to achieve a balance between expected (as per average traffic pattern) and actual data transfer rates. Optical codes and wavelengths are the resources in the hybrid PON under consideration. In our work we adopted a heuristic approach for allocating codes to the ONUs/users which takes into consideration the traffic asymmetry between the upstream and downstream transmissions. We developed an analytical model for system throughput taking into consideration the effects of interference and code contention in the upstream channels which helps in understanding the behaviour of a network with asymmetric traffic. Two separate throughput models based on Binomial and Poisson traffic distributions were formulated and compared. Further we studied the under-provisioned and over-provisioned (with reference to the heuristic allocation) regions using an open search mode of code allocation with fixed resources. We propose a few figures of merit which helped us draw useful conclusions on the overall system performance.

This method of allocating codes might tilt the balance between the bidirectional traffic with reference to the average traffic. In the process the network gets either under-provisioned or over-provisioned with respect to the heuristic estimate. Depending upon the relative traffic intensity in the upstream and downstream, variation in degree of provisioning Δ might in some situation, benefit the data traffic with higher intensity, while sacrificing only a nominal amount of service quality for data traffic with lower intensity.

References

[ChSa89] F. R. K. Chung, J. A. Salehi, "Optical Orthogonal Codes: Design, Analysis and Applications," *IEEE Transactions on Information Theory*, vol. 35, no. 3, pp. 595-604, May 1989.

[FaMR04] C. Fan, M. Maier and M. Reisslein, "The AWG-PSC network: A performance enhanced single-hop network with heterogeneous protection," *IEEE/OSA Journal of Lightwave Technology*, vol. 24, no. 5, pp. 1242 – 1262, May 2004.

[HWWK06]T. Hamanaka, X. Wang, H. Wada, A. Nishiki and K. Kitayama, "Ten-user truly asynchronous gigabit optical CDMA transmission experiment with 511-chip SSFBG En/Decoder," *IEEE/OSA Journal of Lightwave Technology*, vol. 24, no. 1, pp. 95 – 102, Jan 2006.

[Jaya00] R. Jayashree, "Optical CDMA in Broadband Communication - Scope and Applications," *Journal of Optical Communications*, vol. 23 (2002) 1, pp. 11-21.

[Kami05] N. Kamiyama, "A Large-scale AWG-based single-hop WDM network using couplers with collision avoidance," *IEEE/OSA Journal of Lightwave Technology*, vol. 23, no. 7, pp. 2194 – 2205, Jul. 2005.

[Keis97] G. E. Keiser, "*Local Area Networks*," Tata McGraw Hill Ltd., India, 1997 Edition.

[KiWW06]K. Kitayama, X. Wang and N. Wada, "OCDMA over WDMPON- Solution path to gigabit-symmetric FTTH," *IEEE/OSA Journal of Lightwave Technology*, vol. 24, no. 4, pp. 1654-1662, Apr. 2006.

[MaVi98] S. V. Maric and Vincent K. N. Lau, "Multi rate fiber–optic CDMA: System design and performance analysis," *IEEE/OSA Journal of Lightwave Technology*, vol. 16, no. 1, pp. 9 – 17, Jan. 1998.

[RaDa02] Jayashree Ratnam and Debasish Datta, "Performance evaluation of a packet switched multi-wavelength optical CDMA network," *Journal of Optical Communications*, vol. 27 (2006) 5, 273 - 277.

[Rayc81] D. Raychaudhuri, "Performance analysis of random access packet-switched code division multiple access systems," *IEEE Transactions on Communications*, vol. 29. no. 6, pp. 895–901, Jun. 1981.

[SaBr89] J. A. Salehi and C. A. Brackett, "Code division multiple access techniques in optical fiber networks-part II: Systems performance analysis," *IEEE Transactions on Communications*, vol. 37, no. 8, pp. 834–842, Aug. 1989.

[Sale89] J. A. Salehi, "Code Division Multiple - Access Techniques in Optical Fiber Networks-Part I: Fundamental Principles," *IEEE Transactions on Communications*, vol. 37. no. 8., pp. 824 – 833, Aug. 1989.

[StSa02] A. Stok and E. H. Sargent, "The Role of optical CDMA networks in access networks," *IEEE Communication Magazine*, pp. 83- 87, Sept. 2002.

[ToCY99] G. E. Town, K. Chan and G. Yoffe, "Design and performance of high-speed optical pulse-code generators using optical fiber bragg gratings," *IEEE Journal of Selected Topics in Quantum Electronics*, 5(5): 1325-1331, Sep./Oct. 1999.

[TPIR01] P.C. Teh, P. Petropoulos, M. Ibsen, and D. J. Richardson, "A comparative study of the performance of seven- and 63-chip optical code-division multiple-access encoders and decoders based on super structured fiber bragg gratings," *IEEE/OSA Journal of Lightwave Technology*, vol.19, no. 9, 1352-1364, Sept. 2001.

CHAPTER 5

Transmission Impairments in a WDMPON Employing AWG-based Remote Node

5.1 Introduction

As discussed earlier in Chapter 1, a dedicated wavelength-per-channel preserves the bit rate and protocol transparency of a service, both of which are valuable features for a rapid growing access segment. A WDMPON might consist, in general, several clusters of ONUs, each one terminating at a business house or an individual home. The clusters would usually be interconnected in a star or a tree topology to the OLT located on the access backbone. This backbone is usually a ring, which connects the PON to higher levels of network hierarchy as discussed in Chapter 3. Over the last decade, this segment alone has grown to such an extent that, considerable research effort has been made on studying appropriate topologies and device technologies for the PONs to sustain. For such PONs, with medium- to long-reach spans (10-20 km), tree topology would prove more cost effective. Such realization of PONs, with tree topology usually employs one or more stages of RN in between an OLT and ONUs, wherein an RN uses a passive device for collection/distribution of upstream/downstream wavelength channels [McBa00]. The passive device can be a PSC or an AWG. PSC's power splitting losses make it unsuitable for high port-counts. An AWG is an imaging device with wavelength-dependent focusing and dispersive properties. A WDM signal undergoes a wavelength-dependent phase delay as it traverses this AWG towards the output port [SmDa96], which results in a static wavelength-routing pattern for individual channels. Thus it can be an ideal WDM multiplexing/ demultiplexing device for RN without incurring the power-splitting loss experienced in PSC.

Further, AWG is amenable to large scale IC fabrication using waveguide technology and, as such, has been continuously worked upon for improvement by several photonic-component research groups [Smit88], [TSKN90], [Mcgr98]. Silica-based AWGs with very low insertion loss (3-4 dB), good crosstalk levels (30 to 35 dB) [TaOT96], high fiber-coupling efficiency and polarization independence were reported (as discussed in Chapter 2). Since the device loss does not increase with port count, AWG is ideally suitable for scaling up a cost-sensitive WDMPON. Takahashi *et.al* reported 1 nm resolution capability of the AWG-based demultiplexer at 1.3 μm [TSKN90], proving its suitability for PONs supporting dense WDM (DWDM) transmission.

In order to sustain the huge growth potential in the access segment, and to justify the additional inventory costs involved both at the OLT and ONU for WDMPONs, service quality should be ensured within the allocated power budget. Furthermore, for minimizing the budget overheads as well as to ensure fail-safe operation of the network, one needs to gain good insight into the physical layer issues of the optical channels. By identifying major transmission impairments under given operating conditions and by assessing the extent to which they can influence signal quality, one can gain full control over the network operation and its upgradeability. For instance in an RN, a downstream WDM signal might be subjected to several transmission impairments due to signal attenuation, crosstalk from co-propagating channels and beat noise (due to square law photodetection process) apart from the signal-dependent shot noise and the thermal noise at the receiver end. In addition, power variations at various AWG ports and non-ideal lasers with finite linewidth can further deteriorate the receiver performance at both OLT and ONU.

Some useful investigations have been reported on transmission characteristics and crosstalk-related BER degradation in AWG devices through analytical as well as experimental studies [TOTI95]. Further, some important physical-layer limitations of wavelength-routed signals in long-haul networks were examined in [RDFM99]. In the present work, we attempt to model some of the relevant features of AWG, in presence of non-ideal lasers with finite linewidth, and use the model to evaluate the BER performance of various optical channels received at the ONUs through the output ports of AWG. The rest of the chapter is organized as follows. Section 5.2 describes the network configuration and the important characteristics of AWG. In Section 5.3 we discuss about the transmission impairments and analytically evaluate the signal power captured at various output ports through a novel spectral-to-spatial transformation. Thereafter, we develop a BER model for the optical channels, which captures major impairments in the WDMPON. Finally, we discuss the implications of the results obtained from the numerical evaluation of the BER. Section 5.5 presents the summary.

5.2 WDMPON Configuration

We consider a WDMPON configuration which employs an AWG in the RN for distributing the optical channels from OLT to individual ONUs, on specific wavelengths as shown in

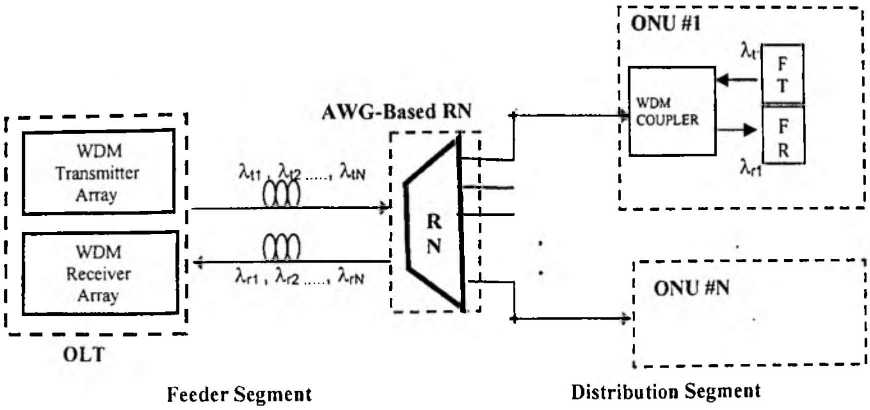

Fig.5.1. AWG-Based WDMPON Configuration

Fig. 5.1. The AWG-based RN demultiplexes the downstream WDM signal from the OLT, via distinct output ports to individual ONUs, through static wavelength-routing mechanism of the AWG. The RN is generally located close to the ONU premises to reduce the fiber cabling costs. The PONs with such configuration may typically have with a 20 Km reach, with about 5 Km between the RN and the constituent ONUs. The OLT consists of a WDM transmitter which can be a single tunable laser source or a laser array, depending upon the speed requirement, the number of ONUs and the power budget allocation of the PON. Each ONU is equipped with a fixed-tuned transceiver (FT, FR) whose transmit-receive frequencies are separated by one FSR of the AWG, so that the same fiber link can support bidirectional ONU traffic (further discussion on FSR is made in Section 5.2.2). Every ONU in this scheme gets the full bandwidth of an optical channel provided the link budget is adhered to. A WDM coupler directs the upstream and downstream to relevant sections in the ONU transceiver. GaAsP or AlGaAs based distributed feedback (DFB) lasers can provide 17 to 20 dBm output powers which are expensive and would be suitable only for the transceivers in the OLT. Low power DFB lasers with -2 to 3 dBm transmit powers are relatively cheap and can be used in the ONU transceivers. Typical values of linewidths for DFB lasers range between 10 GHz to 500 MHz. PIN photodiodes are in general used in ONU receivers, while OLT receiver can afford to have receivers with avalanche photodetectors.

Next we consider the AWG and some specific aspects of its functionality that enable it to be a very useful demultiplexing device.

5.2.1 Wavelength-Routing Mechanism

It is important to understand the mechanism by which an input WDM signal is demultiplexed and routed to the various ports in an AWG. An AWG exhibits periodic wavelength property, which allows the device to reuse the same wavelengths at different input ports, to be routed to distinct output ports as seen in Fig. 5.2. This gives AWG the capability to function as a

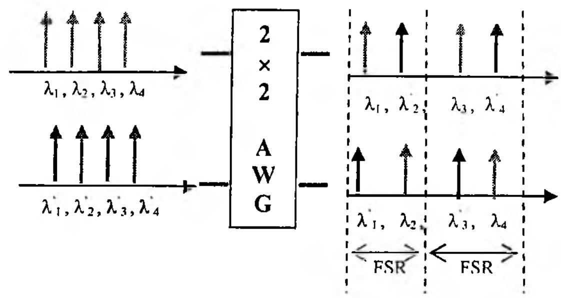

Fig. 5.2. Routing in a 2 × 2 AWG

network element and make use of its $1 \times N$ demultiplexing/wavelength-routing feature in the downstream and $N \times 1$ multiplexing/ wavelength-routing feature in the upstream. Typically a $1 \times N$ AWG consists of an input port, two focusing slab waveguides joined by an array of waveguides and N output ports as shown in Fig. 5.3. Transmitting and receiving waveguides are attached to the input and output ports to couple the data carrying WDM lightwaves into and out of the device. Slab waveguides offer free propagation regions (FPR) within which collimated beams of input lightwaves belonging to the WDM channels, undergo

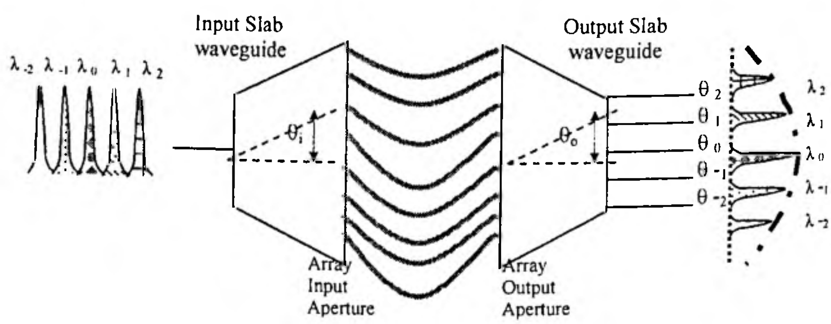

Fig. 5.3. Far Field Pattern of Routed Optical Channels

divergence, diffraction, interference and convergence phenomena in succession. The intermediate section of waveguide array has a constant path difference ΔL between its adjacent waveguides. An incoming lightwave undergoes divergence in the first FPR, and diffraction at the input aperture of the array and interference in the second FPR. Depending on the propagation constant and path length in each section and the wavelength, each lightwave is subjected to progressive phase shifts in the AWG device. At a position where propagating lightwave satisfies the phase match condition, constructive interference takes place and its corresponding focal field appears at the respective output port. Thus the focal position of the output signal field is uniquely determined by the wavelength of the input signal in an AWG.

The plane consisting of focal fields corresponding to all input WDM lightwaves constitutes the image plane of the device along which N receiver ports are located. This image plane is a part of a Rowland circle with a focal length R_a which is an important design parameter [SmDa96]. Thus spatial separation of the demultiplexed lightwaves of respective channels is obtained through a static wavelength-routing mechanism at the output aperture of

Table 5.1 AWG Device Parameters

Parameter	**Description**	**Numerical Value**
m	diffraction order in the AWG/ order of the beam	118
Δf_{FSR}	free spectral range ($=f_c/m$)	1600 GHz
c	velocity of light in vacuum	3299792458m/s
λ_c	central wavelength in vacuum; λ= optical channel wavelength	1.55381 µm
R_a	focal length of focusing slab waveguide	9381 µm
N_c	effective refractive index of channel waveguide	1.4513
N_{FPR}	effective refractive index of slab waveguide/free propagation region	1.4529
β_{FPR}	propagation constant in the free propagation region	
N_g	group index of the w/g mode $= N_c + f\frac{dN_c}{df}$ or $N_c - \lambda\frac{dN_c}{d\lambda}$	1.4752
β	propagation constant in the w/g mode	
ΔL	path length difference between adjacent waveguide	126.46 µm
V	normalized V-parameter of the waveguide material (fiber) $V = \frac{2\pi a}{\lambda}\sqrt{(n_1^2 - n_2^2)}$ where a, n_1, n_2 are the fiber parameters	
w_{wg}	width of the channel waveguide	
w_e	waveguide effective mode width $= w_{wg}\left[0.5 + \frac{1}{V - 0.6}\right]$ $1 < V < 10$	
w_0	FWHM beam width of the far field $= w_e\sqrt{\frac{2}{\pi}}$	4.5 µm
d_a	pitch of the waveguide array	25.0 µm
Δx	spacing of input/output waveguides	25.0 µm
θ	dispersion angle due to path difference between adjacent w/gs	
θ_i	diffraction angle in the input slab region	
θ_o	diffraction angle in the output slab region	

the AWG. In this process, incomplete coupling of power at the junctions between the waveguide array and the slab regions contributes to the insertion loss of AWG. However it is independent of the device port count. This feature of AWG makes it more suitable for a PON with large number of ONUs as compared to a PSC. Table 5.1 gives the list of device parameters, their descriptions along with the numerical values of select parameters as employed by Takahashi et al [TOTI95], which we use in our subsequent analysis. The phase match condition for constructive interference at a given output port can be expressed as

$$N_{FPR} d_a \sin\theta_i + N_g \Delta L + N_{FPR} d_a \sin\theta_o = m\lambda \qquad (5.1)$$

$$\beta_{FPR} d_a \sin\theta_i + \beta_g \Delta L + \beta_{FPR} d_a \sin\theta_o = 2\pi\, m$$

where, $\theta_i = i\dfrac{\Delta x}{R_a}$ and $\theta_o = j\dfrac{\Delta x}{R_a}$ with i and j as the indices of input and output waveguides.

From eqn.5.1 [SmDa96], it is evident that the refractive indices and geometrical dimensions of the constituent sections have to be designed appropriately to obtain the routed outputs at desired ports. Next, we examine various aspects of AWG analytically with the aim to develop a propagation model for the routed lightwaves of the respective WDM channels.

5.2.2 AWG Characteristics

In this section we consider some important characteristics of AWG and express them analytically based on earlier work [SmDa96]. These characteristics of AWG are used in subsequent sections, to evaluate the amount of optical signal power available at the output ports of the AWG. Focusing ability of AWG determines the amount of power that can be collected at the receiver ports. Primarily for the center wavelength λ_c, the parameter ΔL is a crucial factor to realize a well-focused output on the image plane. For λ_c, the group refractive index of the waveguide mode N_g is same as refractive index of channel waveguide N_c in the phase matching condition, so that eqn.5.1 reduces to $N_c \Delta L = m\lambda_c$. Then the adjacent waveguide path difference [SmDa96] can be expressed as

$$\Delta L = \frac{mc}{f_c N_c} \qquad (5.2)$$

Thus, for the same path difference, there is a trade-off between higher diffraction orders and lower refractive index for channel waveguides to ensure optimum focusing levels. On the image plane, maximum channel powers can be obtained for a given diffraction order m, which would reduce significantly for all other orders [SmDa96]. Figure 5.3 shows the demultiplexed channels from m^{th} order, which are obtained around the central output port of the device. Diffraction into undesired orders, absorption and scattering phenomena inside the device add to the insertion loss in the device.

When the wavelength of a lightwave in an input channel deviates from the center wavelength λ_c, the path difference in the waveguide array causes the focal field of the signal to shift from the central port (non-ideal constructive interference) along the image plane. The extent to which this lateral shift takes place per unit frequency change is called dispersion D and is determined by the device parameters. Though this aspect is effectively utilized for spatially separating the multiplexed channels, within a channel, this dispersion can cause some transmission impairments. In particular, when a channel employs an optical source, which does not have an ideal (line) spectrum, a part of the optical power is lost (smeared out) through shifted focal fields of constituent spectral components. Thus the spectral spread of a nonideal laser gets transformed into an undesired spatial spread at the output port of the AWG, leading to interchannel (hetero-wavelength) crosstalk – we address this issue in further details in the following two sections. In Fig. 5.3, for a signal component of frequency f, angle of dispersion θ can be viewed as the output diffraction angle θ_0 corresponding to a 'zero' input diffraction angle θ_i. The phase difference for ideal interference is given as $\beta\Delta L = 2\pi m$ from eqn. 5.1. The phase match condition for zero input and output diffraction angles is given by

$$\beta_{FPR} d_a \sin\theta = \Delta\phi - \beta\Delta L$$

We can express dispersion angle θ in terms of the other parameters [SmDa96] as

$$\theta = \sin^{-1}\left[\frac{\Delta\Phi - m.2\pi}{\beta_{FPR} d_a}\right] \cong \frac{N_g \Delta L}{N_{FPR} d_a} = \frac{N_g mc}{N_{FPR} d_a f_c N_c} \tag{5.3}$$

Further, for waveguide spacing $\Delta x << R$, lateral dispersion and angular dispersion are related through the focal length R_a [SmDa96] as

$$D = \frac{\Delta x}{df} = R_a \frac{d\theta}{df} \tag{5.4}$$

Substituting the expression for θ from eqn. 5.3 in eqn. 5.4, we get angular dispersion as

$$\frac{d\theta}{df} = -\frac{1}{f_c^2} \frac{N_g mc}{N_{FPR} d_a N_c} \tag{5.5}$$

Smit and Dam [SmDa96] approximated the modal field of the array waveguides as a Gaussian beam which in turn determines the far field intensity pattern of the routed signal power. The far-field distribution is obtained along the image plane of the AWG and signal power at the i[th] port [SmDa96] is given by

$$P_o^i(\theta) = P_o\, e^{\frac{-2\theta_i^2}{\theta_w^2}} \tag{5.6}$$

where, P_o is the max. power at a port, θ gives the angular deviation from the midpoint of central port and θ_w is 3dB beam width of focal field (at $1/e^2$ of P_o) $= \frac{\lambda}{N_{FPR}} \frac{1}{w_e\sqrt{2\pi}}$.

θ_w is inversely proportional to the modal field width of input waveguide, and hence, single mode fibers which have low values of modal widths, are used both in the array and in input/output ports. Thus, as seen in Fig. 5.3, the far-field pattern has a Gaussian profile with the peak coinciding with the central channel (at central port) of the m^{th} order diffraction beam. The curvature of the far-field indicates that the field intensity reduces towards the edge-ports, affecting the signal quality of the channel routed to those ports. This gives rise to difference in the signal loss between central and outermost ports called loss non-uniformity.

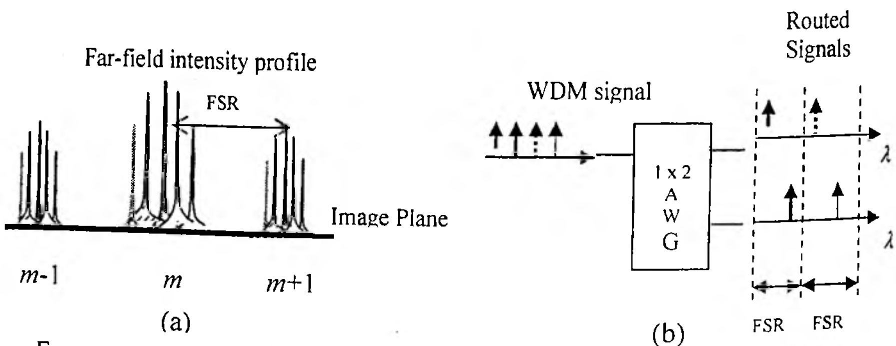

Fig. 5.4. (a) Diffraction order and (b) FSR of AWG-RN

From ... could be satisfied at multiples of f_c, implying that several orders of diffraction is possible along the image plane of the device. Higher orders allow more number of wavelength components to be spatially separated and so diffraction order of the device m is a parameter which denotes the resolution capability of AWG. Takahashi *et. al* took experimental results using AWGs of order 118 [TOTI95]. Depending on the desired value of m and f_c, other parameters can be calculated using eqns. 5.2 through 5.5. The spectral distance between two consecutive diffraction order beams is called the FSR of the AWG. The value of FSR determines the periodicity of the AWG as shown in Fig.5.4. This property can be utilized in a PON to save the port count of AWG since upstream transmissions can be sent on an optical frequency which is separated from the downstream carrier frequency by one FSR using a single fiber per ONU. In fact we included this aspect in our PON configuration.

We examine the impact of these functional parameters on the channel performance through an analytical model and discuss the results in subsequent sections.

5.3 Impact of Laser Spectrum on AWG Performance

Next we consider some of the salient signal impairments that affect the performance of demultiplexed optical channels in a WDMPON. Impairments have two-fold effect on the PON performance. They increase the noise variance of downstream signal transmissions, making data recovery erroneous at the ONU. Similarly, upstream transmissions generated from ONU reach the OLT with reduced signal to noise ratios, demanding additional processing to restore the signal quality. We examine the nature of three such impairments at three different points in the optical link viz., the transmitter, the RN and the receiver.

A typical WDMPON of a moderate size may need to support 16-32 ONUs (and wavelengths), which on demand may have to scale upto 64 or more, in order to justify the deployment costs. In this regard, linewidth of the laser along with the wavelength channel spacing would play crucial role in determining the performance of a WDMPON. The principal cause of line broadening of a laser is associated with quantum fluctuations in photon emissions which give rise to laser phase noise. Random spontaneous emission is intrinsic to Laser operation. Salz described it as a Weiner process, characterized by a zero mean, white Gaussian frequency noise with two-sided spectral density N_o [Salz86]. This gives rise to phase deviation in the radiated field of the laser and reduces its coherence time. As a result the emission spectrum of an optical channel exhibits a spectral spread leading to a non-negligible linewidth. The electromagnetic field of such a lightwave for a given channel can be viewed as a wide sense stationary random process whose power spectral density (PSD) is commonly referred as "Lorentzian". Accordingly, the PSD of the Lorentzian laser emission $S_i(f)$ with a center frequency f_{oi} corresponding to i^{th} wavelength (channel) [Salz86] and is expressed as

$$S_i(f) = \frac{A^2}{4\pi^2 N_O}\left[\frac{1}{1+\left(\frac{f+f_{oi}}{\pi N_o}\right)^2} + \frac{1}{1+\left(\frac{f-f_{oi}}{\pi N_o}\right)^2}\right] \tag{5.7}$$

where, A represents the amplitude of the optical field, N_0 denotes laser frequency noise spectral density and B_L is the 3 dB laser linewidth with $\pi N_0 \approx B_L$.

Though crosstalk in WDM channels may be caused due to various mechanisms, in an AWG-based RN, which operates as a $1 \times N$ demultiplexer in downstream, inter-channel crosstalk may become more significant. The finite laser linewidth causes a spectral spread in its emission spectrum. As a result spectral components deviating from the center frequency but belonging to a single optical channel get routed to adjacent ports on constructive interference in the RN. This leads to an overlap of the focal fields belonging to different wavelength channels and manifests as inter-channel crosstalk. Closely spaced channels undergo further deterioration due to the proximity of the corresponding spectral main lobes. Fig. 5.3 illustrates this effect. Inter-channel crosstalk increases shot noise in the receiver both directly and indirectly through beat noise formation which we discuss in the following section. It can be detrimental to closely spaced WDM channels such as in WDMPON using ≥ 64 channels.

Photodetection in an optical receiver is a non-linear process where the amplitude of the detected electrical signal is proportional to the square of the incident lightwave. When the lightwave consists of other signal components (due to crosstalk) apart from the desired one, the photodetected output consists of sum and difference terms of the constituent signal components. When the difference-frequency terms fall within the photodetector bandwidth, they contribute towards beat noise. This beating phenomenon occurs with all combinations of signal and crosstalk terms and is aggravated by broader laser linewidths. Beat noise effects reduce the receiver sensitivity and have to be contained with appropriate system design. In addition laser transmit powers might also be subjected to small variations due to temperature changes. We consider the effect of these phenomena on the signal quality at various data rates and laser linewidths in our BER analysis and make our observations in Section 5.3.3.

Next we derive the analytical expressions for signal and inter-channel crosstalk components associated with a demultiplexed optical channel at the AWG output port. In the earlier sections we have seen that the routing pattern of the AWG is characterized by its far-field intensity profile which is expressed in terms of the angular position of the routed signal along the image plane (eqn. 5.6). The Gaussian focal field pattern relates the input signal power to the routed output power through an exponential term. Since this term is distinctly determined by device parameters, it can be treated as an equivalent to a transfer function in spatial domain $|H(\theta)|^2$ for the RN. Assuming that AWG is a linear device, we get the output power $P_o = |H(\theta)|^2$ times the input signal power.

Also from eqn. 5.7, which gives the PSD of the laser emission, we observe that the Lorentzian spectrum modifies the input signal power (square of input signal amplitude) in the frequency domain. Combining eqn. 5.6 and 5.7 we get the demultiplexed output power for i^{th} signal as

$$P^i_{sig\_out}(\theta, f) = e^{\frac{-2\theta_i^2}{\theta_w^2}} \left\{ \frac{A^2}{4\pi^2 N_o} \left[\frac{1}{1+\left(\frac{f+f_{oi}}{\pi N_o}\right)^2} + \frac{1}{1+\left(\frac{f-f_{oi}}{\pi N_o}\right)^2} \right] \right\} \quad (5.8)$$

Table 5.2. System Parameters:

Parameter	Description
B_e	Noise Equivalent Bandwidth ($=R_b/2$)
K	Boltzmann Constant
T	Absolute Temperature In Kelvin
R_L	Load Resistance
η_{th}	Noise Power Spectral Density
q	Electronic Charge
ε	Laser Extinction Ratio (=0.01)
R_λ	Photo Detector Responsivity
n_{adj}	No. of Ports (Adjacent) Contributing To Crosstalk
ξ_{pol}	Polarization Mismatch Factor (=0.5)
$p_{r\text{-}on}$	Probability of Data Symbol Being "1" (=0.5)
P_{sig}^i	Optical Signal Power of i^{th} channel
$P_{adj-1}^i / P_{adj+1}^i$	Optical Signal Power From Adjacent Ports of i^{th} channel
P_{xt}^i	Optical Crosstalk Power of i^{th} channel
σ^2_{th}	Thermal Noise Variance
σ^2_{sh0}	Shot Noise Variance For "0" Bit
σ^2_{sh1}	Shot Noise Variance For "1" Bit
σ^2_{xt} (n_{adj}=2)	Crosstalk Variance from n adj. ch.s
$\sigma^2_{sg\_xt}$	Signal-Crosstalk Beat Variance
$\sigma^2_{xt\_xt}$	Crosstalk-Crosstalk Beat Variance

In eqn.5.8, the output signal is acted upon by two transfer functions, one related to the laser linewidth (in frequency domain) and the other related to the far-field pattern of the AWG (in the spatial domain). However we are aware of the fact that, in an AWG, routing mechanism is frequency (i.e., wavelength) dependent. Every input frequency component is subject to angular dispersion and routed to a distinct spatial position. We make use of this fact to develop a model for transformation between the two domains of eqn.5.8 as discussed in the following section.

5.3.1 Spectral-to-Spatial Domain Transformation of Lightwave

In this section we develop a transformation technique to map the frequency domain PSD term of a lightwave in an optical channel to the angular domain variation of the light intensity. By integrating the transformed PSD expressions over the port dimensions, the total captured signal power at each port is estimated. The central idea involved in the transformation is that the frequency deviation of a spectral component from the AWG central frequency f_c (= f_0) is linearly related to the lateral displacement of its focal field. Let $d\theta$ be incremental angular displacement corresponding to an incremental frequency deviation df. Some of the functional parameters which are used in the following are: the center frequency of the central port f_0, the center frequency of the i^{th} port ($i \neq 0$) f_{oi}, the angular separation of the i^{th} channel/ port from the central channel/ port $i\Delta\theta_{ch}$; output channel spacing in the frequency domain Δf_{ch} and output channel spacing in the spatial/angular domain $\Delta\theta_{ch}$. We next consider eqn. 5.4 for integration over θ and f on either side, which gives

$$\int d\theta = \int \frac{D}{R_a} df \Rightarrow \theta = \frac{D}{R_a} f + c$$

where c is the constant determined by the initial condition $f = f_0$. Thus at $f = f_0$, $\theta = 0$ which gives c = $-(D/R_a)f_0$. By substituting the value for c, we get the mapping relation as follows

$$(f - f_o) = \frac{R_a \theta}{D} \tag{5.9}$$

Eqn. 5.9 can be used to obtain the desired transformation between the two domains. We use this relation, to transform the frequency difference term $f - f_{oi}$ of eqn.5.9, into the angular domain. The i^{th} channel center frequency f_{oi} can thus be expressed in terms of channel frequency deviation from the central channel ($i = 0$) frequency f_o as

$$f_{oi} = f_o + i\Delta f_{ch}$$

Using eqn. 5.9, f_{oi} can be mapped into its corresponding angular dispersion θ_{oi}, given by

$\theta_{oi} = \theta_o + i\Delta\theta_{ch} = i\Delta\theta_{ch}\ (\theta_o = 0)$

Using the above results, the difference frequency term can be expressed as

$$f - f_{oi} = \frac{R_a\theta}{D} - i\frac{R_a\Delta\theta_{ch}}{D} \qquad (5.10)$$

Next we consider the PSD of the laser emission spectrum as expressed by eqn. 5.7., in order to compute the routed signal powers at output ports. Taking into consideration only the positive frequencies of the laser emission spectrum and using eqn.5.10, we get

$$S_i(f) = \frac{A^2}{2\pi^2 N_O}\left[\frac{1}{1+\left(\frac{f-f_o-i\Delta f_{ch}}{\pi N_o}\right)^2}\right]$$

By using the eqn. 5.9, we get the transformed laser emission in spatial domain (θ) as

$$S_i(\theta) = \frac{A^2}{\pi B_L}\left[\frac{1}{1+\left(\frac{2R_a\theta}{B_L D} - i\frac{2R_a\Delta\theta_{ch}}{B_L D}\right)^2}\right]$$

The transformed PSD for the i^{th} output port can be expressed as the product of peak optical power and a normalized PSD $S_n^i(\theta)$ as

$$S_i(\theta) = P_o^i\ S_n^i(\theta) \qquad (5.11)$$

where,

$$S_n^i(\theta) = \left[\frac{1}{1+\left(\frac{2R_a\theta}{B_L D} - i\frac{2R_a\Delta\theta_{ch}}{B_L D}\right)^2}\right] \text{ and}$$

$$P_O^i = \frac{A^2}{\pi B_L}$$

We can now substitute the normalized PSD in the angular domain in eqn. 5.8, to get the overall transfer function as

$$\left[e^{\frac{-2(i\Delta\theta_{ch})^2}{\theta_w^2}}\ S_n^i(\theta)\right]$$

Thus the lightwave power at the i^{th} output port can be expressed in terms of the spatial variable θ as

$$P_{sig}^{i}(\theta) = \frac{A^2}{\pi B_L} e^{\frac{-2(i\Delta\theta_{ch})^2}{\theta_w^2}} \left[1 \Big/ \left\{ 1 + \left(\frac{2R_a\theta}{B_L D} - i\frac{2R_a\Delta\theta_{ch}}{B_L D} \right)^2 \right\} \right] \tag{5.12}$$

Therefore, the total desired signal power captured at the i^{th} port can be obtained by integrating eqn. 5.12 over the angular width $\Delta\theta_{wg}$ of the output port as follows

$$P_{t\_sig}^{i} = \int_{i\Delta\theta_{ch}-\frac{\Delta\theta_{wg}}{2}}^{i\Delta\theta_{ch}+\frac{\Delta\theta_{wg}}{2}} \frac{A^2}{\pi B_L} e^{\frac{-2(i\Delta\theta_{ch})^2}{\theta_w^2}} \left[1 \Big/ \left\{ 1 + \left(\frac{2R_a\theta}{B_L D} - i\frac{2R_a\Delta\theta_{ch}}{B_L D} \right)^2 \right\} \right] d\theta \tag{5.13}$$

On applying the limits of integration, we get the desired signal power captured at the i^{th} port as

$$P_{sig}^{i} = \frac{A^2}{2\pi} e^{\frac{-2(i\Delta\theta_{ch})^2}{\theta_w^2}} \left\{ 2\tan^{-1}\left(\frac{R_a\Delta\theta_{wg}}{B_L D} \right) \right\} = \frac{A^2}{\pi} e^{\frac{-2(i\Delta\theta_{ch})^2}{\theta_w^2}} \tan^{-1}\left(\frac{R_a\Delta\theta_{wg}}{B_L D} \right) \tag{5.14}$$

At the central port where i = 0, power at the central channel is given by

$$P_{sig}^{0} = \frac{A^2}{\pi} \tan^{-1}\left(\frac{R_a\Delta\theta_{wg}}{B_L D} \right)$$

Next we evaluate the crosstalk power at an output port by considering the overlapping tails of the light intensity profiles from the two neighbouring adjacent channels. Optical powers at each of the adjacent ports $P_{i+1}(\theta)$ and $P_{i-1}(\theta)$ are given by

$$P_{i+1}^{i}(\theta) = P_o^{i+1}\, S_n^{i+1}(\theta) = \frac{A^2}{\pi B_L} e^{\frac{-2(\overline{i+1}\Delta\theta_{ch})^2}{\theta_w^2}} \left[\frac{1}{1 + \left(\frac{2R_a\theta}{B_L D} - i\frac{2R_a(i+1)\Delta\theta_{ch}}{B_L D} \right)^2} \right]$$

and

$$P_{i-1}^{i}(\theta) = P_o^{i-1}\, S_n^{i-1}(\theta) = \frac{A^2}{\pi B_L} e^{\frac{-2(\overline{i-1}\Delta\theta_{ch})^2}{\theta_w^2}} \left[\frac{1}{1 + \left(\frac{2R_a\theta}{B_L D} - i\frac{2R_a(i-1)\Delta\theta_{ch}}{B_L D} \right)^2} \right] \tag{5.15}$$

Inter-channel crosstalk at a port can be estimated by integrating the terms in eqn 5.15 over the desired port dimensions i.e., $(i\Delta\theta_{ch} \pm \Delta\theta_{wg})$. Thus the total crosstalk appearing at i^{th} port is given by

$$P_{xt}^{i} = \int\limits_{i\Delta\theta_{ch}-\frac{\Delta\theta_{wg}}{2}}^{i\Delta\theta_{ch}+\frac{\Delta\theta_{wg}}{2}} P_{adj+1}^{i}\ d\theta + \int\limits_{i\Delta\theta_{ch}-\frac{\Delta\theta_{wg}}{2}}^{i\Delta\theta_{ch}+\frac{\Delta\theta_{wg}}{2}} P_{adj-1}^{i}\ d\theta$$

By substituting eqn. (5.15) in the above expression, we get the inter-channel crosstalk power as

$$P_{xt}^{i} = \int\limits_{i\Delta\theta_{ch}-\frac{\Delta\theta_{wg}}{2}}^{i\Delta\theta_{ch}+\frac{\Delta\theta_{wg}}{2}} \frac{A^2}{\pi B_L}\left(e^{\frac{-2(\overline{i+1}\Delta\theta_{ch})^2}{\theta_w^2}}\right)\left[\frac{1}{1+\left(\frac{2R_a\theta}{B_LD}-i\frac{2R_a(i+1)\Delta\theta_{ch}}{B_LD}\right)^2}\right]d\theta$$

$$-\int\limits_{i\Delta\theta_{ch}+\frac{\Delta\theta_{wg}}{2}}^{i\Delta\theta_{ch}-\frac{\Delta\theta_{wg}}{2}} \frac{A^2}{\pi B_L}\left(e^{\frac{-2(\overline{i-1}\Delta\theta_{ch})^2}{\theta_w^2}}\right)\left[\frac{1}{1+\left(\frac{2R_a\theta}{B_LD}-i\frac{2R_a(i+1)\Delta\theta_{ch}}{B_LD}\right)^2}\right]d\theta \qquad (5.16)$$

On integrating eqn. 5.16 we get the total crosstalk appearing at the i^{th} port, given by

$$P_{xt}^{i} = \frac{A^2}{2\pi}e^{\frac{-2(\overline{i+1}\Delta\theta_{ch})^2}{\theta_w^2}}\left[\tan^{-1}\left\{\frac{2R_a}{B_LD}\left(\Delta\theta_{ch}+\frac{\Delta\theta_{wg}}{2}\right)\right\}-\tan^{-1}\left\{\frac{2R_a}{B_LD}\left(\Delta\theta_{ch}-\frac{\Delta\theta_{wg}}{2}\right)\right\}\right]$$

$$-\frac{A^2}{2\pi}e^{\frac{-2(\overline{i-1}\Delta\theta_{ch})^2}{\theta_w^2}}\left[\tan^{-1}\left\{\frac{2R_a}{B_LD}\left(\Delta\theta_{ch}-\frac{\Delta\theta_{wg}}{2}\right)\right\}-\tan^{-1}\left\{\frac{2R_a}{B_LD}\left(\Delta\theta_{ch}+\frac{\Delta\theta_{wg}}{2}\right)\right\}\right] \qquad (5.17)$$

For the central port $(i = 0)$, this reduces to

$$P_{xt}^{0} = \frac{A^2}{\pi}e^{\frac{-2\Delta\theta_{ch}^2}{\theta_w^2}}\left[\tan^{-1}\left\{\frac{2R_a}{B_LD}\left(\Delta\theta_{ch}+\frac{\Delta\theta_{wg}}{2}\right)\right\}-\tan^{-1}\left\{\frac{2R_a}{B_LD}\left(\Delta\theta_{ch}-\frac{\Delta\theta_{wg}}{2}\right)\right\}\right] \qquad (5.18)$$

The signal and the crosstalk powers, derived in this section, are incorporated in the BER model developed in the next section

5.3.2 BER Evaluation

In this section we develop an analytical model for evaluating the BER performance of the demultiplexed optical channels by using the models developed in the foregoing sections, for the transmission impairments and the signal powers received at various AWG ports. We consider the intensity-modulated direct-detection (IM-DD) communication scheme for the evaluation of BER at receiving end. Like thermal noise, for binary data, inter-channel crosstalk affects both for 'on' (data bit 1) and 'off' (data bit 0) signal pulses. We consider crosstalk contribution from only two neighboring ports/channels. Since beat noise practically affects only the 'on' pulse (ε = 0.01 from Table. 5.2), the corresponding probability of occurrence of data bit 1 is included. The various noise components corresponding to a channel (given as a superscript for signal and crosstalk powers) are expressed in terms of their respective noise variances. The thermal σ_{th}^2 and shot noise variances for "0" bit σ_{sh0}^2 and "1" bit σ_{sh1}^2 are given by

$$\sigma_{th}^2 = \frac{4KTB_e}{R_L}$$

$$\sigma_{sh0}^2 = 2q\varepsilon R_\lambda P_{sig}^i B_e \text{ and } \sigma_{sh1}^2 = 2qR_\lambda P_{sig}^i B_e$$

where the symbols used in the above expressions represent the variables as defined in Table 5.2.

Further shot noise variances from crosstalk from n_{adj} adjacent channels (considering only two adjacent channels) can be expressed as

$$\sigma_{xt}^2 = 2q\, R_\lambda P_{xt}^i\, n_{adj}\, B_e\, p_{r-on}$$

As discussed earlier, the beat noise variance between signal and crosstalk can be expressed as

$$\sigma_{sg\_xt}^2 = 2\xi_{pol} R_\lambda{}^2 P_{sig}^i P_{xt}^i\, p_{r-on}$$

and the crosstalk-to-crosstalk beat noise variance is given by

$$\sigma_{xt\_xt}^2 = 2\xi_{pol} R_\lambda{}^2 P_{adj+1}^i P_{adj-1}^i p_{r-on}^2 (n_{adj} - 1)$$

Considering all the constituent noise components, the standard deviations of total noise for "0" and "1" bits are given as

$$\sigma_0 = \sqrt{\sigma_{th}^2 + \sigma_{sh0}^2 + \sigma_{xt}^2 + \sigma_{xt\_xt}^2} \text{ and } \sigma_1 = \sqrt{\sigma_{th}^2 + \sigma_{sh1}^2 + \sigma_{xt}^2 + \sigma_{xt\_xt}^2 + \sigma_{sig\_xt}^2}$$

At the receiver we choose a value for the decision threshold which is kept independent of beat noise to make the receiver electronics simple [RDFM99]. Accordingly we compute the decision threshold term I_{th} using the noise variances as

$$I_{th} = \frac{R_\lambda P^{i}_{sig}\sigma'_0 + \varepsilon R_\lambda P^{i}_{sig}\sigma'_1}{\sigma'_1 + \sigma_0'}$$

where, ε = extinction ratio of the optical source

P^{i}_{sig} = Captured optical signal power over i^{th} output port

$\sigma'_0 = \sqrt{\sigma^2_{th} + \sigma^2_{sh0} + \sigma^2_{xt}}$ and

$\sigma'_1 = \sqrt{\sigma^2_{th} + \sigma^2_{sh1} + \sigma^2_{xt}}$

Finally, using Gaussian statistics for receiver noise processes for the "zero" and "one" receptions (with σ_0^2 and σ_1^2 as the variances, respectively), the receiver BER [RDFM99] is expressed as

$$P_e = \frac{1}{4}\left\{erfc\left[\frac{R_\lambda P_{sig} - I_{th}}{\sqrt{2}\sigma_1}\right] + erfc\left[\frac{I_{th} - \varepsilon R_\lambda P_{sig}}{\sqrt{2}\sigma_0}\right]\right\} \tag{5.19}$$

Here we ignore the signal losses and possible crosstalk encountered in WDM coupler at the ONU, which can be duly accommodated in our model, when necessary, in the received signal and cross talk power levels. Using the above expression, we evaluate BERs of the routed optical channels at various ports for relevant transmission parameters.

5.4 Results and Discussion

In this section, we present the results of our BER analysis for routed optical channels through AWG. We employ the values used by Takahashi [TOTI95] for device specifications in our numerical computation. Several AWG- related device parameters are taken from [TOTI96], based on which other functional parameters were calculated using the expressions developed in Section 5.2. A 1 × 16 AWG is considered with an insertion loss of 6.5 dB and a propagation loss of 4 dB. Two operating speeds for PON, viz., OC-3 (155 Mbps) and OC-12 (622 Mbps) in C-band (1525 nm-1565 nm) are assumed. Class B PONs have typically 20-25 dB power budgets which our configuration can easily support. Further, we considered 100 GHz (=0.8 nm) channel spacing for 16 WDM channels which specifies the minimum value of FSR as 1600 GHz. We assumed that effective spectral width of the main lobe of the received signal is the root mean square value of the data rate and laser linewidth in all cases.

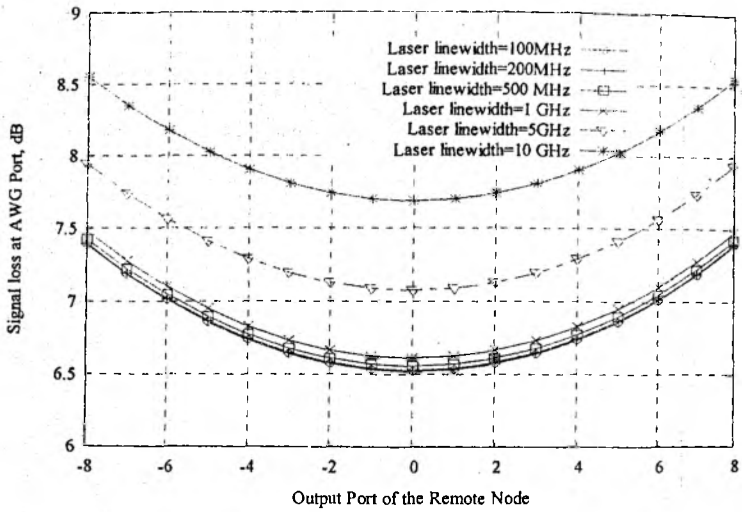

Fig. 5.5. Loss characteristics of AWG at 155Mbps; P_OLT=-22.5 dBm; Channels=16; Ch-spacing=100 GHz; Beat independent

Figures 5.5 and 5.6 illustrate the loss characteristics of routed optical channels at the AWG output ports for different laser linewidth values at 155 Mbps and 622 Mbps. The total signal loss is inclusive of the fixed amount of insertion loss of AWG and a variable component which depends on the location of the output port along the output aperture. It is evident from Figs. 5.5 and 5.6 that, though the total signal loss for a channel increases with source

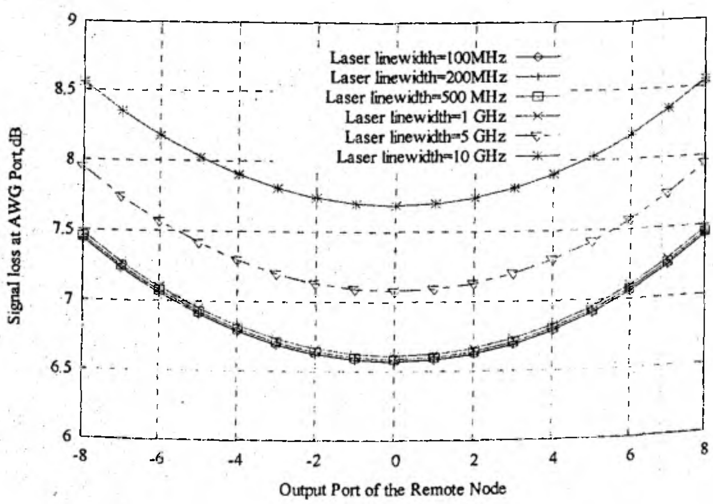

Fig. 5.6. Loss characteristics of AWG at 622Mbps; P_OLT=-16.5 dBm; Channels=16; Ch-spacing=100 GHz; Beat independent

linewidth, the differential loss between innermost (port #0) and outermost (port #8) receiving ports remains constant for both transmission rates. Further, we find that at higher data rates, the signal loss becomes relatively less sensitive to laser linewidth within 100 MHz -1 GHz range. On the other hand, for signals transmitted with linewidths far exceeding the data rates (5 GHz – 10 GHz), the absolute value of signal loss increases at all ports though to the same extent for both the channel rates. We observe a 0.5 dB additional loss as the linewidth value increases from 1 GHz to 5 GHz. This loss can be attributed to incomplete captured optical power from the main lobe of the routed signal spectrum, whose intensity is spatially

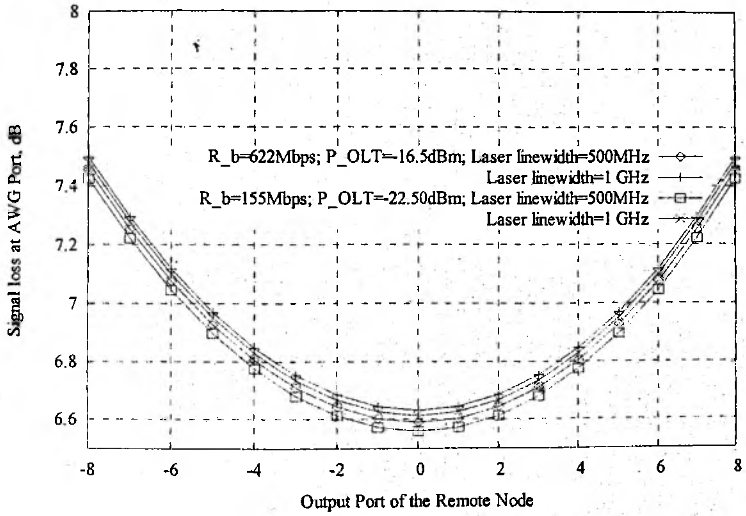

Fig. 5.7. Comparative loss profiles at different data rates and linewidths; Channels=16; Ch-spacing=100 GHz; Beat independent

modulated by the Gaussian focal-field pattern at the image plane. On the other hand, channel data rate and source linewidth broaden the main spectral lobe of the routed emission spectrum, which results in further loss of the captured signal power at a port. Their individual influence on the loss profile depends on the relative dominance of data rate and linewidth in determining the "effective" bandwidth of the transmitted signal.

Figure 5.7 compares the loss characteristics of the AWG at 155 Mbps and 622 Mbps for 500MHz and 1GHz linewidths. It is observed that at 155 Mbps, inner channels (channels routed to port-location close to port #0) are somewhat more susceptible to loss with increasing source linewidth than the outer channels (port near the edge of the output aperture). However the sensitivity to linewidth reduces at the higher data rate. We examine this aspect in Fig. 5.8

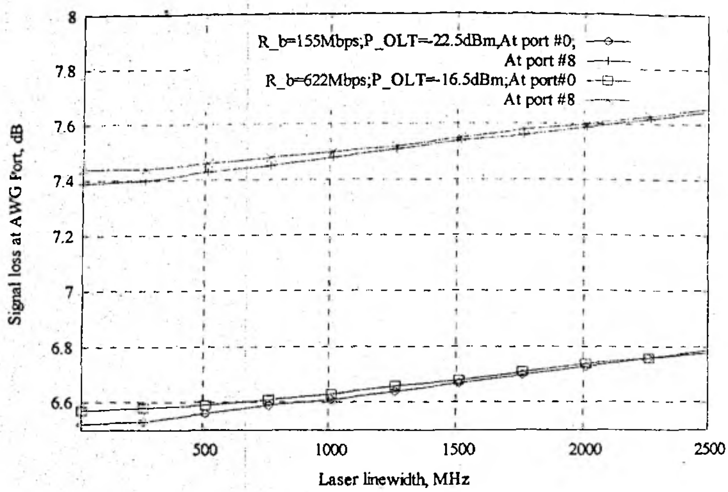

Fig. 5.8. Signal loss versus laser linewidth; Channels=16; Ch-spacing=100 GHz; Beat independent

over a much wider range of laser linewidth (100 MHz-2.5 GHz) values. As expected, for broader linewidths, signal losses become independent of data rates over the observed linewidth range of 100 MHz to 2.5 GHz [Fig. 5.6 & Fig. 5.8].

Figure 5.9 shows inter-channel crosstalk characteristics of 155 Mbps data channels at different AWG ports with laser linewidth as a variable parameter. We find that the crosstalk variation with port is small, with less than 1 dB margin at both inner and outer ports. As

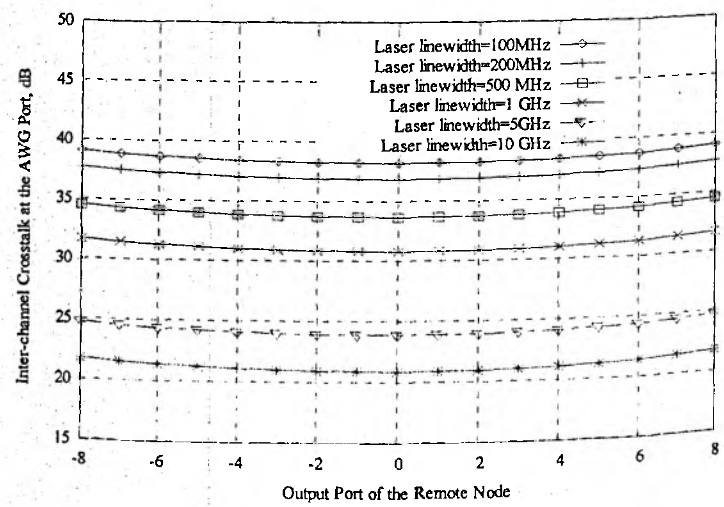

Fig. 5.9. Inter-channel crosstalk Characteristics for 155 Mbps Channels; P_OLT=-22.5 dBm; Channels=16; Ch-spacing=100 GHz; Beat independent

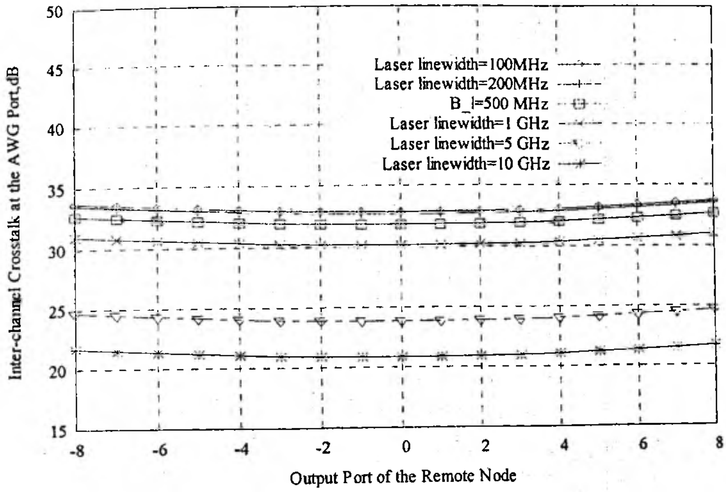

Fig. 5.10. Inter-channel crosstalk Characteristics for 622 Mbps channels; P_OLT=-16.5 dBm; Channels=16; Ch-spacing=100 GHz; Beat independent

indicated earlier, inter-channel crosstalk is a spill-over from neighboring channels and depends on both spectral spread and optical power from adjacent ports, and is more for innermost ports. For this reason, inner ports accumulate slightly more crosstalk from adjacent ports. As expected, it is evident from Fig.5.9 that crosstalk is a strong function of linewidth over the observed range of 100MHz to 10GHz for OC-3 channels. For instance, data channels at all the 16 port-locations accumulate approximately 3 to 5dB additional crosstalk with every 3 dB increase in linewidth. Figure 5.10 shows that at a higher data rate (622 Mbps) for

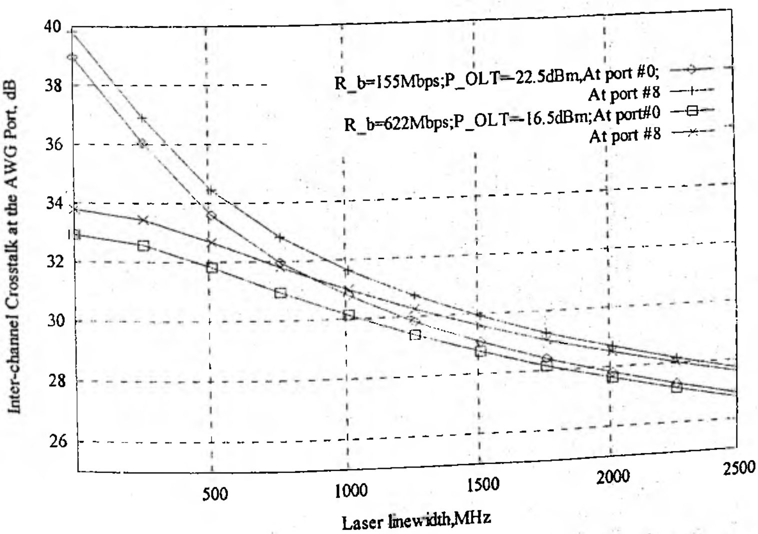

Fig. 5.11. Inter-channel crosstalk Characteristics versus laser linewidth at different data rates; Channels=16; Ch-spacing=100 GHz; Beat independent

linewidths below 1GHz, the absolute value of crosstalk increases more rapidly with linewidth than at 155 Mbps, though the crosstalk variation with port is very small.

In Fig. 5.11, we observe the impact of laser linewidth on crosstalk at the central and outer ports for the two data rates. It is evident that the differential crosstalk across 8 ports is 1

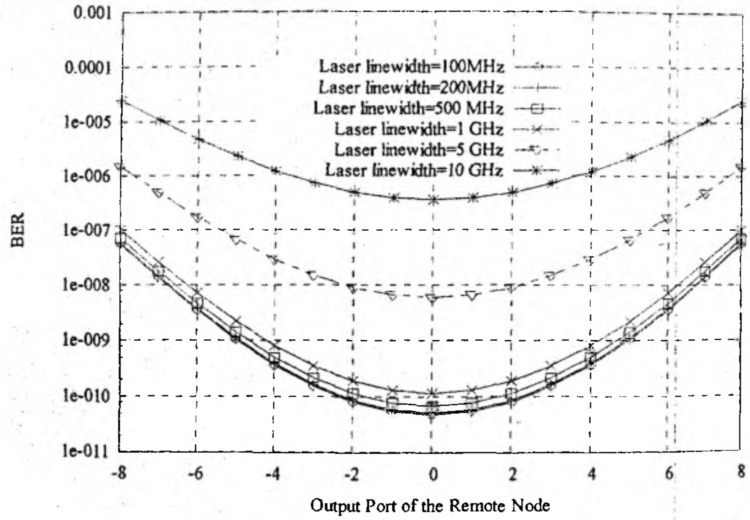

Fig. 5.12. BER Characteristics of routed 155 Mbps channels without beat noise effects; P OLT=-22.5 dBm; Channels=16; Ch-spacing=100 GHz

dB irrespective of any change in either the data rate or the output port. Further, we find that at 155 Mbps, crosstalk in the data channels becomes sensitive to linewidth within 100-500 MHz range and all ports are affected equally. However at 622 Mbps, sensitivity to laser linewidth

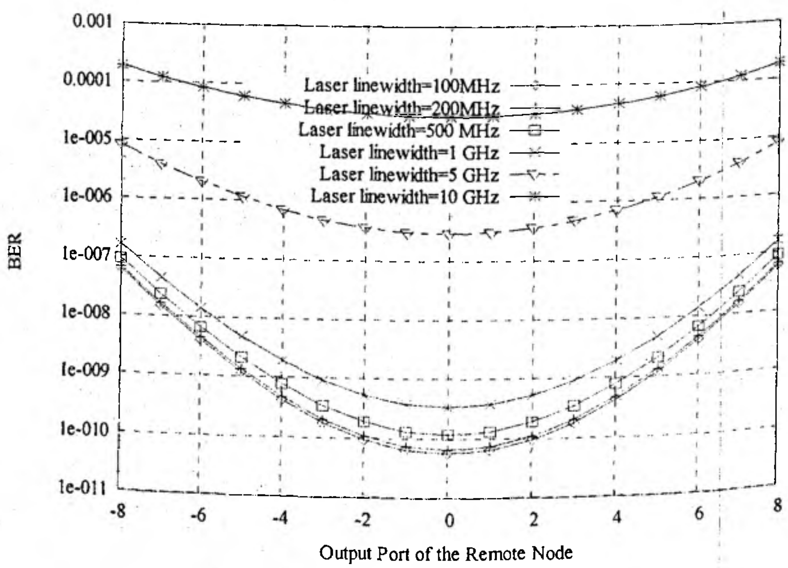

Fig. 5.13. BER Characteristics for routed 155 Mbps channels considering beat noise effects; P_OLT=-22.5 dBm; Channels=16; Ch-spacing=100 GHz;

reduces considerably. Crosstalk dependence on data rate gradually decreases for larger laser linewidths, and beyond 1.75 GHz becomes insignificant with an overall deterioration in crosstalk performance.

Next we examine the impact of signal loss and crosstalk on the data channels in terms of their BER performance. In Fig. 5.12, we present the BER plots for 155 Mbps data channels at various ports for varying source linewidths ≤10GHz. Figure 5.13 shows the corresponding performance when beat noise impairments are also taken into consideration. As depicted in Fig. 5.12, signal degradation of the routed optical channels is lowest at the central port and increases by 3 orders near the edge ports for linewidth values ≤500MHz. However laser linewidths of higher values affect the inner ports more seriously than the outer ports where the BER degradation with location is only by 2 orders. Comparing the two figures, it is evident that for laser linewidths ≤ 1 GHz, beat noise effects on channel BER are relatively more prominent at the central port, where the amount of power captured is maximum, be it the signal or crosstalk power. We noticed that channel quality at the extreme-end ports are only slightly affected by beat noise implying that the observed drop in BER is mainly due to lower available power levels. This in turn makes shot noise-dependent impairments less tangible at these locations. On the other hand, for channels using source linewidths exceeding 1GHz, at all ports, beat noise degrades the signal quality significantly. However BER variation with port is much less as evident from the corresponding curves at 5GHz and 10 GHz.

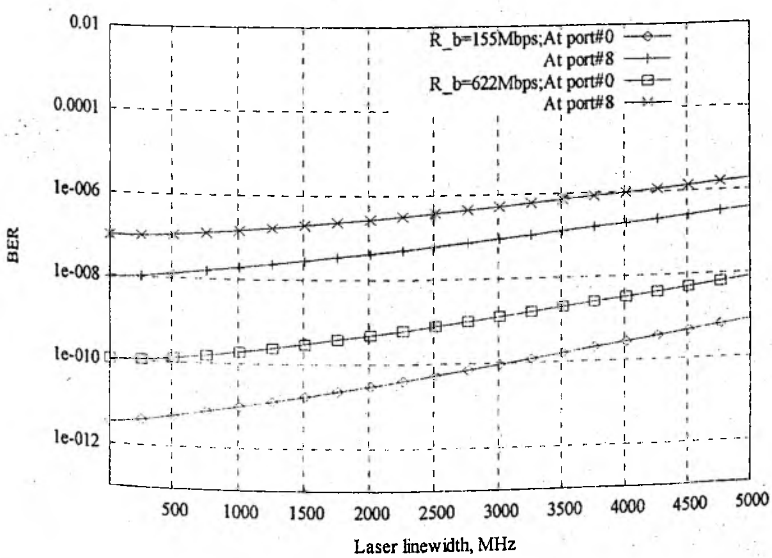

Fig. 5.14. BER versus laser linewidth without beat noise effect for different data rates; Channels=16; Ch-spacing=100 GHz

In Figs.5.14 and 5.15, we examine the impact of laser linewidth on BER, at innermost and outermost ports for two different operating speeds with and without beat noise respectively. From Fig.5.15, we find that the inner channels are more sensitive to the laser linewidth variation at the lower data rate especially for linewidths ≤ 750MHz. Channels routed to port #8 are less sensitive to linewidth variation and at both data rates. They register a BER drop of about one order compared to more than two orders by data channels at port #0. As seen from Fig. 5.15, beat noise effects are felt conspicuously at the inner ports for laser linewidth values

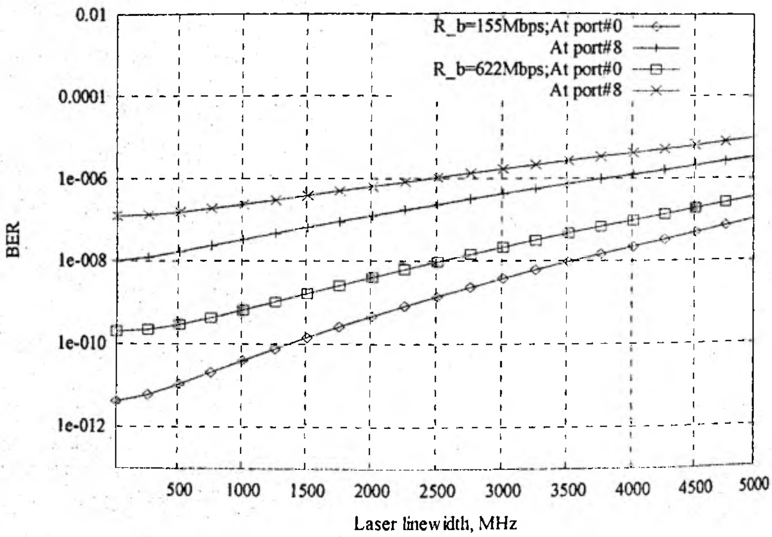

Fig. 5.15. BER versus laser linewidth with beat noise effect at different data rates; Channels=16; Ch-spacing=100 GHz

exceeding 1 GHz, and relatively more for lower data rates.

In Fig. 5.16, we compare the BER performance of the optical channels with 100 GHz channel spacing and different port counts. We neglect the beat noise effects as our focus is on the device functionality with modified parameters. As per the analysis carried out in Section 5.2, when FSR of the device is altered (corresponding to change in port count), for rest of the device parameters to be same, order of AWG which is inversely proportional to FSR also changes. We find in Fig. 5.16, that for RNs with smaller port-counts, channel BER becomes very sensitive to the port it is routed to. Thus 3-order variation in BER is observed across 4 output ports in a 8-port RN. In comparison there is hardly 0.5 order drop in BER even across 16 ports in the case of a 32-port RN. This is due to the fact that in an AWG-RN dispersion coefficient increases with the diffraction order, which causes the spectral components of a wavelength channel to spread laterally across the image plane. This in turn results in more inter-channel crosstalk to be coupled from adjacent ports giving higher BER values both at the inner channels as well as the outer ones. This is verified from the figure where central inner channels in a 32-port AWG have better BER values than those in 8-port AWG. Outer port performance is far better in lower-order AWGs with larger FSRs. Similarly BER performance at the inner ports is relatively better in such AWGs due to the corresponding lower values of dispersion coefficient. However it may be noted that a trade-off exists between channel performance and frequency resolution associated with lower value of *m*.

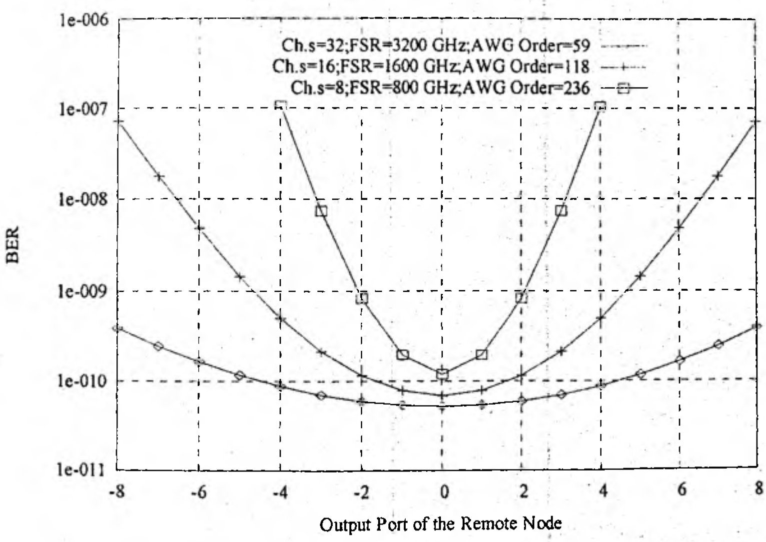

Fig. 5.16.BER performance with different port count and fixed channel spacing; P_OLT=-22.5 dBm; Channels=16; Laser linewidth=500 MHz; Ch-spacing=100 GHz; Without beat noise

Next we compare the channel performance of AWGs with the same FSR supporting WDM channels with different channel frequency spacing as shown in Fig. 5.17. Here the BER profiles for different port-count AWGs are similar to the earlier case but converge to a common point at the central channel in this case. If we compare the corresponding curves in Fig. 5.16, we find that error performance improves slightly for the inner channels in an 8-port AWG when the channel spacing is increased from 100 GHz to 200 GHz. In the case of 32-port AWG, BER performance slightly deteriorates at the central channel for reducing the channel spacing from 100 GHz to 50 GHz. This is because in spite of the unchanged lateral dispersion coefficient (FSR being constant), channels are more closely spaced in the frequency spectrum for the 32-port AWG which increases interchannel crosstalk. The converse happens in the case of 8-port AWG which experience less inter-channel crosstalk at its output port.

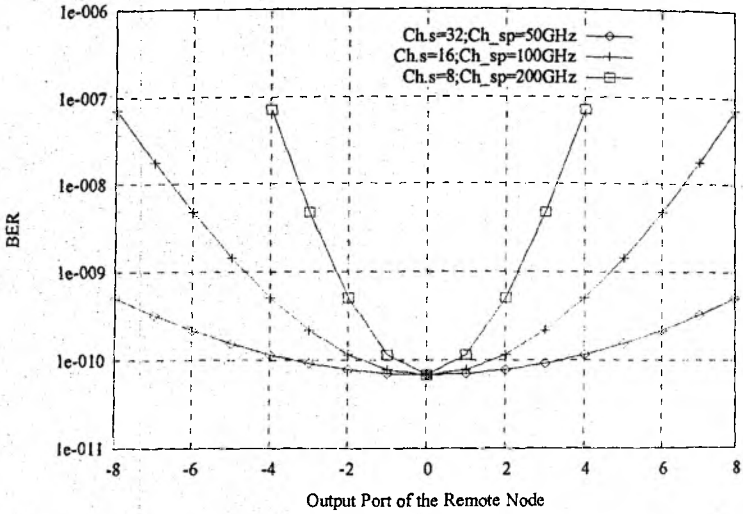

Fig. 5.17. BER performance of RNs with different port count and FSR; P_OLT=-22.5 dBm; FSR=1600 GHz; Laser linewidth=500 MHz; Without beat noise: AWG order=118

5.5 Summary

In this chapter, we presented our studies on a wavelength-routed WDMPON employing an AWG device in the RN. The AWG-based router demultiplexes the downstream WDM signal to distinct output ports, through static wavelength-routing mechanism providing distinct optical channels for every ONU. Each ONU is equipped with a fixed-tuned transceiver whose transmit-receive frequencies are separated by one free spectral range of the AWG, so that the same fiber link can support bidirectional ONU traffic. However several physical-layer issues related to the transmitter, AWG and receiver can affect the signal quality at the high operating data rates in a WDMPON. Our work dealt with the analytical modeling of routed optical channels taking into account transmission impairments of the propagation path of the lightwaves. Our model takes into consideration Lorentzian emission spectrum of the source laser, angular dispersion and far-field intensity profile of AWG. Our analytical model indicated that variation of signal strength of demultiplexed optical channels was largely determined by the Gaussian focal-field pattern of the AWG. It was noted that for linewidths ranging from 100MHz to 500MHz, BER of the routed channel deteriorated by 3-4 orders at all AWG ports. Interchannel crosstalk accumulation was found to be considerably more for higher rate channels with slight advantage to outer port channels compared to the inner ones.

References

[Henr82] C. H. Henry "Theory of linewidth of semiconductor lasers," *IEEE Journal of Quantum Electronics*, pp. 259-264, Feb. 1982.

[Keis91] G. E. Keiser, "*Optical Fiber Communications*," McGraw Hill Inc, USA, 1991 Edition.

[Mcgr98] K. A. McGreer, "Arrayed waveguide gratings for wavelength routing," *IEEE Communication Magazine*, pp. 62- 68, Dec. 1998.

[Peeb02] P. Z. Peebles, "Probability, Random Variables and Random Signal Principles," Tata McGraw Hill Ltd., India, 2002 Edition.

[RDFM99]B. Ramamurthy, D. Datta, H. Feng, J. P. Heritage and B. Mukherjee, "Impact of transmission impairments on the teletraffic performance of wavelength-routed optical networks," *IEEE/OSA Journal of Lightwave Technology*, 17(10): 1713-1723, Oct. 1999.

[Salz86] J. Salz, "Modulation and Detection for Coherent Communication," *IEEE Communications Magazine*, pp. 38-49, Jun. 1986.

[SmDa96] M. K. Smit and C. V. Dam, "PHASAR-Based WDM-Devices: Principles, design and applications," *IEEE Journal of Selected Topics in Quantum Electronics*, 2(2): 237-250, Jun. 1996.

[Smit88] M. K. Smit, "New focusing and dispersive planar component based on an optical phased array," *Electronics Letters*, vol. 24, no. 7, Feb. 1988.

[TaOT96] H. Takahashi, K. Oda and H. Toba, "Impact of Crosstalk in an Arrayed-Waveguide Multiplexer on N x N Optical Interconnection," *IEEE/OSA Journal of Lightwave Technology* 14 (6): 1097-1105, June 1996.

[TOTI95] H. Takahashi, K. Oda, H. Toba and Y. Inoue, "Transmission characteristics of arrayed waveguide N x N wavelength multiplexer," *IEEE/OSA Journal of Lightwave Technology*, 13(3): 447-445, Mar. 1995.

[TSKN90] H. Takahashi, S. Suzuki, K. Kato, I. Nishi, "Arrayed-waveguide grating for wavelength division multi/demultiplexer with nanometer resolution," *Electronics Letters*, vol. 26, no. 2, Jan. 1990.

[TWLH93] H. Takahashi, E. K. Wildermuth, M. Lanker, W. Hunziker and H. Melchior, "Polarization-insensitive arrayed-waveguide grating multiplexer with birefringence compensating film," *IEEE Photonic Technology Letters*, vol. 5, pp. 707-709,1993.

CHAPTER 6

Conclusions

WDM-based optical access technology is indeed emerging as the most powerful means for realizing future-proof, wired last-mile solutions. However, there are several challenging issues to be investigated before the benefits of the optical solutions in the access segment reach the customer end as well as the service providers. Extensive research activities have been reported over the last two decades to improve both the device and networking related issues. In view of this we examined in the present thesis some of the relevant issues concerning the design and resource provisioning of some candidate realizations of WDMOANs. In particular, we considered three different realizations of WDMOANs and investigated some of the MAC-layer and physical-layer issues therein.

First, we considered a WDMOAN in Chapter 3 with two-level hierarchical topology of a backbone ring connecting several passive-star-based clusters of ONUs at the customer premises with ANs interconnected by a WDM ring. The network employs both active and passive subsystems for the collection and distribution segment. We proposed an AN configuration that handles both intracluster and intercluster communications through appropriate scheduling functionalities. For the proposed AN configuration, we studied the performance of two candidate MAC protocols, that are employed in the scheduler-based AN to manage the transport of data packets. For intracluster traffic, the protocol incorporates pre-transmission co-ordination based scheduling, whose performance has been evaluated through computer simulation. The delay performance has been found to improve on increasing the number of control channels but with an early take-off of the delay curves. Further, our results indicate that, incorporating a few SCM subcarriers on a single control wavelength reduces the number of collisions between the control packets, without reducing the number of wavelengths needed for data traffic. This in turn improves the delay performance, albeit with some additional hardware complexity at ONUs as well as ANs. The problem of receiver contention could also be alleviated in the given network setting by incorporating "look-ahead" feature in the scheduler. For intercluster traffic, we examined a MAC protocol employing priority-based queuing to differentiate between RT and NRT services. An analytical model was developed for evaluating the network performance and a comparative study of the two priority queuing schemes in terms of end-to-end delay was carried out to understand the mutual impact effect of RT and NRT service traffic. The methodologies used in this study are expected to serve as useful tools for designing a WDMOAN with ring-on-star topology, both for intracluster and inter cluster communications.

Next, we considered a PON, referred to as W-OCDM PON (Chapter 4) with tree topology employing OCDMA over WDM, which can accommodate a large number of ONUs through two stages of RNs using AWGs and PSCs. We first investigated the resource allocation issue for such a network using a heuristic method, taking into account the natural traffic asymmetry in an access network. We developed analytical models for data throughput with binomial and Poisson distributed traffic, with due considerations to (a) multi-user interference from bidirectional traffic and (b) code contention in the upstream transmission. It was observed that our heuristic estimate for code allocation offered a handy reference point to initiate the search for an optimum solution for resource (code) provisioning. This approach enables the designer to examine some of the network design aspects of W-OCDM PONs viz., trade-off between per-user throughput and user count (PON size); interplay between contention relief in the upstream channels and data packet size etc. In general, it is understood that the PONs with lower traffic ratio can support more number of users with reasonably good overall throughput performance as compared to the PONs with higher traffic ratios. This study is expected to help designers to allocate resources with the objective to improve overall throughput performance of the network.

Finally, we considered a wavelength-routed WDMPON in Chapter 5, with tree topology with an AWG as the RN and examined the transmission impairments affecting the downstream BER at the output ports of AWG. An analytical model was developed for studying the impact of transmission impairments and various system design parameters on the BER performance of such WDMPONs. We observed that variation of signal strength of the demultiplexed wavelength channels across the AWG ports is largely determined by the Gaussian focal-field pattern of the AWG. The non-ideal lasers with finite linewidth and crosstalk limitations of the routing mechanism were found to cause variations in the quality of the received signal at various output ports. Moreover the beat noise effects deteriorate the signal quality of channels routed to innermost ports significantly than other ports. It was noted that, for increasing linewidths, beat noise effects on the optical signal at the receiver are strong enough to deteriorate the BER values by 2-3 orders at the outer ports and by 3-4 orders at the inner ones. The proposed theoretical model gives useful insight into the various transmission impairments affecting the WDMPON performance and the results obtained from the model can be utilized as a design tool for optimizing the overall power budget of WDMPONs.

It may be also worthwhile eventually to look into the possible directions for future extension of the present work. While analyzing the delay performance of the MAC protocols for inter-cluster traffic in WDMOAN with ring-on-stars topology, we considered only the queuing delay at the exit point of the AN. The delay that these packets encounter while waiting to be scheduled in the local cluster (through control channel/s common to both intra- and inter-cluster packets) was ignored. This may not be justified for a network with high intra-cluster loads. Therefore it may be worthwhile to include also the delay incurred in the local cluster to get a more realistic estimate of the RT/NRT delay profiles in presence of high intra-cluster traffic.

In W-OCDM PON, if the RSOA in the ONU is replaced by a fixed-tuned transmitter whose wavelength is one FSR away from the downstream, the data packets will experience MUI only from unidirectional traffic. The performance analysis for this modified network can be explored as it is expected to give more scope for higher throughput and better link power budget. Moreover, to make the code strong in both scalability and performance, two dimensional (2D) code sequences have been explored in recent times, in which data is encoded both in temporal and wavelength domains avoiding long codes [RaDa02]. Since each 'ON' chip pulse in such two dimensional (2D) code sequence is on a distinct wavelength, there is less probability of interference. Similarly, two dimensions offer more combinations of the chip-pulse sequences allowing a larger code dictionary. Such configurations can be used in W-OCDM PONs with larger split ratios with better connectivity (due to larger cluster size) and service quality (due to reduced impact of MUI).

Furthermore, in the last problem on WDMPON studied in Chapter 5, we considered a single-stage AWG in the RN for evaluating the transmission impairments. In a practical situation, a multi-stage-AWG in RN might be more useful to connect clusters of ONUs, geographically spread out over a wide range. Signal loss and BER performance in multi-stage-AWG RNs can give useful results for improving the end-to-end link design for scalable configurations. It would indeed be worthwhile to investigate the transmission impairments in such WDMPONs by making use of the analytical models we developed in Chapter 5.

Author's Publications

(2002-2007)

Journal:

- "Medium Access Control Protocols for WDM-based Optical Access Networks with Passive-Star Clusters Interconnected by a Backbone Ring," Jayashree Ratnam, Ritesh Shyamsukha, Satyanarayana Vuta, Amogh Joglekar, Goutam Das and Debasish Datta, *Computer Communications* (Elsevier Publication), vol. 30, Issue 18, pp. 3614 -3626, Dec. 2007 (*special issue on "Optical Networking: Systems and Protocols)*
- "Performance Evaluation of a Packet Switched Multi-wavelength Optical CDMA Network," Jayashree Ratnam and Debasish Datta, *Journal of Optical Communications* (Fachverlag Schiele & Schön Publication, Berlin), vol. 27 (2006)5, 273 - 277.
- "Optical CDMA in Broadband Communication - Scope and Applications," R. Jayashree, *Journal of Optical Communications* (Fachverlag Schiele & Schön Publication, Berlin), vol. 23 (2002) 1, pp. 11-21.

Conference:

- "Performance Analysis of a Light Path in WDM-Based Passive Optical Network Employing an AWG-Based Demultiplexer," Jayashree Ratnam, Debasish Datta and Saswat Chakrabarti, *Proceedings of National Conference on Communications*, NCC 2007, IIT Kanpur, Jan.27th-28th, 2007.
- "Performance Evaluation of a Packet Switched Multi-wavelength Optical CDMA Network", Jayashree Ratnam and Debasish Datta, *Proceedings of National Conference on Communications* (NCC 2004), IISc., Bangalore, Jan. 30th – Feb. 1st 2004.
- "MAC Protocols for a WDM based Optical Access Network with two level Hierarchical Topology", Jayashree Ratnam, Satyanarayana Vuta, Amogh Joglekar, Goutam Das and Debasish Datta, Proceedings of *Proceedings of Conference on Horizons of Telecommunications* (HOT2003)", Institute of Radio physics and Electronics, University of Calcutta, Kolkata on Feb.3rd-5th, 2003.

(2008-2009)

- "Resource Provisioning Through Traffic-Aware Code Allocation in a Hybrid PON Employing WDM and OCDMA," Jayashree Ratnam, Debasish Datta and Saswat Chakrabarti, *Proceedings of IEEE Conference on Advanced Network and Telecommunication Systems (ANTS 2008)*, IIT Bombay, Dec.15th-17th, 2008 (Won the **Best paper award)**

- "A Heuristic Approach for Designing Hybrid PONs Employing WDM and OCDMA with Asymmetric Traffic Distribution," Jayashree Ratnam, Debasish Datta and Saswat Chakrabarti, (**communicated on invitation** to Elsevier Journal of "Optical Switching and Networking" in May 2009) .

- "Impact of Transmission Impairments on Performance of WDMPONs Employing AWG-based Remote Nodes," Jayashree Ratnam, Debasish Datta and Saswat Chakrabarti (**to be communicated** to IEEE/OSA Journal of Lightwave Technology)

Author's Biography

Jayashree Ratnam received the B. Tech degree in Electronics and Communication Engineering in 1985 from Jawaharlal Nehru Technological University, Hyderabad, India and the M. Tech. degree in Fiber Optics and Lightwave Engineering in 1997 from Indian Institute of Technology, Kharagpur, India. During the periods, 1986-1989 and 1994 -1995 she worked as a Research Staff member for several sponsored research projects in the Department of Electronics and Electrical Communication Engineering, IIT Kharagpur. From 1998 to 2008, she served as Scientific Officer in G. S. Sanyal School of Telecommunications, IIT Kharagpur. During this period, she was involved as a Project Investigator on topics like "Design and Development of WDM-Based Optical Access Networks" and "Design and Development of Telecom Convergence Switch". She also coordinated and lectured in several short term courses on topics related to telecommunication engineering and networking. During the period 2002-2007, she carried investigations on wavelength-division-multiplexing passive optical networks (WDMPONs) for a PhD degree and published her work in several international journal as well as conference proceedings. She mainly worked on medium access control and physical layer issues of WDM and optical CDMA-based access networks. Her current research interests also include reconfigurable architectures for QoS-aware access network solutions.